



Lepton-Nucleus Interactions — Part II

International Neutrino Summer School
Fermilab, August 10, 2023

Noemi Rocco

Summary of electron-nucleon scattering

- We consider the process:

$$\ell^-(k) + N(p) \rightarrow \ell^-(k') + N(p')$$

$$\left(\frac{d\sigma}{d\Omega}\right)_{\text{Mott}} = \frac{\alpha^2}{4E_k^2 \sin^4 \theta/2} \cos^2 \frac{\theta}{2} \quad \longleftarrow \quad \text{Scattering on a point-like spinless target}$$

$$\left(\frac{d\sigma}{d\Omega}\right) = \left(\frac{d\sigma}{d\Omega}\right)_{\text{Mott}} \left[1 - \frac{q^2}{2M^2} \tan^2 \frac{\theta}{2}\right] \quad \longleftarrow \quad \text{Scattering on a point-like 1/2 spin target}$$

- Protons and neutrons have an internal structure: described by electric and magnetic form factors

$$\left(\frac{d\sigma}{d\Omega}\right) = \left(\frac{d\sigma}{d\Omega}\right)_{\text{Mott}} \left[\frac{G_E^2 - \frac{q^2}{4M^2} G_M^2}{1 - \frac{q^2}{4M^2}} - \frac{q^2}{2M^2} G_M^2 \tan^2 \frac{\theta}{2} \right] \quad \text{Rosenbluth separation}$$

Determination of nucleon form factors

- A **reduced** cross section can be defined as

$$\left(\frac{d\sigma}{d\Omega}\right) = \left(\frac{d\sigma}{d\Omega}\right)_{\text{Mott}} \times \frac{\epsilon G_E^2 + \tau G_M^2}{\epsilon(1 + \tau)}$$

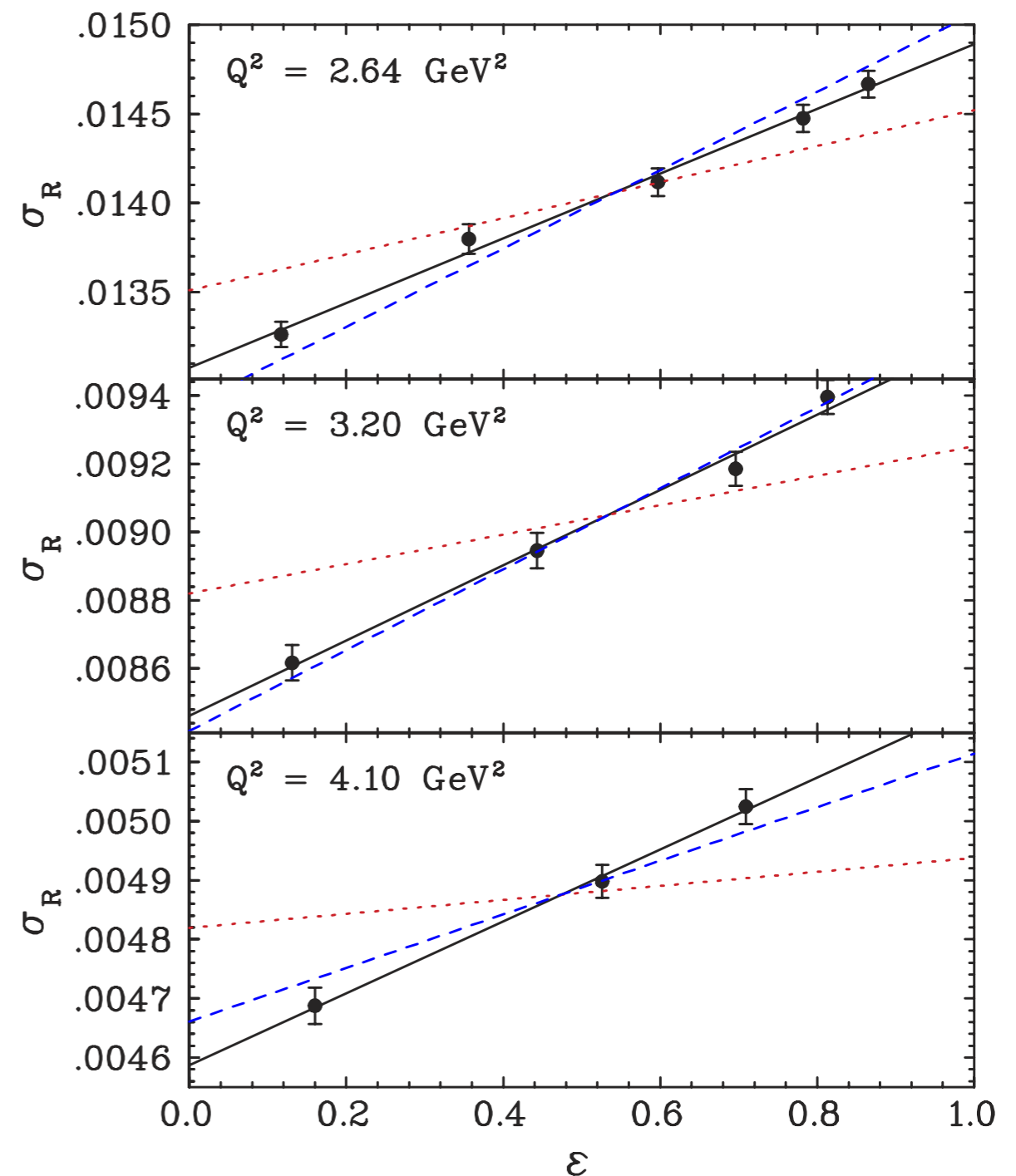
- The **virtual photon polarization** parameter is

$$\epsilon = \left[1 + 2(\tau + 1) \tan^2 \frac{\theta}{2}\right]^{-1}$$

- Measuring angular dependence of the cross section at fixed Q^2

$$\sigma_R = \epsilon(1 + \tau) \frac{\sigma}{\sigma_{\text{Mott}}} = \epsilon G_E^2 + \tau G_M^2$$

Qattan et al., PRL 94, 142301 (2005)



- In Born approximation: G_E^2 is the slope and the intercept is τG_M^2
- polarization transfer experiment
--- previous Rosenbluth

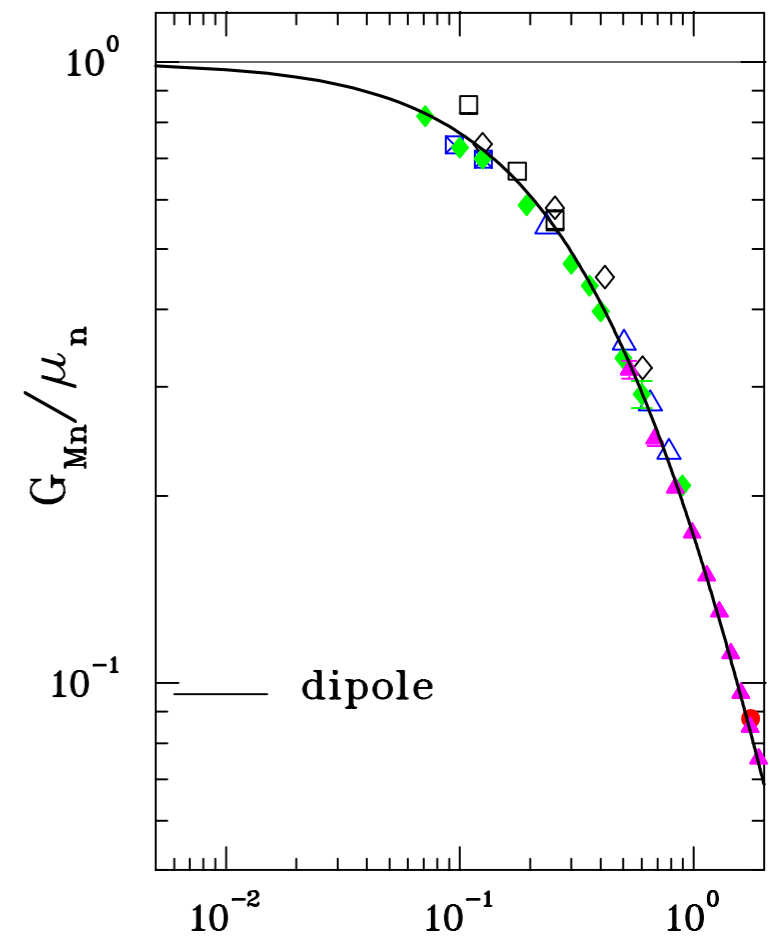
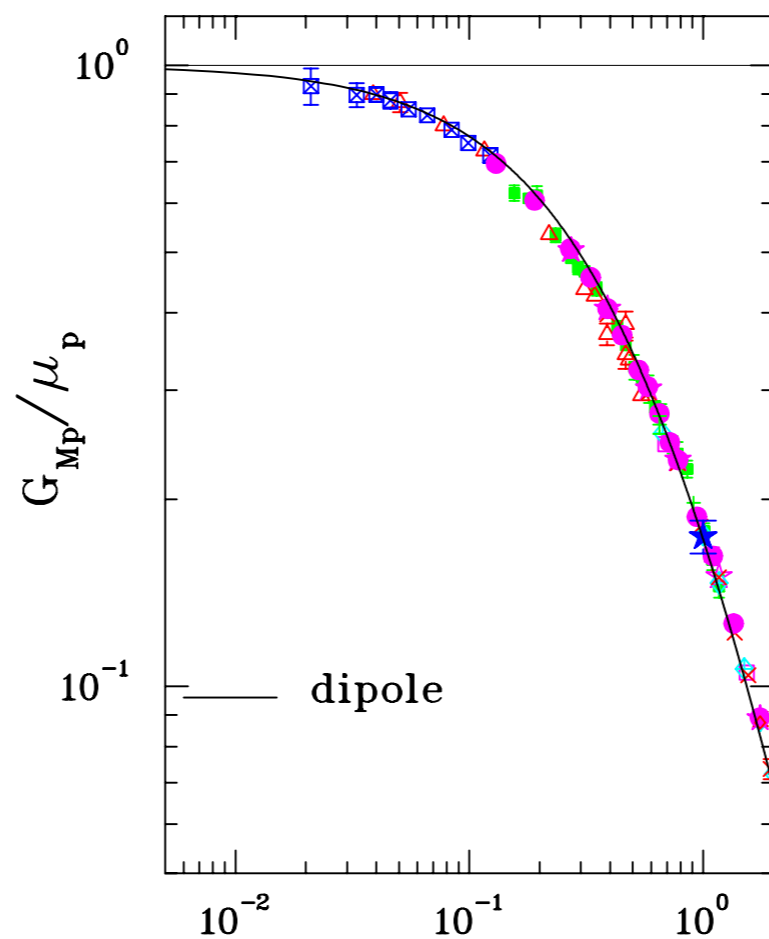
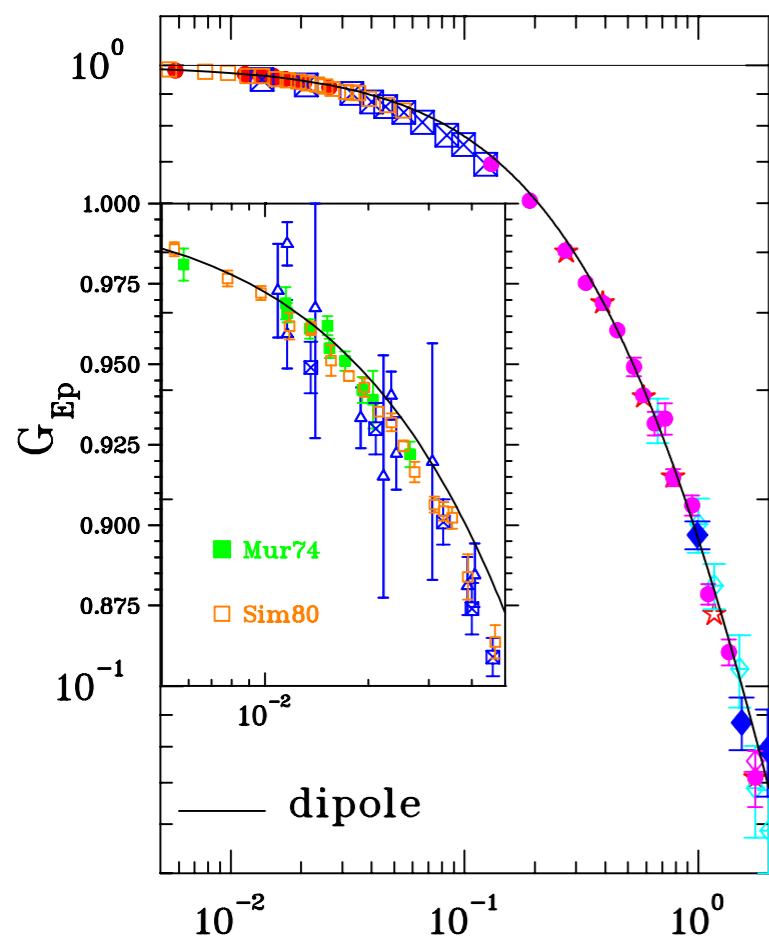
Determination of nucleon form factors

$$G_E^p(q^2) = G_D(q^2) \ , \ G_M^p(q^2) = \mu_p G_D(q^2) \ , \ G_M^n(q^2) = \mu_n G_D(q^2) \ , \ G_D = \left(1 - \frac{q^2}{M_V^2}\right)^{-2}$$

$$\mu_p = 2.793, \ \mu_n = -1.913,$$

$$M_V^2 = 0.71 \text{ GeV}^2$$

 Perdrisat et al., Prog.Part.Nucl.Phys. 59 (2007) 694–764



Lattice QCD in a Nutshell

- Lattice QCD is a technique in which space-time is discretized into a four-dimensional grid
- The QCD path integral over the quark and gluon fields at each point in the grid is performed in Euclidean space-time using Monte Carlo methods
- The quark mass is a parameter of the calculation : m_π
- Space time is discretized, step a : UV cutoff
- Finite volume L : infrared cutoff
- The physical limit is recovered by imposing that

$$m_\pi \rightarrow m_\pi^{\text{phys}}, a \rightarrow 0, L \rightarrow \infty$$

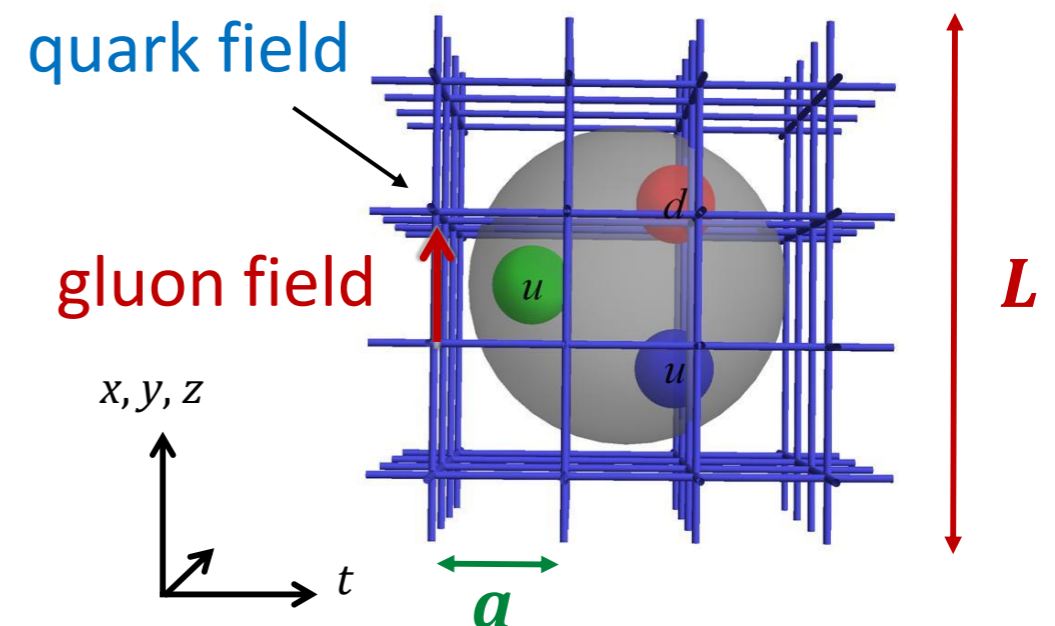
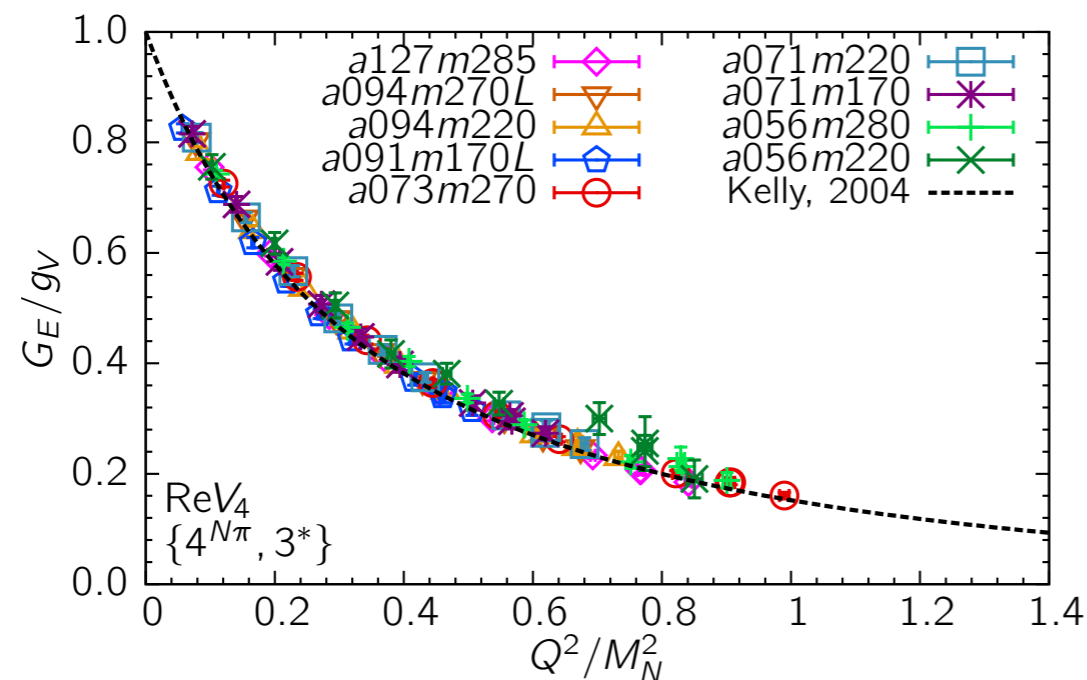


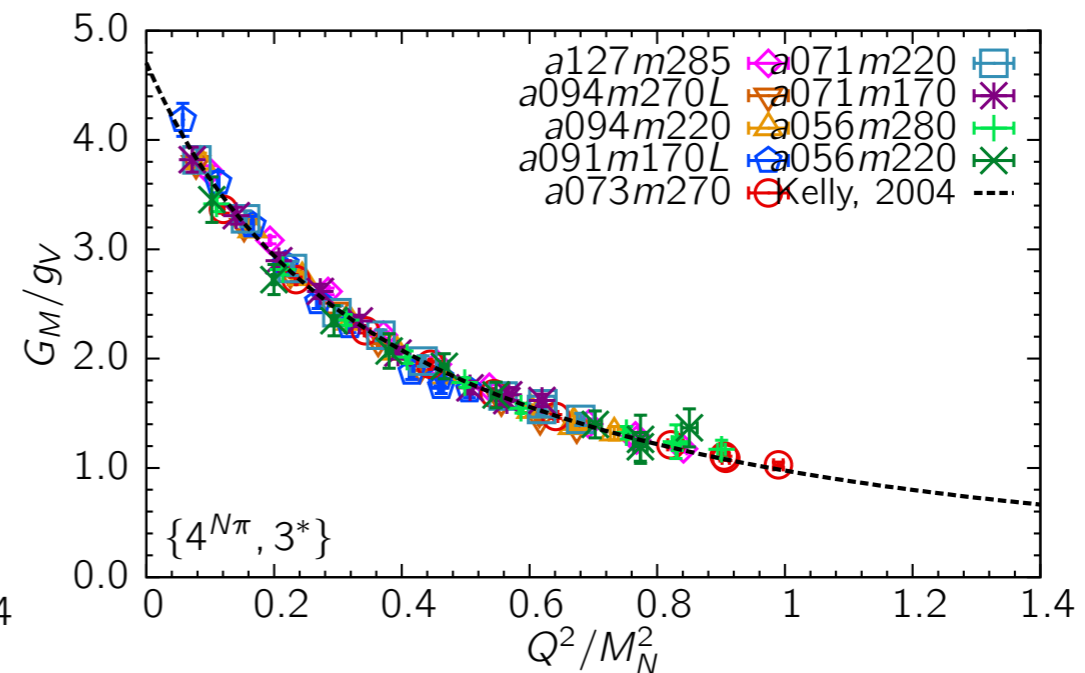
Figure by Huey-Wen Lin

Lattice QCD form factors

Gupta's talk @Lattice2023



Electric



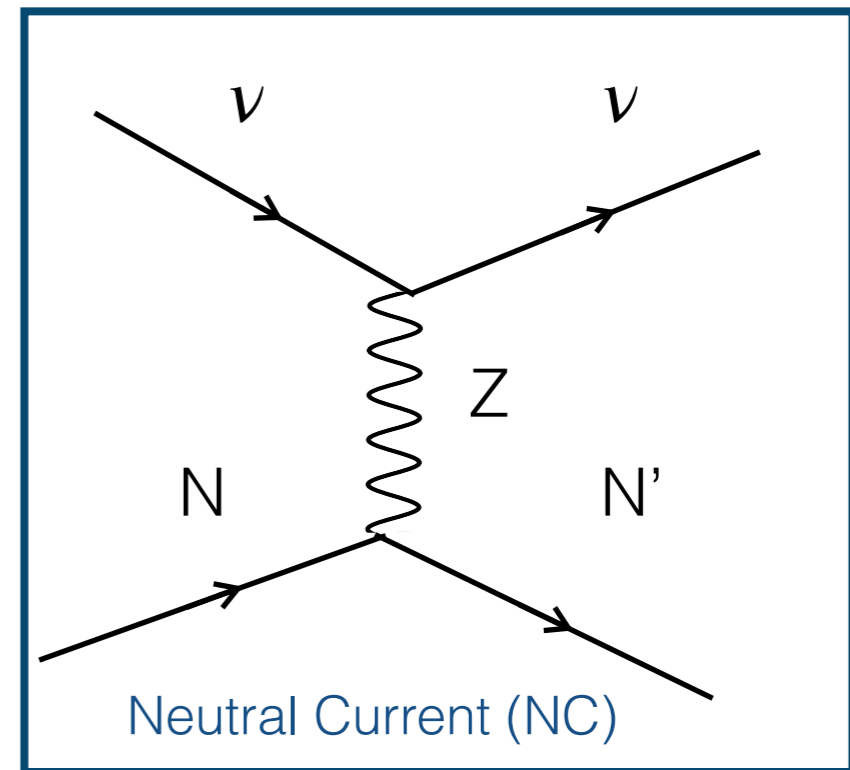
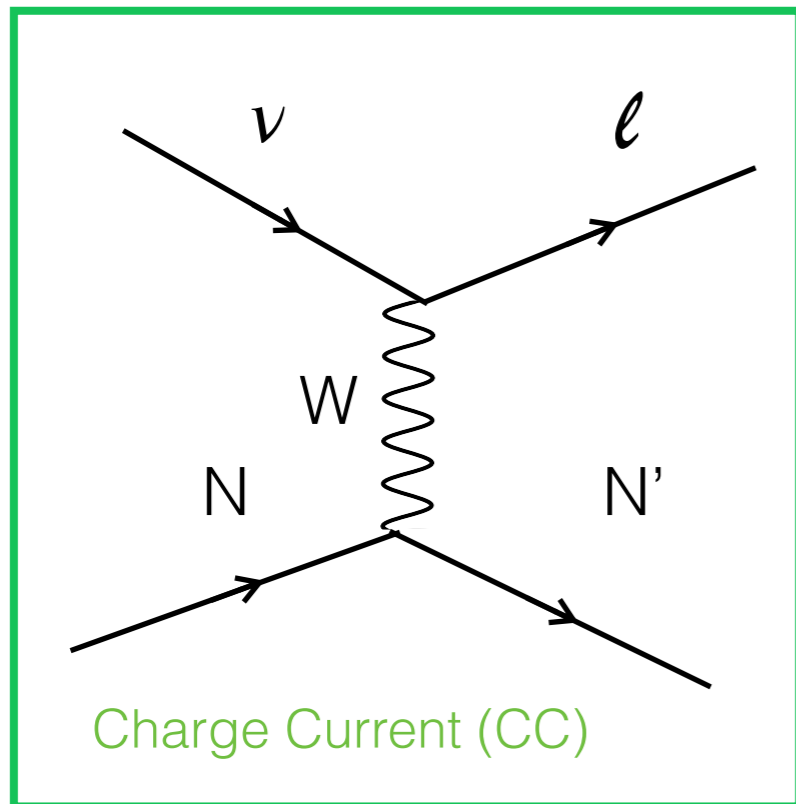
Magnetic

- Isovector electric and magnetic form factors
- The form factors do not show significant dependence on the lattice spacing or the quark mass
- Good agreement with the Kelly curve. Validates the lattice methodology



R. Gupta, [Introduction to Lattice QCD, arXiv:hep-lat/9807028](https://arxiv.org/abs/hep-lat/9807028)

Neutrino-Nucleon scattering



- Exchange of the W boson
- Lepton produced has the same flavor of the neutrino
- Initial and final nucleon have different isospin

- Exchange of the Z boson
- Independent of the neutrino flavor
- Initial and final nucleon have same isospin



F. Close, An Introduction to quark and partons

Neutrino-Nucleon scattering

- Differential cross section for CC and NC processes

$$\frac{d^2\sigma}{dE'd\Omega'} = \frac{1}{16\pi^2} \frac{G^2}{2} L_{\mu\nu} W^{\mu\nu}$$

- For NC

$$G = G_F$$

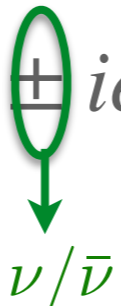
- For CC

$$G = G_F \cos \theta_c$$

$$G_F = 1.1803 \times 10^{-5} \text{ GeV}^{-2}, \quad \cos \theta_c = 0.97425$$

- Leptonic Tensor:

$$L_{\mu\nu} = 2[k_\mu k'_\nu + k'_\mu k_\nu - g_{\mu\nu} k \cdot k' \pm i\epsilon_{\mu\nu\alpha\beta} k'^\alpha k^\beta]$$

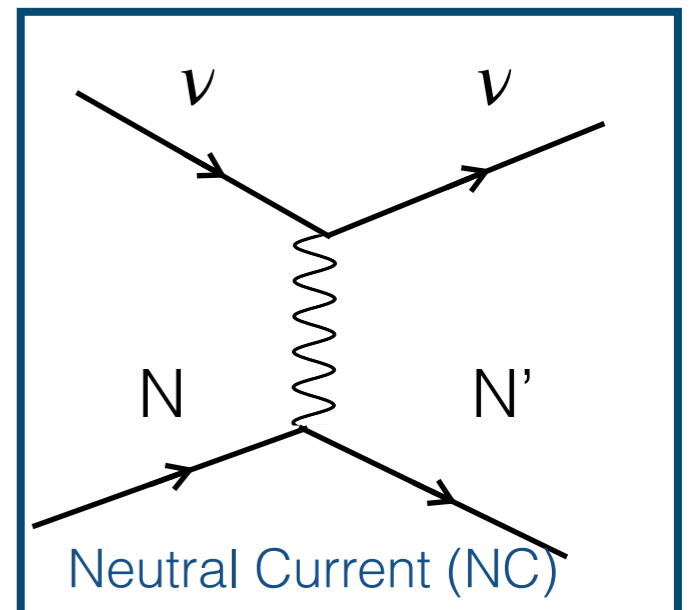
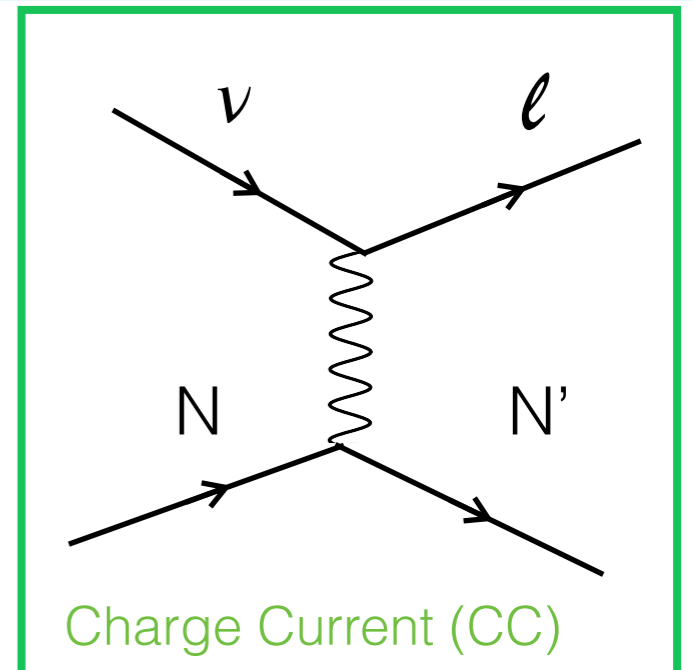


 $\nu/\bar{\nu}$

- Hadronic Tensor:

$$W_{\mu\nu} = \sum_{\sigma_i \sigma_f} \frac{1}{2E_p} \int \frac{d^3 p'}{2E_{p'}} \langle N(p) | J^\mu | N'(p') \rangle \langle N'(p') | J^\nu | N(p) \rangle$$

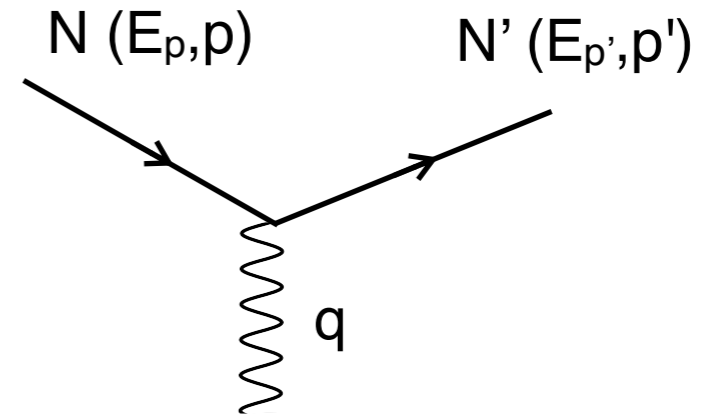
$$\times \delta^{(4)}(p' + k' - p - k)$$



Neutrino-Nucleon scattering

- Electroweak current operator:

$$\langle N' | J^\mu | N \rangle = \bar{u}(p') \Gamma^\mu u(p) = \underbrace{J_V^\mu}_{\text{Vector}} + \underbrace{J_A^\mu}_{\text{Axial}}$$



- The vector contribution is given by:

$$J_V^\mu = \mathcal{F}_1 \gamma^\mu + i \sigma^{\mu\nu} q_\nu \frac{\mathcal{F}_2}{2M}$$

- The axial contribution is given by:

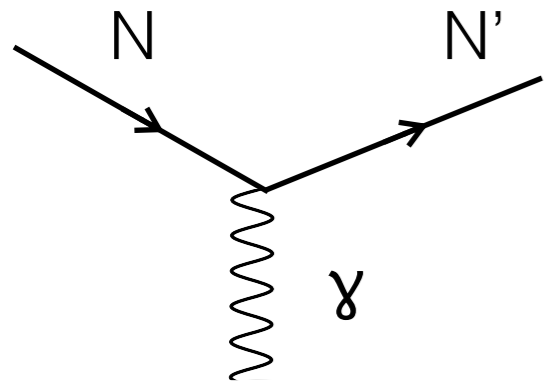
$$J_A^\mu = -\gamma^\mu \gamma_5 \mathcal{F}_A - q^\mu \gamma_5 \frac{\mathcal{F}_P}{M}$$

- General expression for both neutral- and charge current processes. The iso-spin dependence of these form factors is different (see next slide).
- The Vector current is the same of the electromagnetic: Conserved Vector Current hypothesis



T. Leitner, O. Buss, L. Alvarez-Ruso, and U. Mosel, Electron- and neutrino-nucleus scattering from the quasielastic to the resonance region, Phys. Rev. C 79, 034601 (2009).

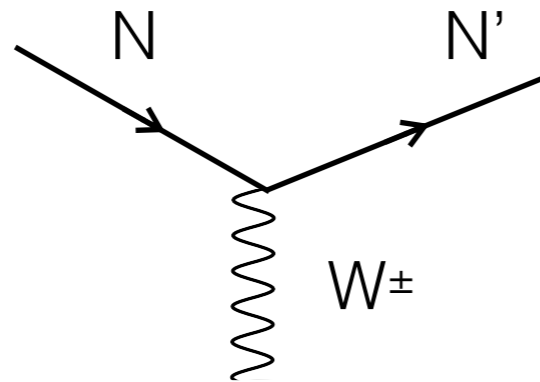
Neutrino-Nucleon scattering



- EM

$$\mathcal{F}_1 = \frac{1}{2}[F_1^S + F_1^V \tau_z]$$

$$\mathcal{F}_2 = \frac{1}{2}[F_2^S + F_2^V \tau_z]$$



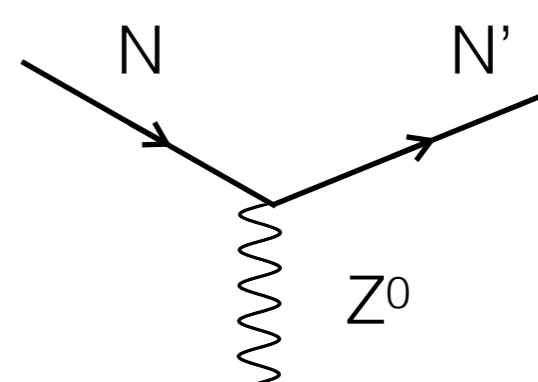
- CC

$$\mathcal{F}_1 = F_1^V \tau_{\pm}$$

$$\mathcal{F}_2 = F_2^V \tau_{\pm}$$

$$\mathcal{F}_A = F_A \tau_{\pm}$$

$$\mathcal{F}_P = F_P \tau_{\pm}$$



- NC

$$\mathcal{F}_1 = \frac{1}{2}[-2\sin^2\theta_W F_1^S + (1 - 2\sin^2\theta_W)F_1^V \tau_z]$$

$$\mathcal{F}_2 = \frac{1}{2}[-2\sin^2\theta_W F_2^S + (1 - 2\sin^2\theta_W)F_2^V \tau_z]$$

$$\mathcal{F}_A = \frac{1}{2}F_A \tau_z$$

$$\mathcal{F}_P = \frac{1}{2}F_P \tau_z$$

- We used the Conserved Vector Current hypothesis:

$$F_1^V \tau_z \rightarrow F_1^V \tau_{\pm} , \quad F_2^V \tau_z \rightarrow F_2^V \tau_{\pm}$$

- PCAC:

$$F_P = \frac{2m_N^2}{(m_\pi^2 - q^2)} F_A$$

Axial form factor determination

- The axial form-factor has been fit to the dipole form

$$F_A(q^2) = \frac{g_A}{(1 - q^2/m_A^2)^2}$$

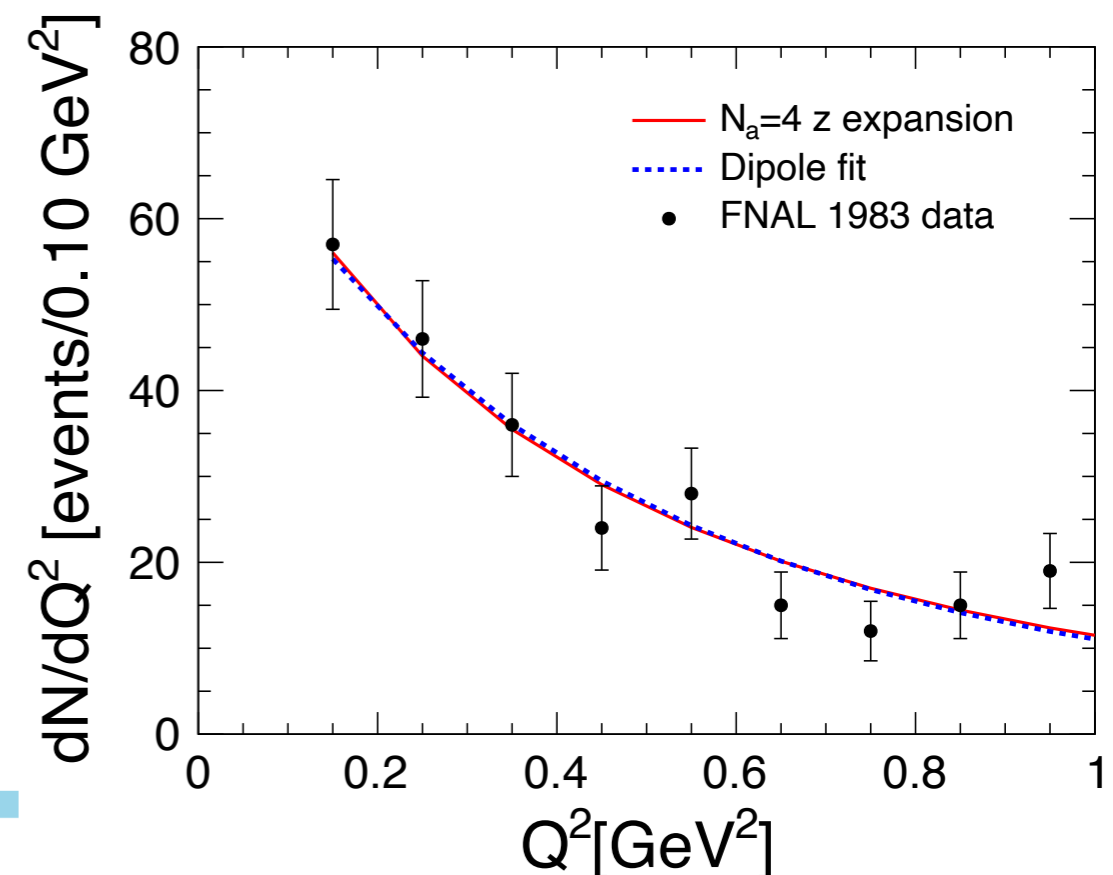
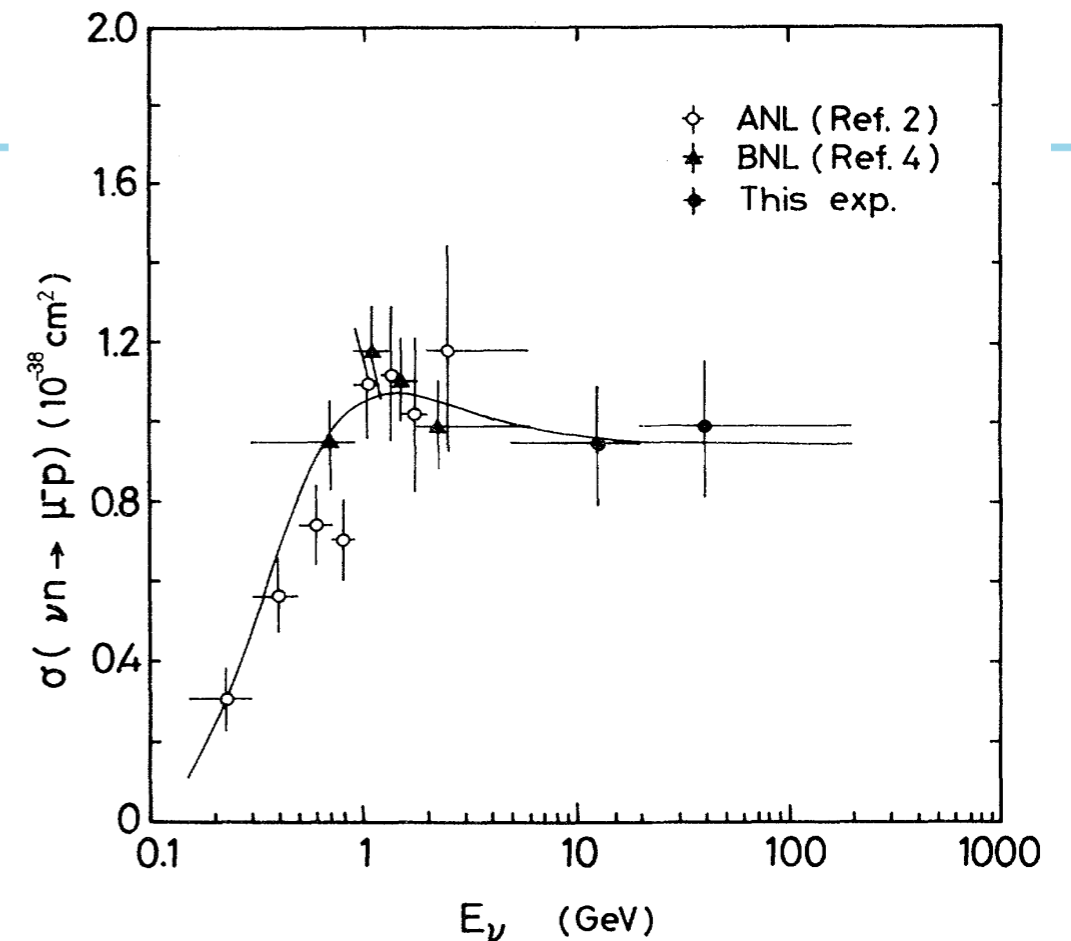
- The intercept $g_A = -1.2723$ is known from neutron β decay
- Different values of m_A from experiments
 - $m_A = 1.02$ GeV q.e. scattering from deuterium
 - $m_A = 1.35$ GeV @ MiniBooNE
- Alternative derivation based on **z-expansion**
—model independent parametrization

$$F_A(q^2) = \sum_{k=0}^{k_{\max}} a_k z(q^2)^k,$$

free parameters known functions

Bhattacharya, Hill, and Paz PRD 84 (2011) 073006

A.S.Meyer et al, Phys.Rev.D 93 (2016) 11, 113015



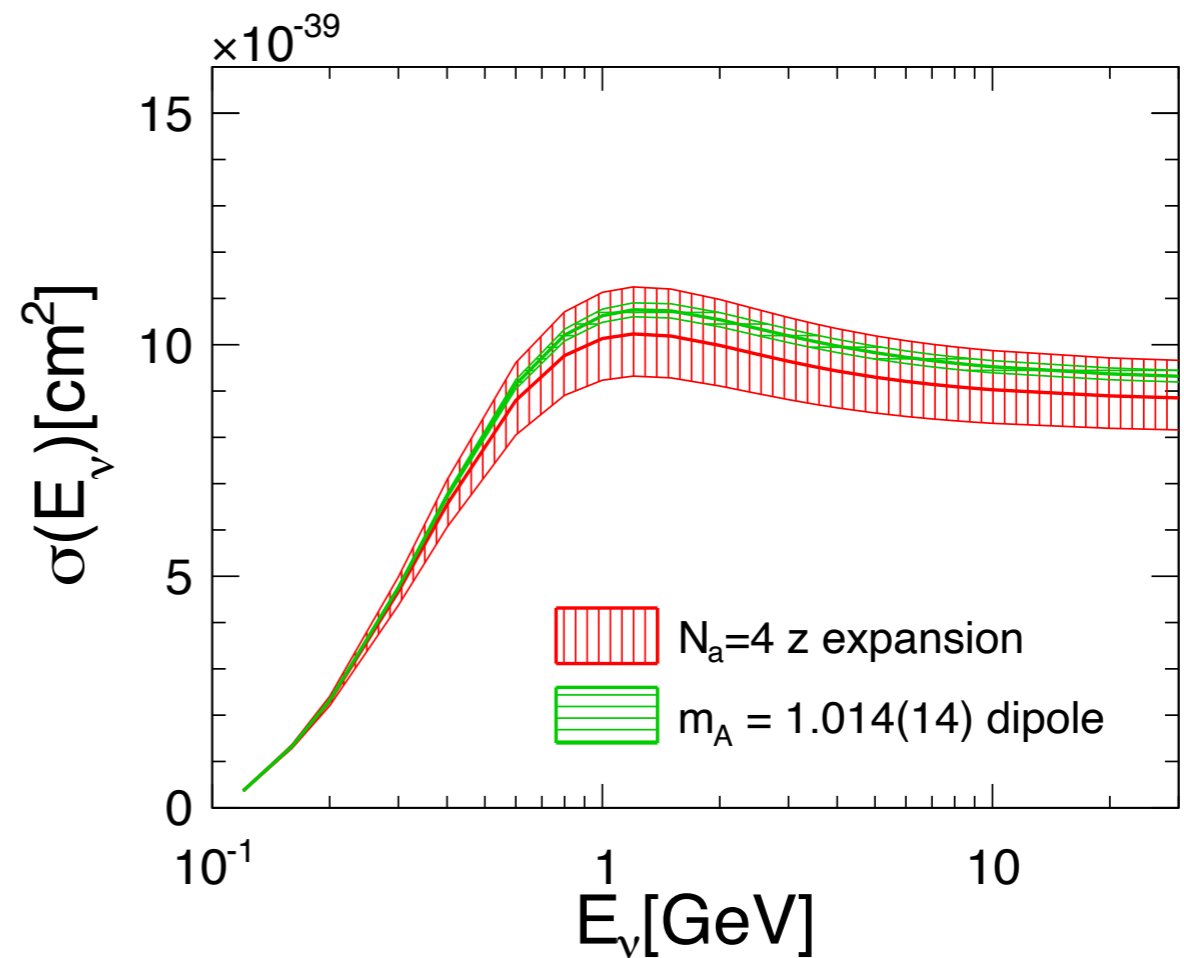
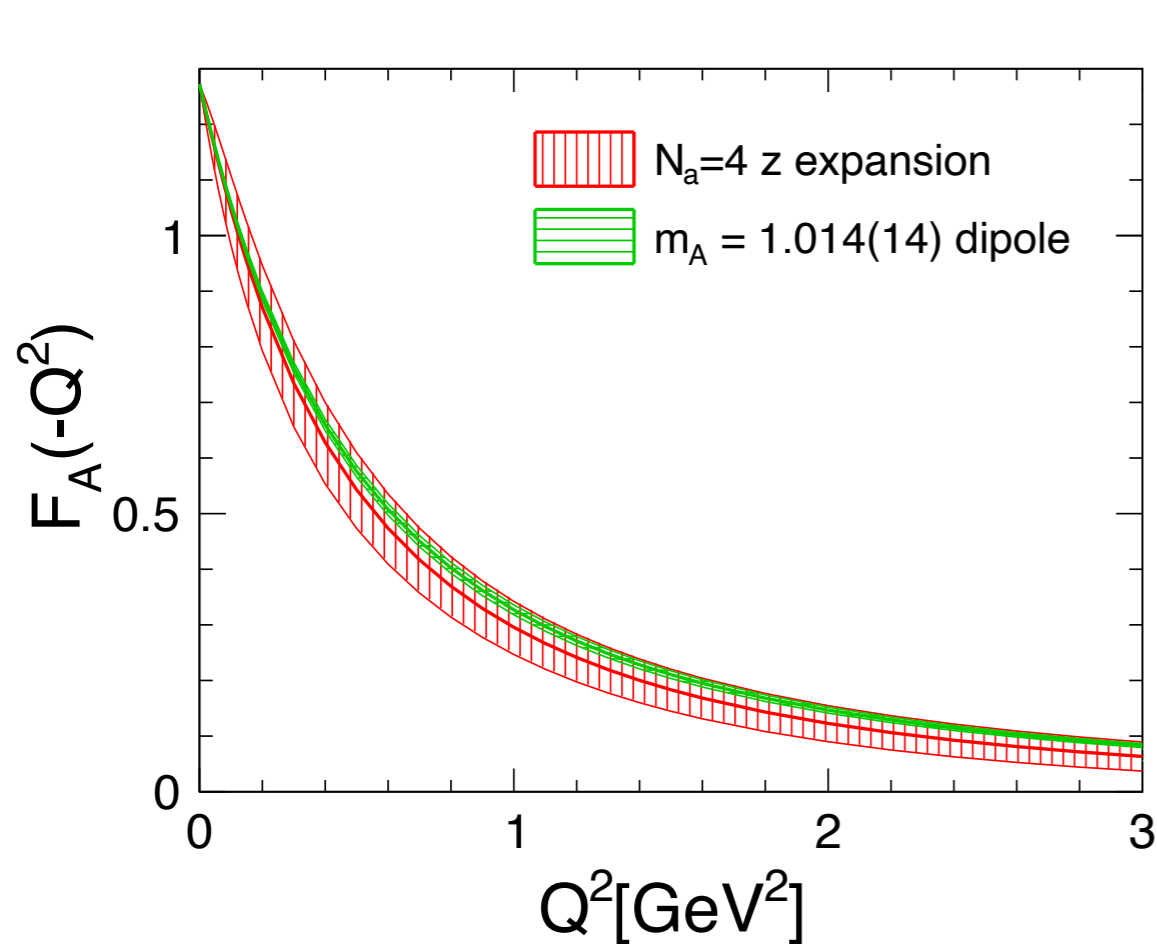
Neutrino-Nucleon scattering

- Sum rule can be enforced ensuring that the form factor falls smoothly to zero at large Q^2

$$z(q^2, t_{\text{cut}}, t_0) = \frac{\sqrt{t_{\text{cut}} - q^2} - \sqrt{t_{\text{cut}} - t_0}}{\sqrt{t_{\text{cut}} - q^2} + \sqrt{t_{\text{cut}} - t_0}},$$

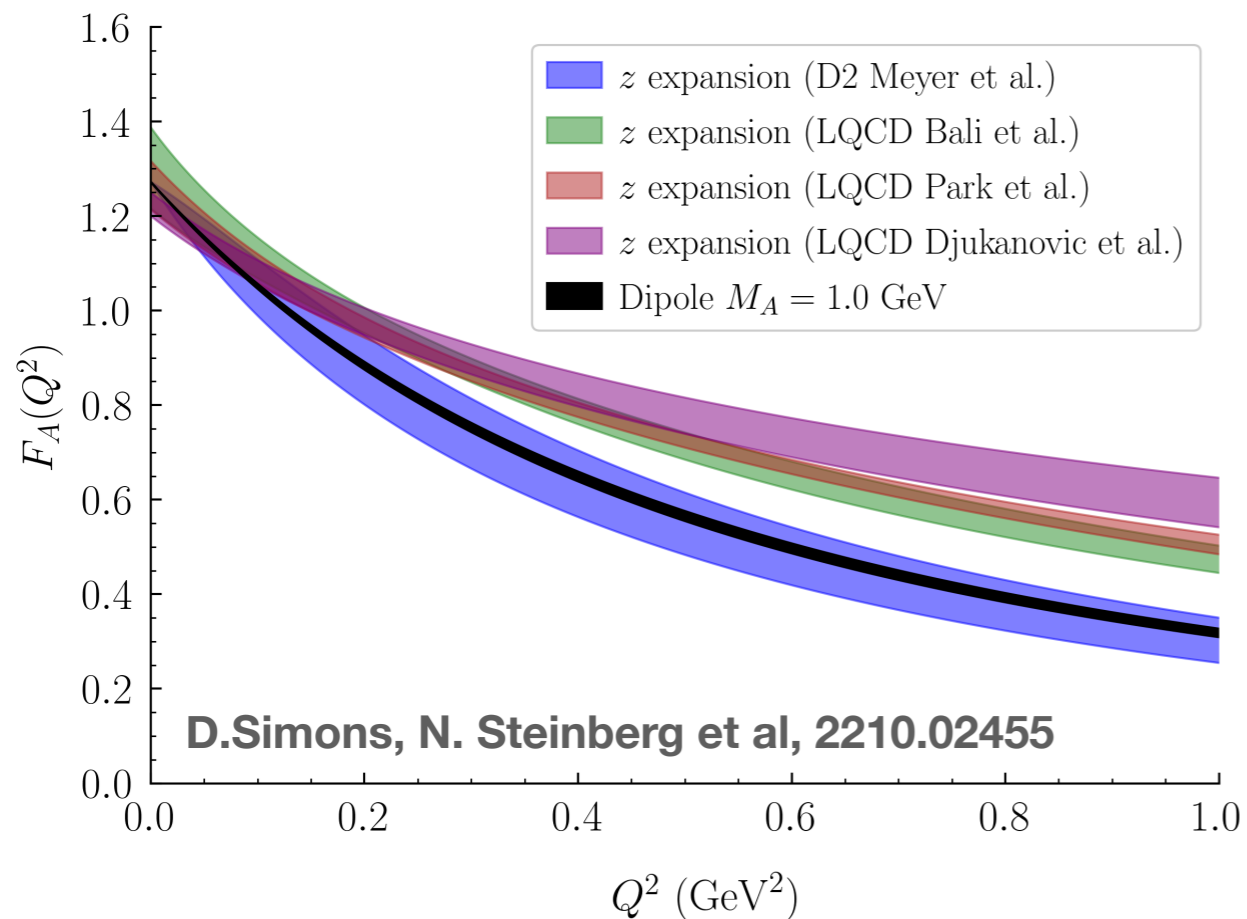
$$\sum_{k=n}^{\infty} k(k-1) \cdots (k-n+1) a_k = 0, \quad n = 0, 1, 2, 3$$

Fit deuteron data replacing dipole axial form factor with z-expansion, enforce the sum rule constraints



A.S.Meyer, Phys.Rev.D 93 (2016) 11, 113015

Axial form factor determination



Comparison with recent MINERvA antineutrino-hydrogen charged-current measurements

1-2 σ agreement with MINERvA data and LQCD prediction by PNDME Collaboration

Novel methods are needed to remove excited-state contributions and discretization errors

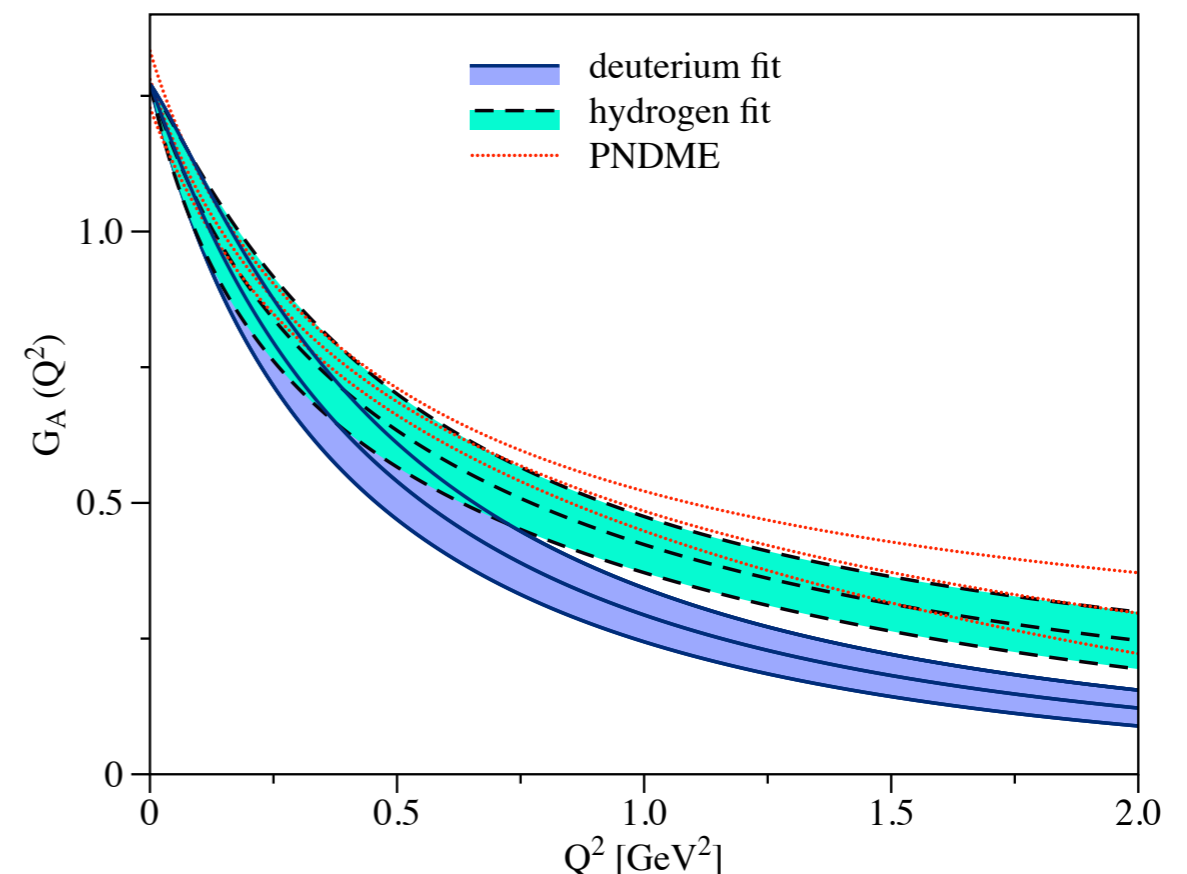
A. Meyer, A. Walker-Loud, C. Wilkinson, 2201.01839

D2 Meyer et al: fits to neutrino-deuteron scattering data

LQCD result: general agreement between the different calculations

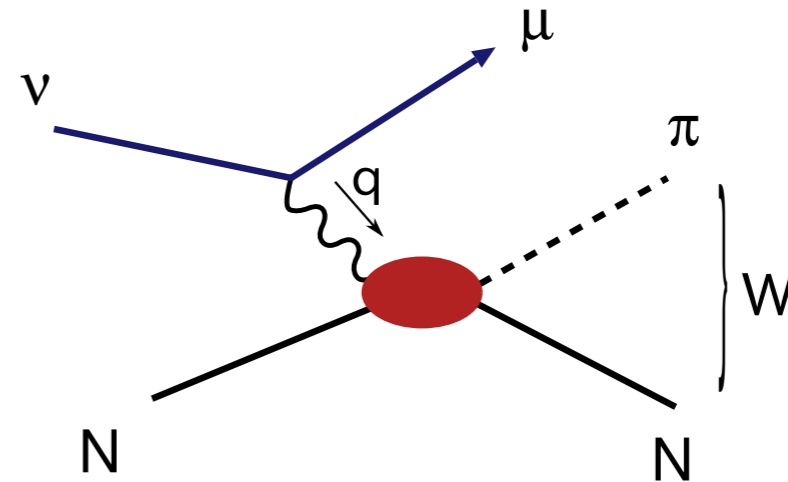
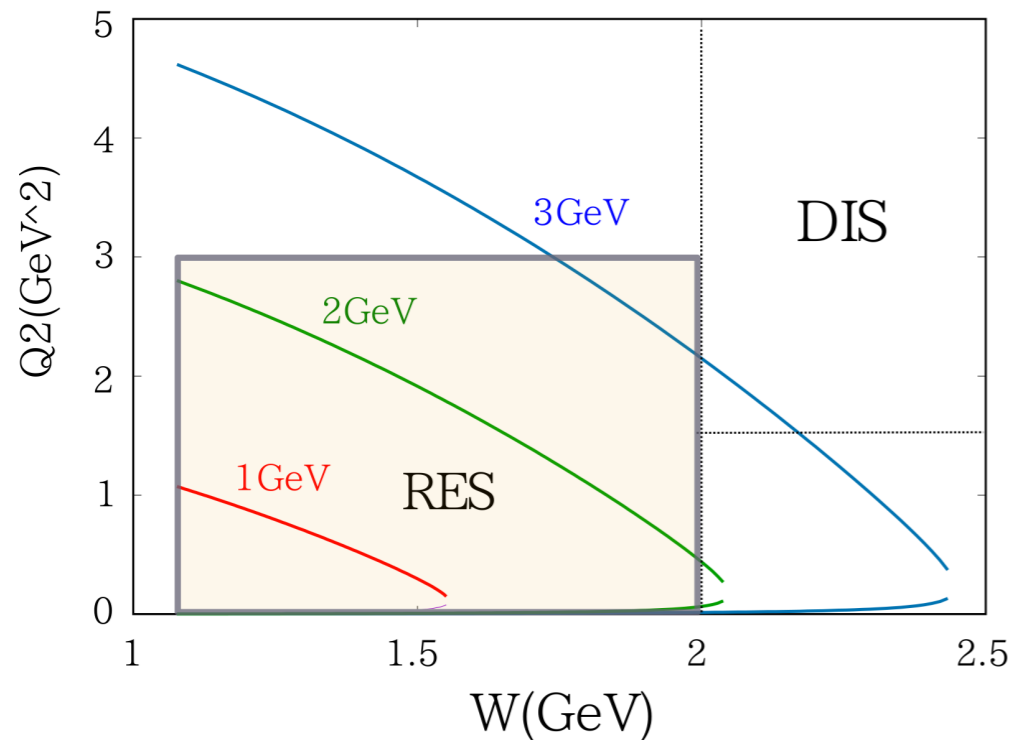
LQCD results are 2-3 σ larger than D2 Meyer ones for $Q^2 > 0.3 \text{ GeV}^2$

O. Tomalak, R. Gupta, T. Battacharaya, 2307.14920



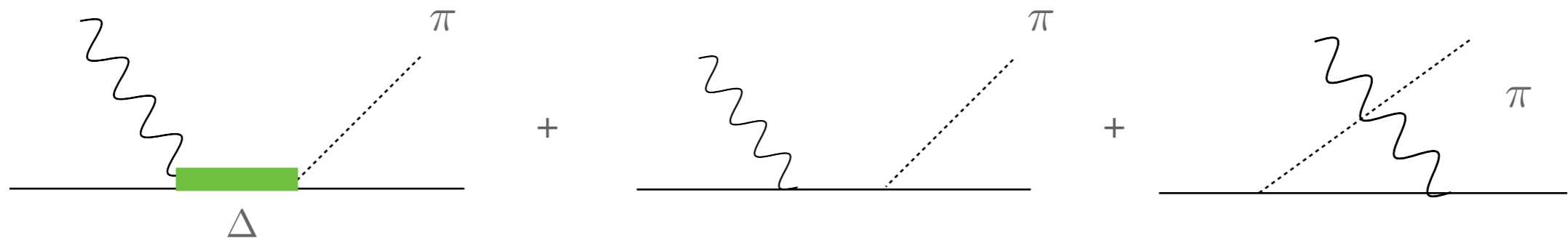
Pion Production

T.Sato talks @ NuSTEC Workshop on Neutrino-Nucleus
Pion Production in the Resonance Region



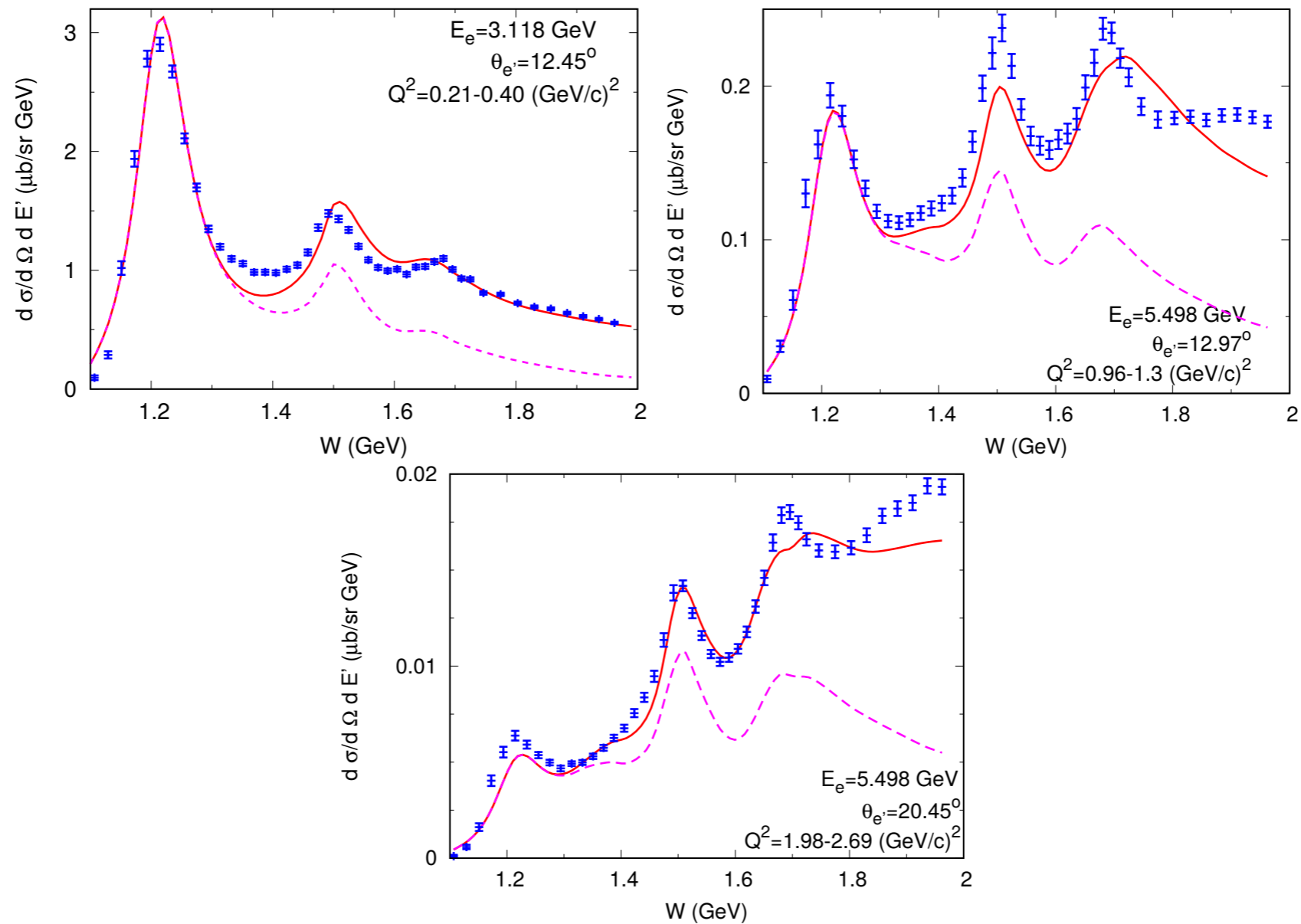
$$W^2 = (p_N(f) + p_\pi)^2 = (p_\nu + p_N(i) - p_\mu)^2$$

$$Q^2 = -q^2 = -(p_\nu - p_\mu)^2$$



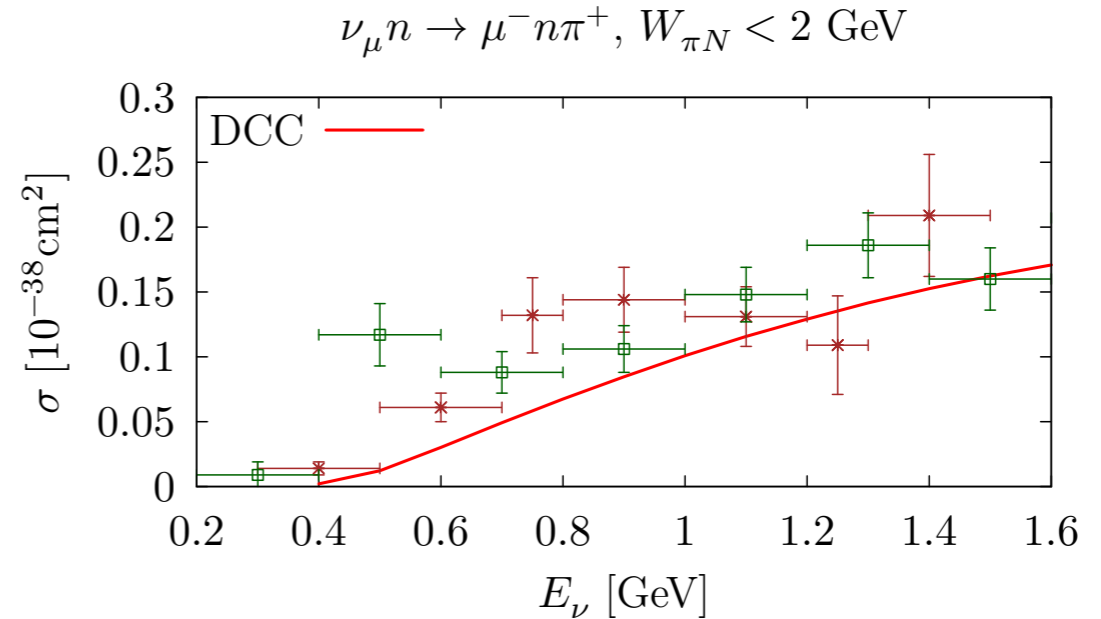
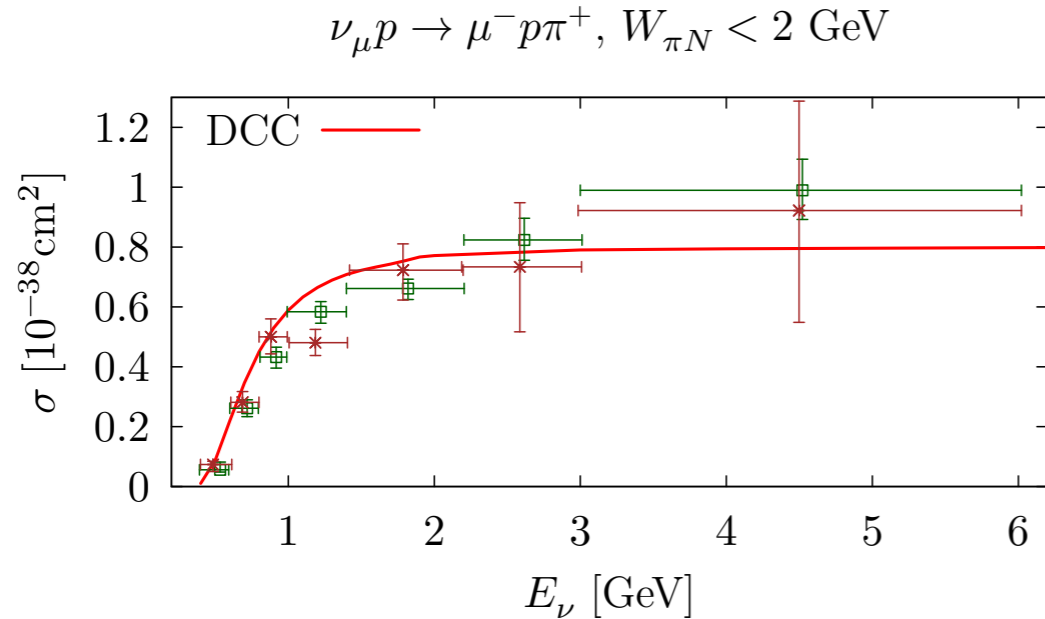
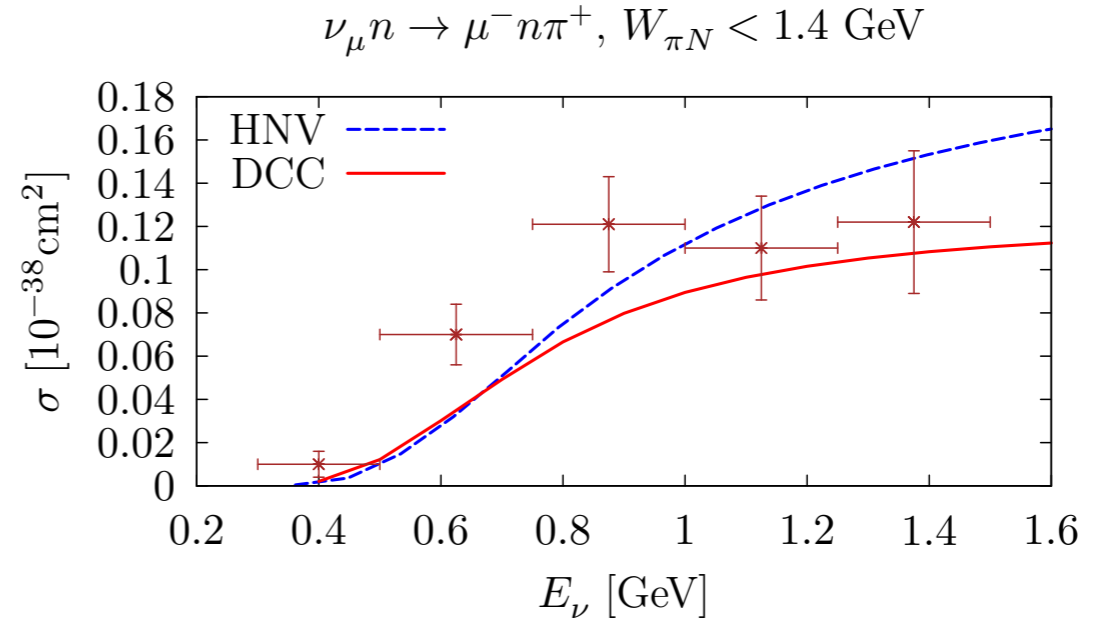
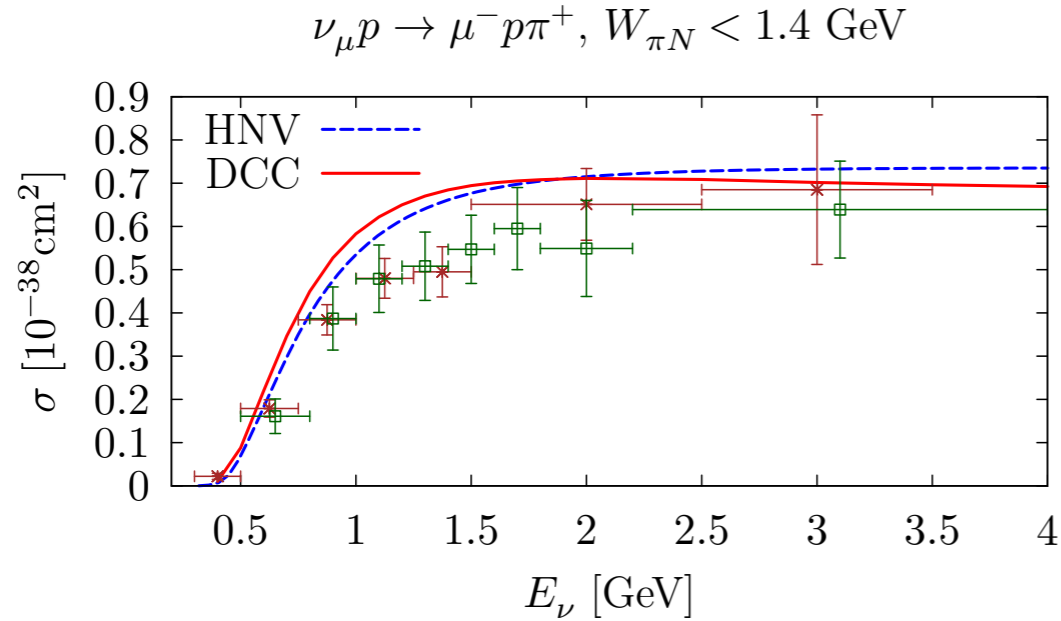
Contribution from both background and Δ -resonance states (but also higher resonances)

Pion Production



ANL-Osaka Partial-Wave Amplitudes (PWA) H.Kamano, T.-S. Lee, S.X. Nakamura, T.Sato, arXiv:1909.11935v1

Pion Production



J. Sobczyk, E. Hernandez, S.X. Nakamura, J. Nieves, T. Sato PRD 98 (2018) 073001

Pion Production

Summary of models for neutrino reaction in RES

	Res	Non-res	Unit.	1pi	2pi	Tot
RS	Delta,N*	-	X	O		O
LPP	Delta,N*	X	X	O		O
HVM	Delta(1232)	chiral	O	O		
	Delta(1232)+N(1440)	chiral	X	O	O	
Giessen	Delta, N*	phen.	X	O		O
ANL-Osaka	Delta, N*	O	O	O	O	O

RS: D. Rein, L. M. Sehgal AP133(81), LPP: O. Lalakulich, E.A. Paschos, G. Piranishvili, PRD74(2006)
HNV: E. Hernandez, J. Nieves, M. Valverde PRD76(2007) Giessen: T. Leitner, O. Buss, L. Alvarez-Ruso, U. Mosel, PRC79(2009)
ANL-Osaka DCC: S.X. Nakamura, H. Kamano, TS, PRD92(2015) , TS, D. Uno, T.-S.H. Lee PRC67(2003)

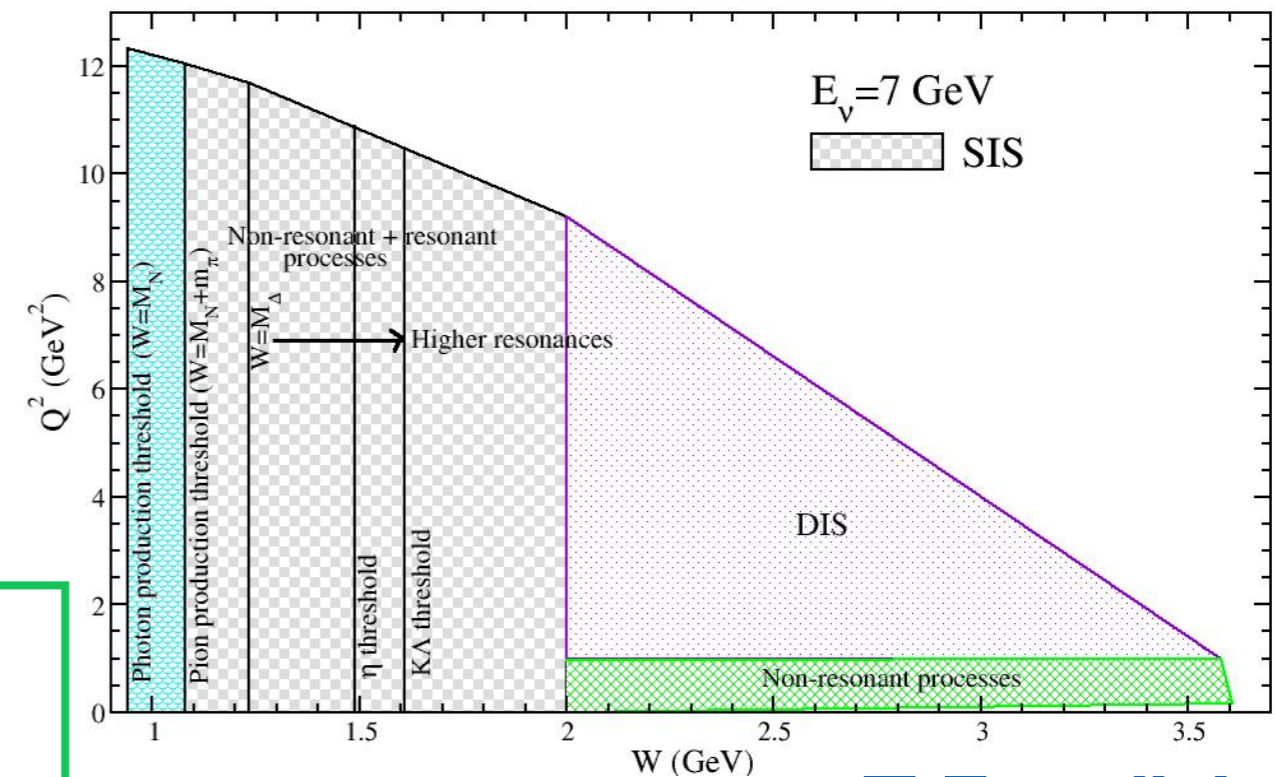
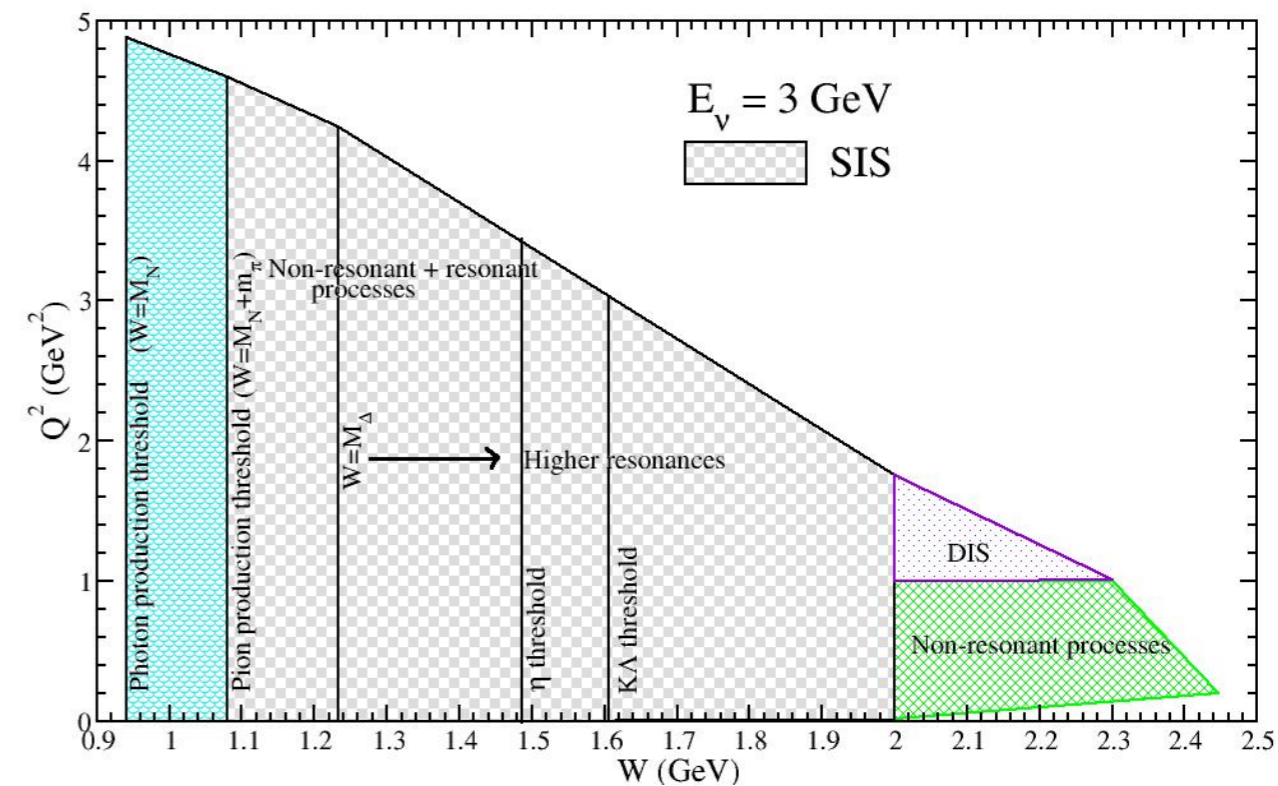
R. Gonzales-Jimenes et al. PRD95,113007(2017)+Regge

Parton Structure of the nucleon

Above the pion production threshold $W \approx 1080$ MeV the excitation of the $\Delta(1232)$ dominates, but at higher W the dynamics results from the interplay of overlapping baryon resonances, non-resonant amplitudes and their interference.

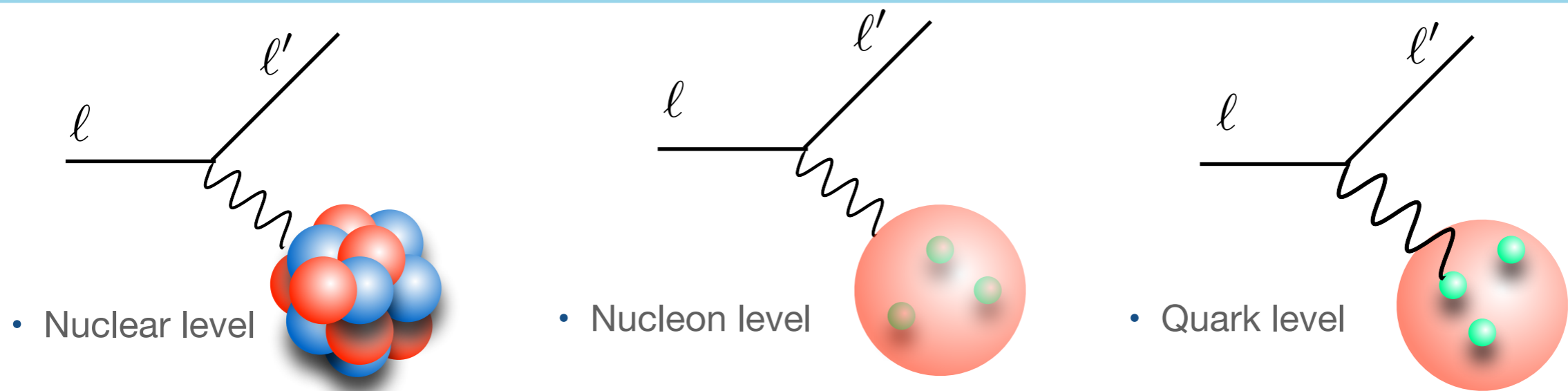
It is this region of W above the $\Delta(1232)$ and at moderate $Q^2 > 1$ GeV² that we refer to as **Shallow Inelastic Scattering (SIS)**. As Q^2 grows, one approaches the onset of Deep Inelastic Scattering (DIS).

Transition from **strong interactions** described in terms of **hadronic degrees of freedom** to those among **quarks and gluons** described by perturbative QCD.



Theoretical tools for neutrino scattering,
Contribution to: 2022 Snowmass Summer Study

Parton Structure of the nucleon



Parton model is analogous to the notion that a nucleus is a collection of noninteracting nucleons—but with a critical difference. Nucleons are rather easily liberated from nuclei, but the **division of a hadron into its constituent partons has never been observed**

$$\frac{d^2\sigma}{dQ^2 d\nu} = \frac{\pi}{EE'} \frac{d^2\sigma}{dE' d\Omega'} = \frac{4\pi\alpha^2}{Q^4} \frac{E'}{E} \left[2W_1(Q^2, \nu) \sin^2 \left(\frac{\theta}{2} \right) + W_2(Q^2, \nu) \cos^2 \left(\frac{\theta}{2} \right) \right].$$



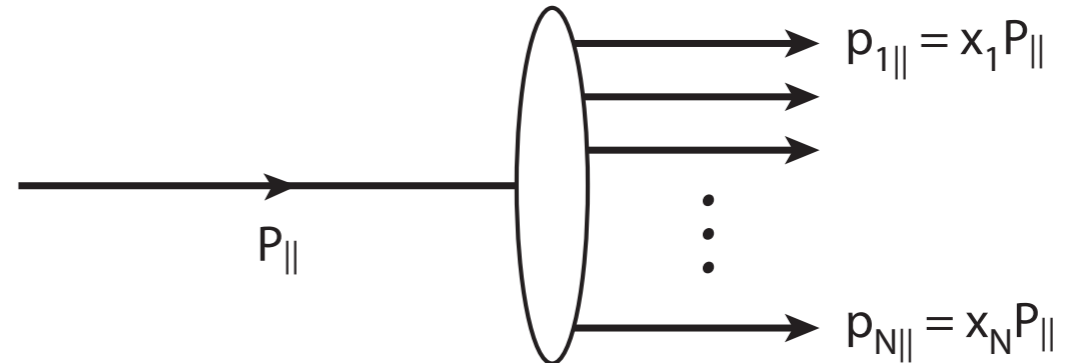
C. Quigg, Gauge Theories of the strong, weak, and electromagnetic interaction

Parton Structure of the nucleon

The transition to the parton model is made in the infinite- momentum frame, in which the longitudinal momentum of the proton is extremely large

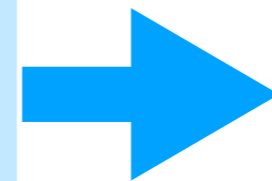
Momentum of individual partons is:

$$p_i^\mu = x_i P^\mu$$



Elastic electron-proton

$$W_1 = \frac{Q^2}{4m_N^2} (F_1 + F_2)^2 \delta\left(\omega - \frac{Q^2}{2m_N}\right)$$
$$W_2 = \left(F_1^2 + F_2^2 \frac{Q^2}{4m_N^2}\right) \delta\left(\omega - \frac{Q^2}{2m_N}\right)$$

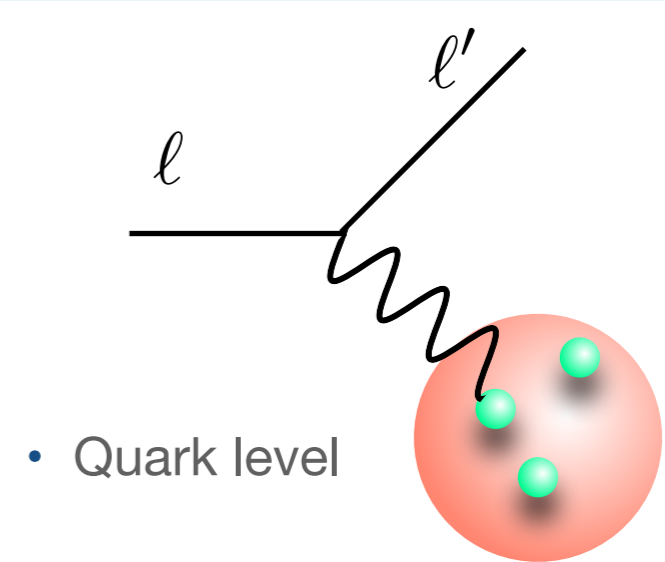
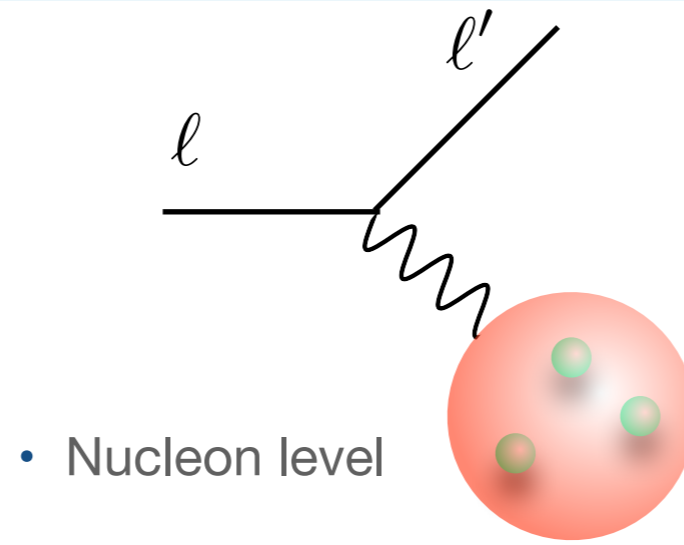
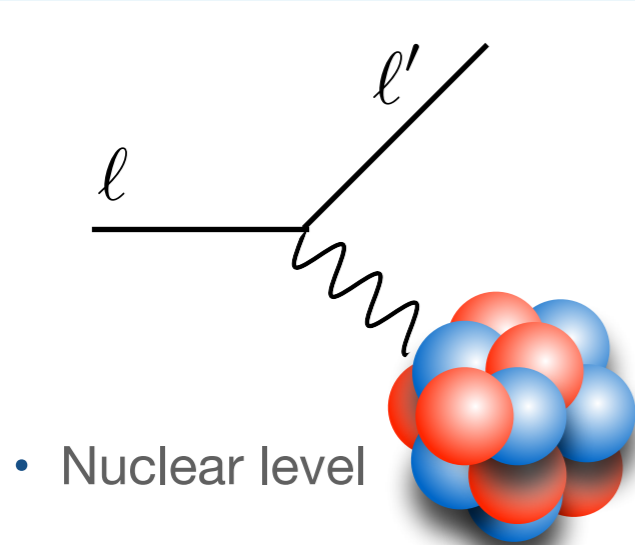


Electron-point-like particle

$$W_1^{\text{point}} = \frac{Q^2}{4m^2} \delta\left(\omega - \frac{Q^2}{2m}\right)$$
$$W_2^{\text{point}} = \delta\left(\omega - \frac{Q^2}{2m}\right)$$

* Let's move to the blackboard

Parton Structure of the nucleon



$$\frac{d^2\sigma}{dQ^2 d\nu} = \frac{\pi}{EE'} \frac{d^2\sigma}{dE' d\Omega'} = \frac{4\pi\alpha^2}{Q^4} \frac{E'}{E} \left[2W_1(Q^2, \nu) \sin^2\left(\frac{\theta}{2}\right) + W_2(Q^2, \nu) \cos^2\left(\frac{\theta}{2}\right) \right].$$



$$\frac{d^2\sigma^\nu}{dQ^2 d\nu} = \frac{G_F^2}{2\pi} E' E \left[2W_1^\nu \sin^2\left(\frac{\theta}{2}\right) + W_2^\nu \cos^2\left(\frac{\theta}{2}\right) + W_3^\nu \frac{(E + E')}{M} \sin^2\left(\frac{\theta}{2}\right) \right]$$

$\nu + N$ has the contribution of an additional structure function

$$\mathcal{F}_3(x) \equiv \nu W_3^\nu(x)$$

Quark-Hadron Duality

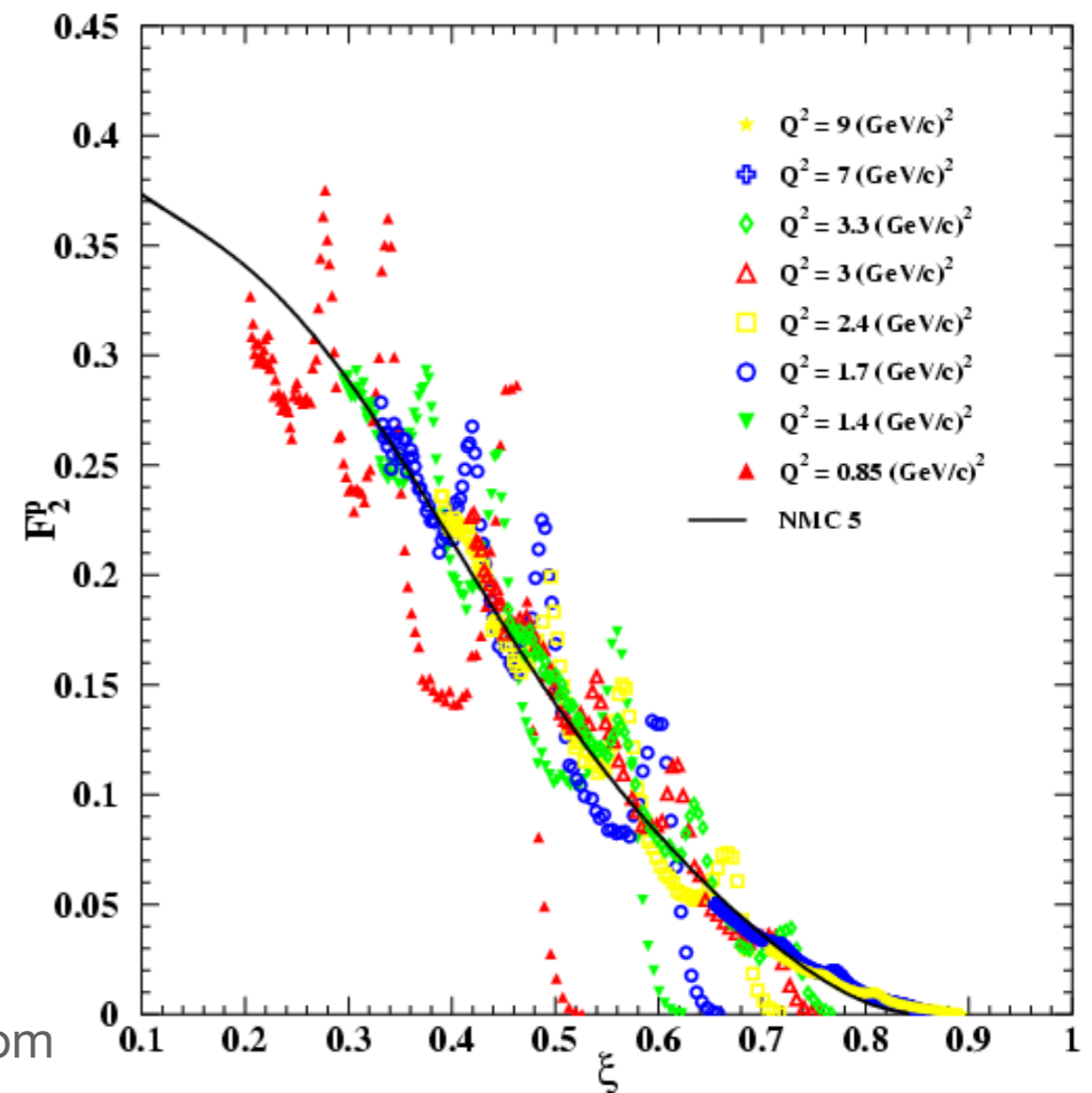
Duality can then be considered as a conceptual experimental bridge between **free** and **confined partons**.

Language of quarks/gluons in the DIS region and, as W decreases, one transitions to hadrons; in the SIS region that includes both resonant and non-resonant pion production.

- 1970 Bloom-Gilman duality in (e,e') experiments on p

DIS scaling curve extrapolated down into the resonance region passes through the average of the "peaks and valleys" of the resonant structure.

Comparison of F_2^p from the **series of resonances** measured by E94-110 vs the **Nachtmann variable ξ** compared to the **extrapolated DIS measurement** from the NMC collaboration at 5 GeV^2



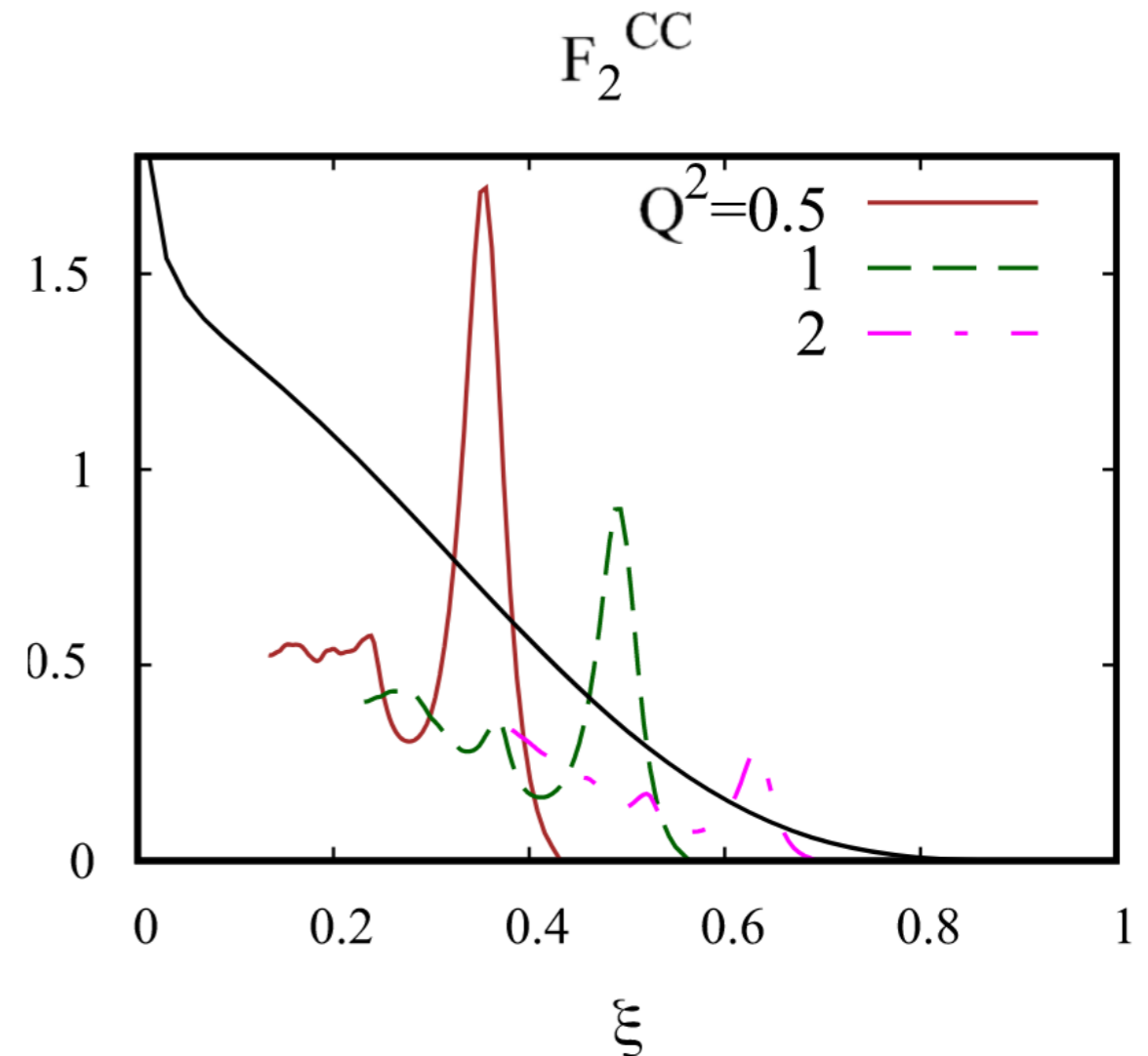
For $Q^2 > 0.5 \text{ GeV}^2$ resonances follow the extrapolated DIS curve showing quark-hadron duality

Quark-Hadron Duality in ν

The experimental study of duality with neutrinos is very restricted since the measurement of resonance production by ν -N interactions is confined to **low-statistics data obtained in hydrogen and deuterium bubble chamber experiments from the 70's and 80's**.

For CC ν scattering

ANL-Osaka DCC model
underestimates F_2 from DIS



[T. Sato EPJ:ST (2021) 230:4409-4418 (2022)]

see also:

[O. Lalakulich et al. PRC79 015206 (2009)]

Quark-Hadron Duality in ν

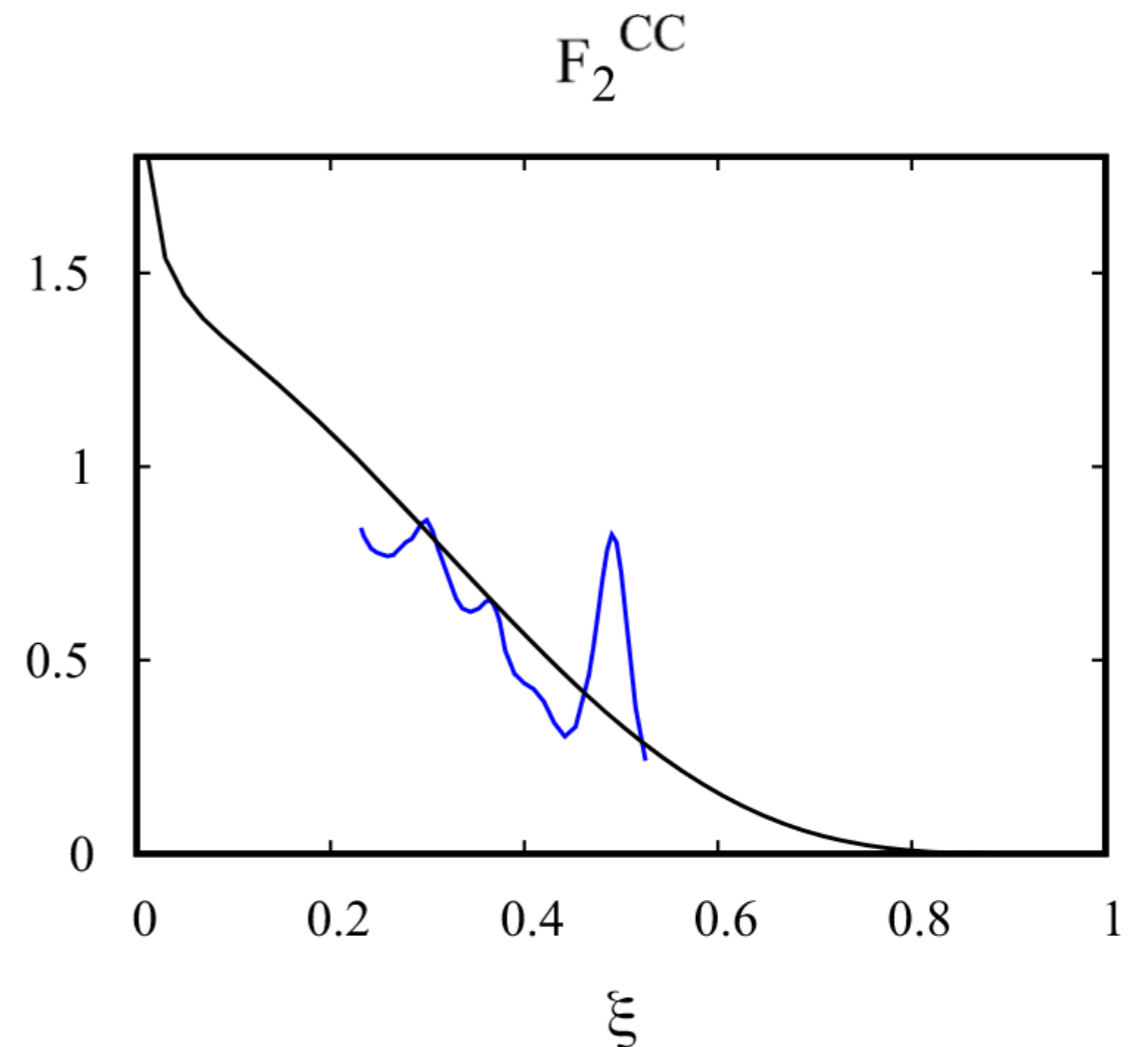
The experimental study of duality with neutrinos is very restricted since the measurement of resonance production by ν -N interactions is confined to **low-statistics data obtained in hydrogen and deuterium bubble chamber experiments from the 70's and 80's**.

For CC ν scattering

ANL-Osaka DCC model
underestimates F_2 from DIS

Improvement with DIS upon
modifying the Q^2 - dependence of the
axial form factor:

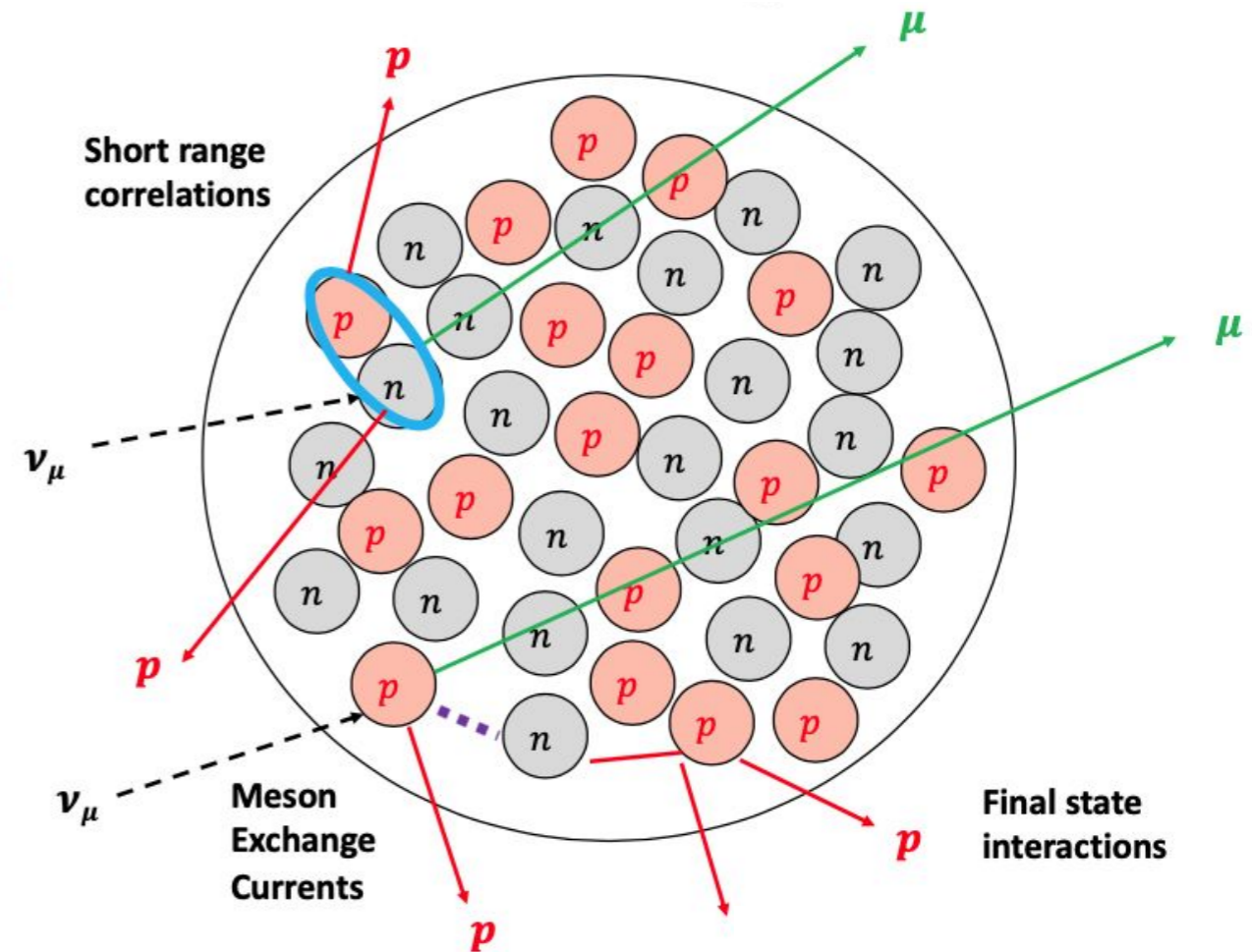
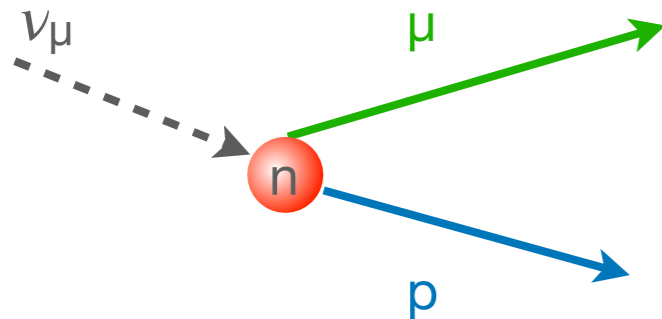
$$A_{\lambda}^A(Q^2) = A_{\lambda}^A(0) \frac{A_{\lambda}^V(Q^2)}{A_{\lambda}^V(0)}$$



- More data are needed to better constrain/understand ν -N scattering

From theory to experiment

Free nucleon scattering case



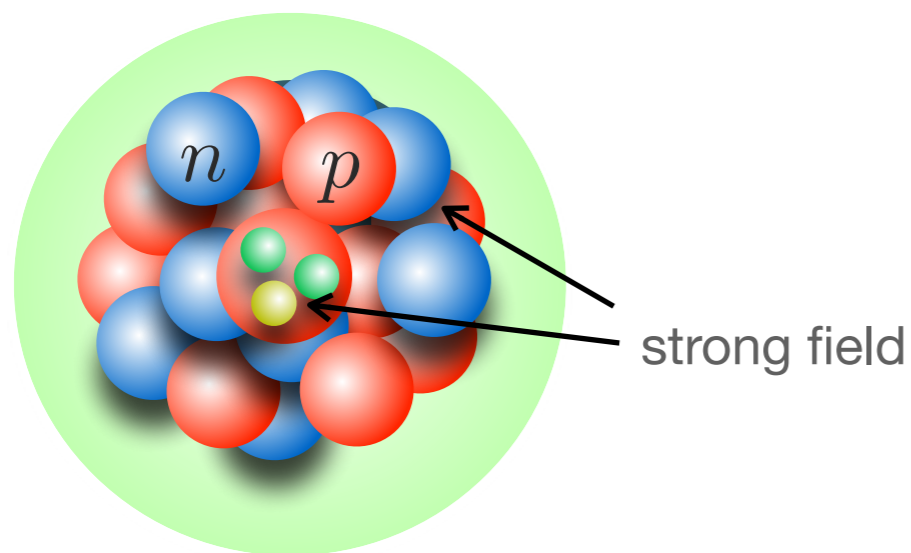
Nuclear model describing the target nucleus

Different reaction mechanisms depending on the momentum transferred to the the nucleus

Final state interactions: describe how the particles propagate through the nuclear medium

The Nucleus internal structure

Nuclei are **strongly interacting** many body systems exhibiting fascinating properties



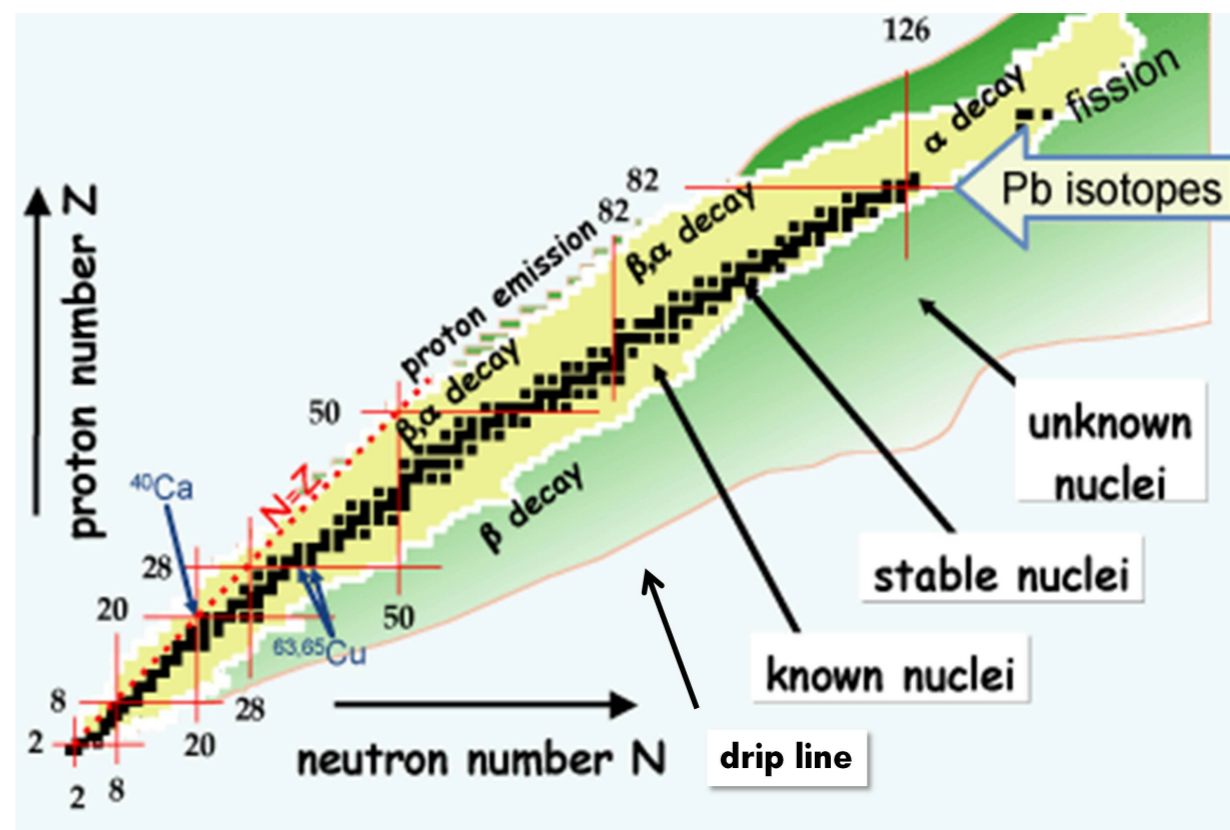
The nucleus is formed by **protons** and **neutrons**: nucleons.

Each nucleon is made of three **quarks** held together by strong interactions → mediated by **gluons**

The nucleus is held together by the strong interactions between quark and gluons of neighboring nucleons

Nuclear Physicists **effectively** describe the interactions between protons and neutrons in terms of **exchange of pions**

Nuclear chart. **Magic numbers** N or $Z = 2, 8, 20, 28, 50$ and 126 ; major shell complete and are more stable than other elements



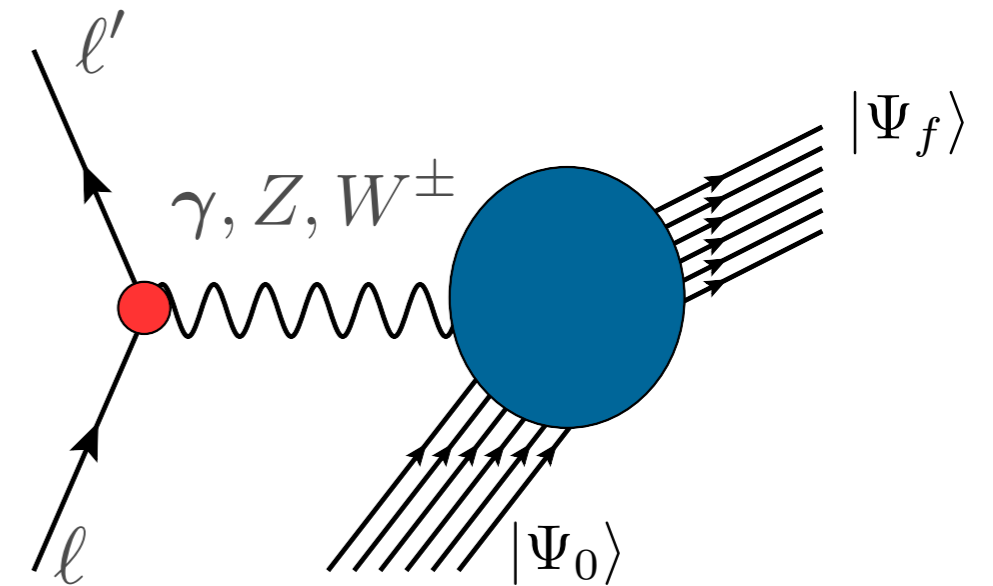
Theory of lepton-nucleus scattering

- The cross section of the process in which a lepton scatters off a nucleus is given by

$$d\sigma \propto L^{\alpha\beta} R_{\alpha\beta}$$

Leptonic Tensor: is the same as before, completely determined by lepton kinematics

Hadronic Tensor: nuclear response function



$$R_{\alpha\beta}(\omega, \mathbf{q}) = \sum_f \langle 0 | J_\alpha^\dagger(\mathbf{q}) | f \rangle \langle f | J_\beta(\mathbf{q}) | 0 \rangle \delta(\omega - E_f + E_0)$$

The initial and final wave functions describe many-body states:

$$|0\rangle = |\Psi_0^A\rangle, |f\rangle = |\Psi_f^A\rangle, |\psi_p^N, \Psi_f^{A-1}\rangle, |\psi_k^\pi, \psi_p^N, \Psi_f^{A-1}\rangle \dots$$

For inclusive reactions, the hadronic final state is not detected. We need to sum over all the possible ones

Comparing electron- and neutrino-nucleus

- We start by defining the nuclear response functions, for a given value of \mathbf{q} and ω

$$W^{\mu\nu}(\mathbf{q}, \omega) = \sum_f \langle 0 | (J^\mu)^\dagger(\mathbf{q}, \omega) | f \rangle \langle f | J^\nu(\mathbf{q}, \omega) | 0 \rangle \delta^{(4)}(p_0 + \omega - p_f)$$

- Electron case we write the **inclusive** double differential cross section as:

$$\frac{d\sigma}{dE' d\Omega} = \sigma_{\text{Mott}} \left[\left(\frac{q^2}{\mathbf{q}^2} \right)^2 R_L + \left(\frac{-q^2}{2\mathbf{q}^2} + \tan^2 \frac{\theta}{2} \right) R_T \right]$$

where: $R_L = W_{00}$, $R_T = W_{xx} + W_{yy}$

- Neutrino case:

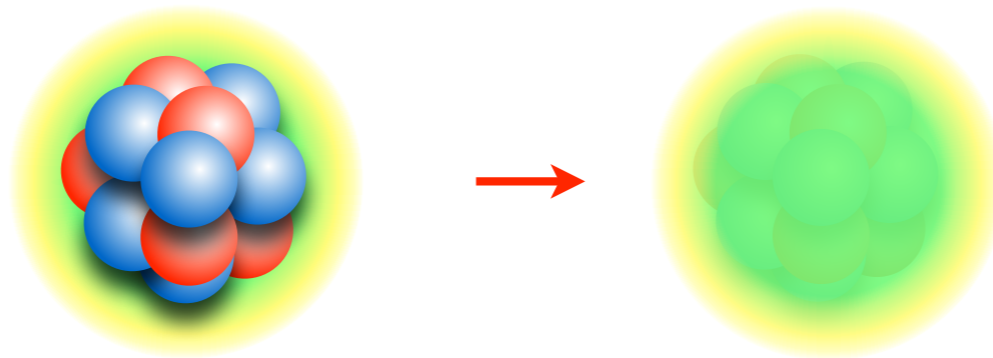
$$\left(\frac{d\sigma}{dE' d\Omega} \right)_{\nu/\bar{\nu}} = \frac{G^2}{4\pi^2} \frac{k'}{2E_\nu} \left[\hat{L}_{CC} R_{CC} + 2\hat{L}_{CL} R_{CL} + \hat{L}_{LL} R_{LL} + \hat{L}_T R_T \pm 2\hat{L}_{T'} R_{T'} \right] ,$$

- Where the nuclear responses are given by

$$\begin{aligned} R_{CC} &= W^{00} & R_{LL} &= W^{33} & R_{T'} &= -\frac{i}{2}(W^{12} - W^{21}) \\ R_{CL} &= -\frac{1}{2}(W^{03} + W^{30}) & R_T &= W^{11} + W^{22} \end{aligned}$$

Liquid Drop Model

- The nucleus is treated as a drop of incompressible nuclear fluid. The fluid is made of nucleons which are held together by the strong nuclear forces.



- This model explains the spherical shape and the binding energy of nuclei.
- The nuclear binding is given by the Weizsäcker formula

$$B(A, Z) = a_V A + a_S A^{2/3} + a_C \frac{Z^2}{A^{1/3}} + S_N \frac{(N - Z)^2}{A} + a_P \frac{(-1)^Z + (-1)^N}{2A^{1/2}}$$



Volume



Surface



Coulomb



Symmetry



Pairing

Liquid Drop Model

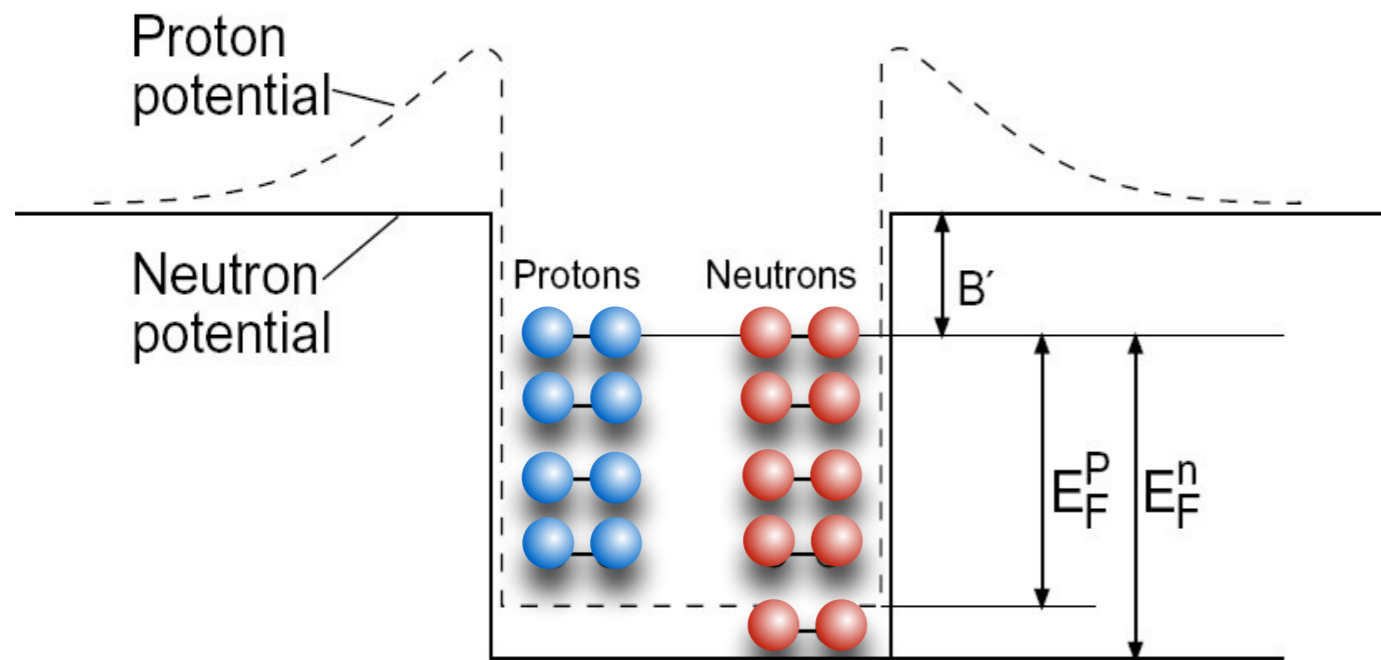
- The nuclear binding is given by the Weizsäcker formula

$$B(A, Z) = a_V A + a_S A^{2/3} + a_C \frac{Z^2}{A^{1/3}} + S_N \frac{(N - Z)^2}{A} + a_P \frac{(-1)^Z + (-1)^N}{2A^{1/2}}$$



- **Volume Term:** This term represents the attractive nuclear force that acts over the entire volume of the nucleus
- **Surface Term:** This term accounts for the fact that nucleons at the surface of the nucleus have fewer neighboring nucleons than those in the interior
- **Coulomb Term:** This term represents the electrostatic repulsion between protons in the nucleus due to their positive charges.
- **Asymmetry Term:** It reflects the preference for equal numbers of protons and neutrons, which contribute to greater nuclear stability. Deviations from this balance result in less binding energy.
- **Pairing Term:** This term considers the additional binding energy due to the pairing of nucleons (protons with protons and neutrons with neutrons) in even numbers.

Initial state: global Fermi gas



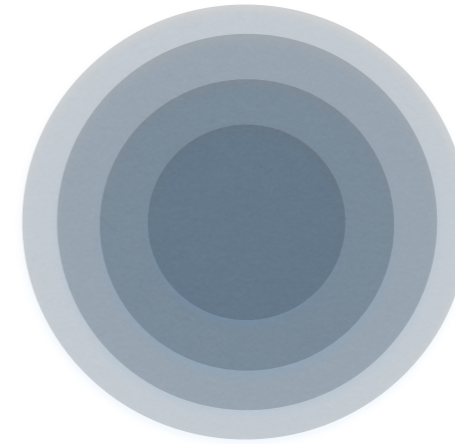
- Simple picture of the nucleus: only statistical correlations are retained (Pauli exclusion principle)
- Protons and neutrons are considered as moving freely within the nuclear volume

- The nuclear potential wells are rectangular: constant inside the nucleus and goes sharply to zero at its edge
- The energy of the highest occupied state is the Fermi energy: E_F
- The difference B' between the top of the well and the Fermi level is constant for most nuclei and is just the average binding energy per nucleon $B'/A \sim 7-8$ MeV

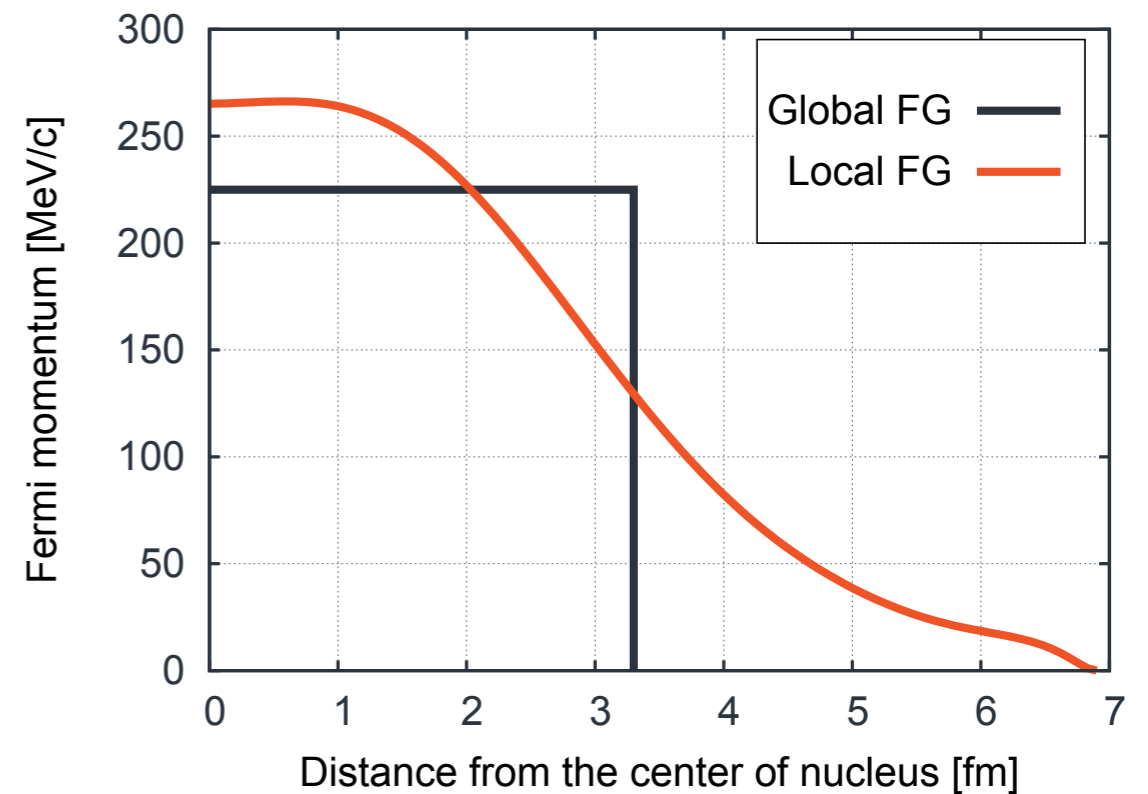
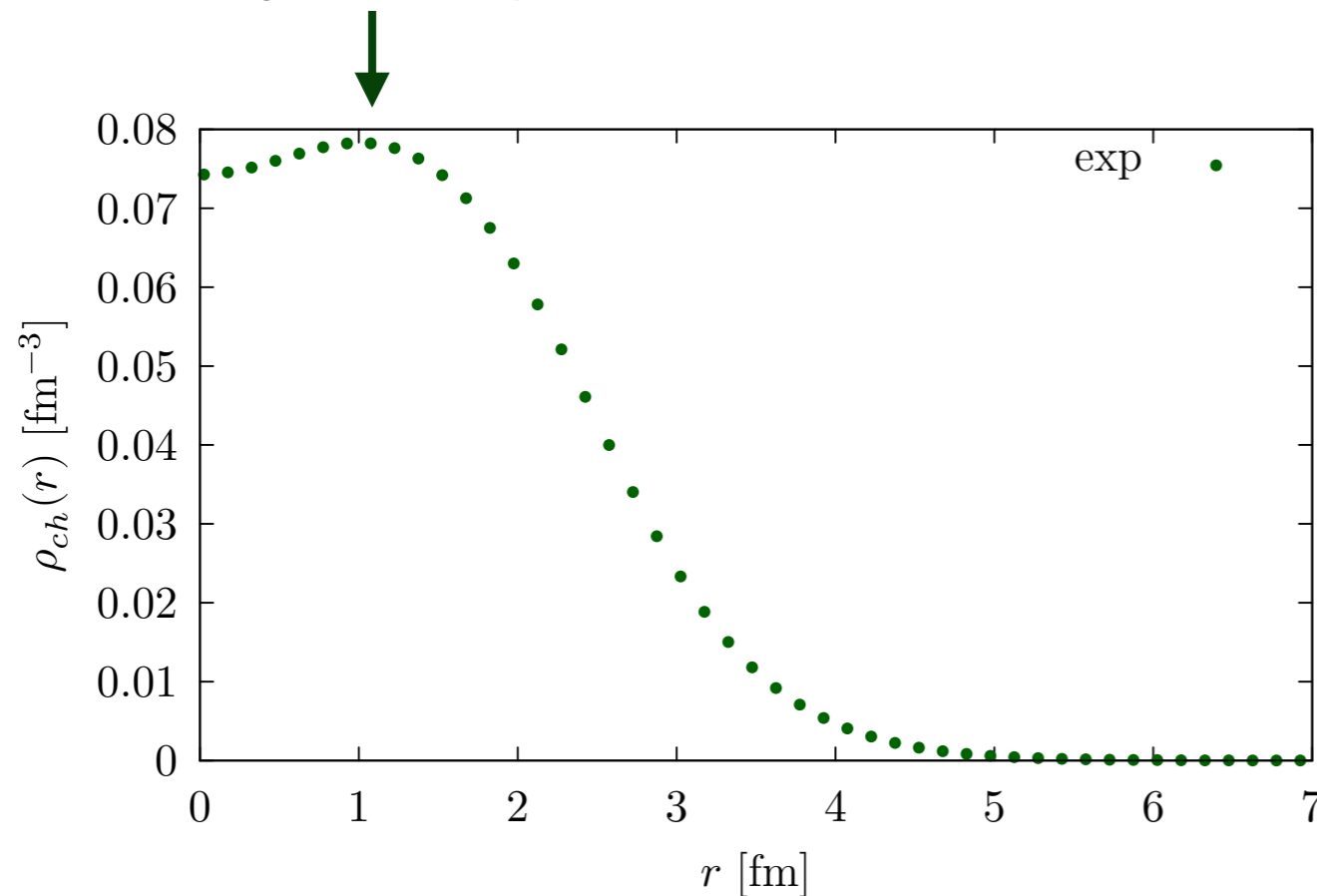
C. Bertulani, Nuclear Physics in a Nutshell

Initial state: Local Fermi gas

- A spherically symmetric nucleus can be approximated by concentric spheres of a constant density.



More likely to find a particle $r \sim r_{ch} \sim 2.5$ fm



• Global Fermi Gas

$$p_F = \left(\frac{9\pi \cdot n}{4A} \right)^{1/3} \cdot \frac{\hbar}{R_0}$$

Figure by T. Golan

• Local Fermi Gas

$$p_F = \hbar \left(3\pi^2 \rho(r) \frac{n}{A} \right)^{1/3}$$

Initial state: shell Model

- As in the Fermi Gas model: the nucleons move within the nucleus independently of each other
- Difference: the nucleons are not free: subject to a central potential



- Each nucleon moves in an average potential created by the other nucleons, the potential should be chosen to best reproduce the experimental results

$$H = \sum_i \frac{p_i^2}{2m} + \sum_{i < j} v_{ij} + \dots \quad \longrightarrow \quad H = \sum_i \frac{p_i^2}{2m} + \sum_i^A U_i + H_{\text{res}}$$

- We solve the Schrödinger Equation:

$$H \psi = E \psi \quad \left\{ \begin{array}{l} E = E_1 + E_2 + \dots + E_A \\ \psi(1, \dots, A) = \mathcal{A}[\phi_1(1) \dots \phi_A(A)] \end{array} \right.$$

Initial state: shell Model

- Example: Particles are subject to an harmonic oscillator potential

$$U(r) = \frac{1}{2}m\omega^2 r^2$$

The frequency should be adapted to the mass number A

- We will seek solutions of the type $\psi(r) = \frac{u(r)}{r} Y_l^m(\theta, \phi)$ ← Spherical Harmonics
- Solving the Schrödinger Equation reduces to a solution of u:

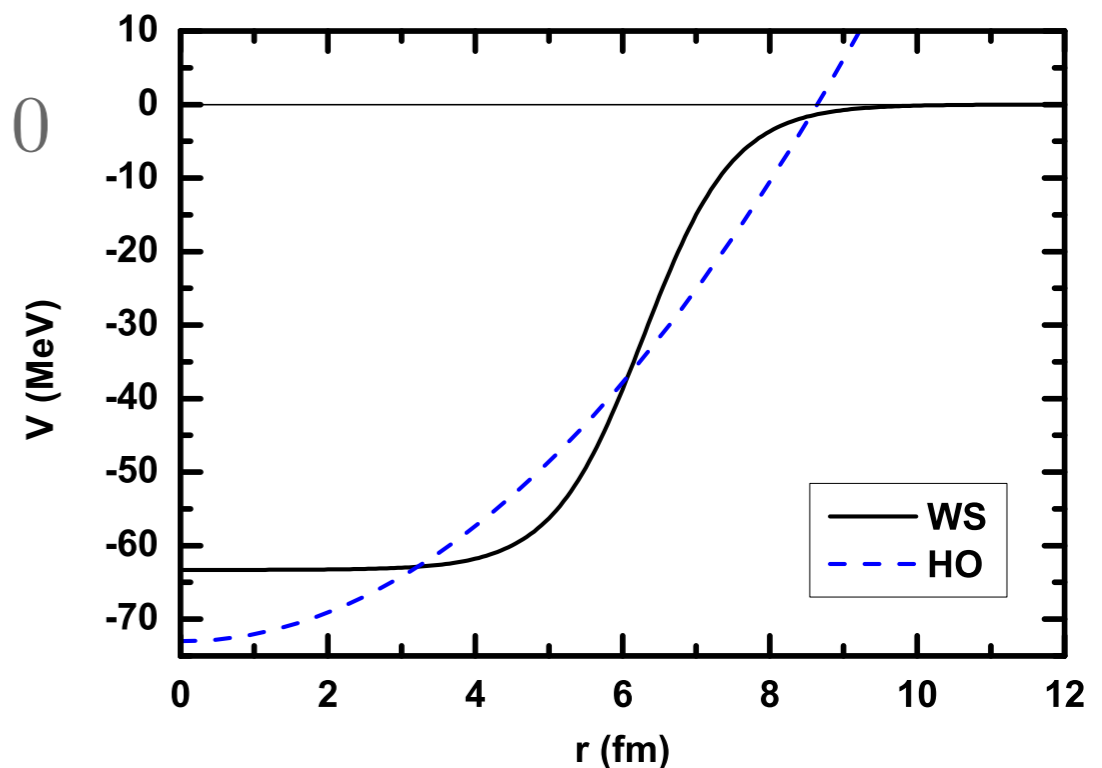
$$\frac{d^2 u}{dr^2} + \left\{ \frac{2m}{\hbar^2} [E - U(r)] - \frac{l(l+1)}{r^2} \right\} u(r) = 0$$

$$E_{nl} = \hbar\omega \left(2n + l + \frac{1}{2} \right) \text{ Eigenvalues}$$

- A more realistic potential is the Wood Saxon:

$$V = V_0 / [1 + \exp[(r - R)/a]]$$

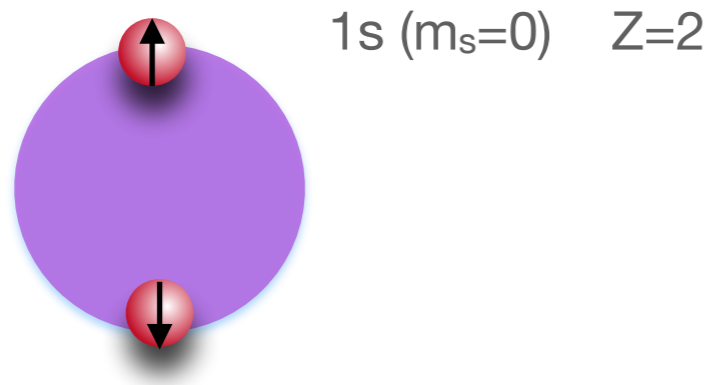
V_0 , r , a , are adjustable parameters chosen to best reproduce the **experimental results**



Physical Review C 87(1):014334

Nuclear Shell Model

The lowest level, s shell, can contain 2 protons



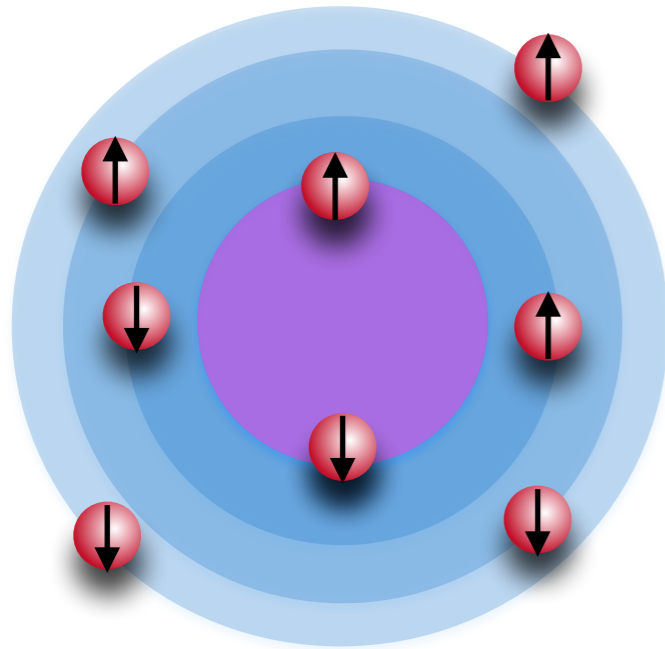
Our assumption: central potential

$$H = \sum_i \frac{p_i^2}{2m} + \sum_i V(r_i)$$

n is the principal quantum number, **l** orbital momentum, **m** magnetic quantum number

Nuclear Shell Model

The p shell can contain up to 6 protons



1s ($m_s=0$)
1p ($m_p=-1,0,1$)
Z=8

Our assumption: central potential

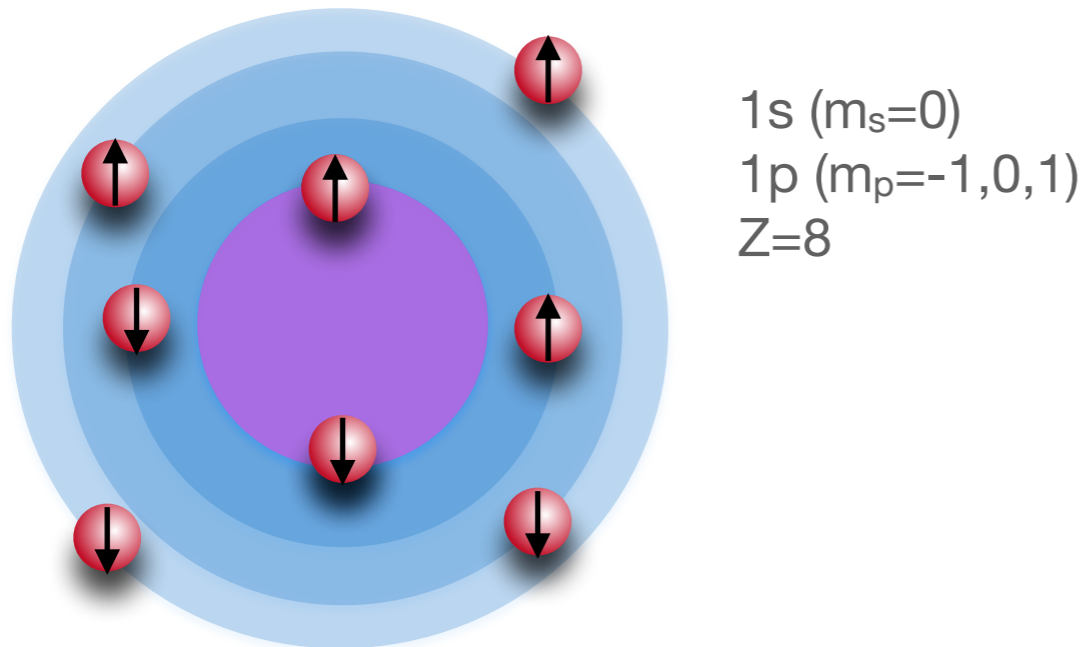
$$H = \sum_i \frac{p_i^2}{2m} + \sum_i V(r_i)$$

We explained the first two magic numbers: 2 and 8.
We can follow the same strategy for the Z=20 case;
but at the next step we obtain Z=40 **while**
experimentally Z=50

n is the principal quantum number, **l** orbital
momentum, **m** magnetic quantum number

Nuclear Shell Model

The p shell can contain up to 6 protons



Our assumption: central potential

$$H = \sum_i \frac{p_i^2}{2m} + \sum_i V(r_i)$$

We explained the first two magic numbers: 2 and 8. We can follow the same strategy for the Z=20 case; but at the next step we obtain Z=40 **while experimentally Z=50**

In 1963, Goeppert Mayer, Jensen, and Wigner shared the Nobel Prize for Physics "for their discoveries concerning nuclear shell structure."

The solution to the puzzle lies in the **spin-orbit coupling**. This effect in the nuclear potential is 20 times larger than in Atomic Physics

$$V(r) \rightarrow V(r) + W(r)\mathbf{L} \cdot \mathbf{S}$$

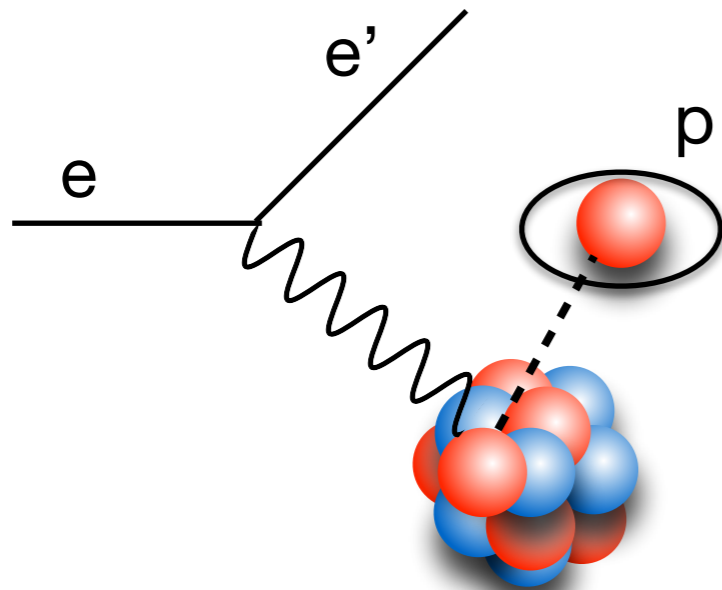
The spin-orbit introduces an energy split which modifies the shell structure and reproduces magic number up to Z=126



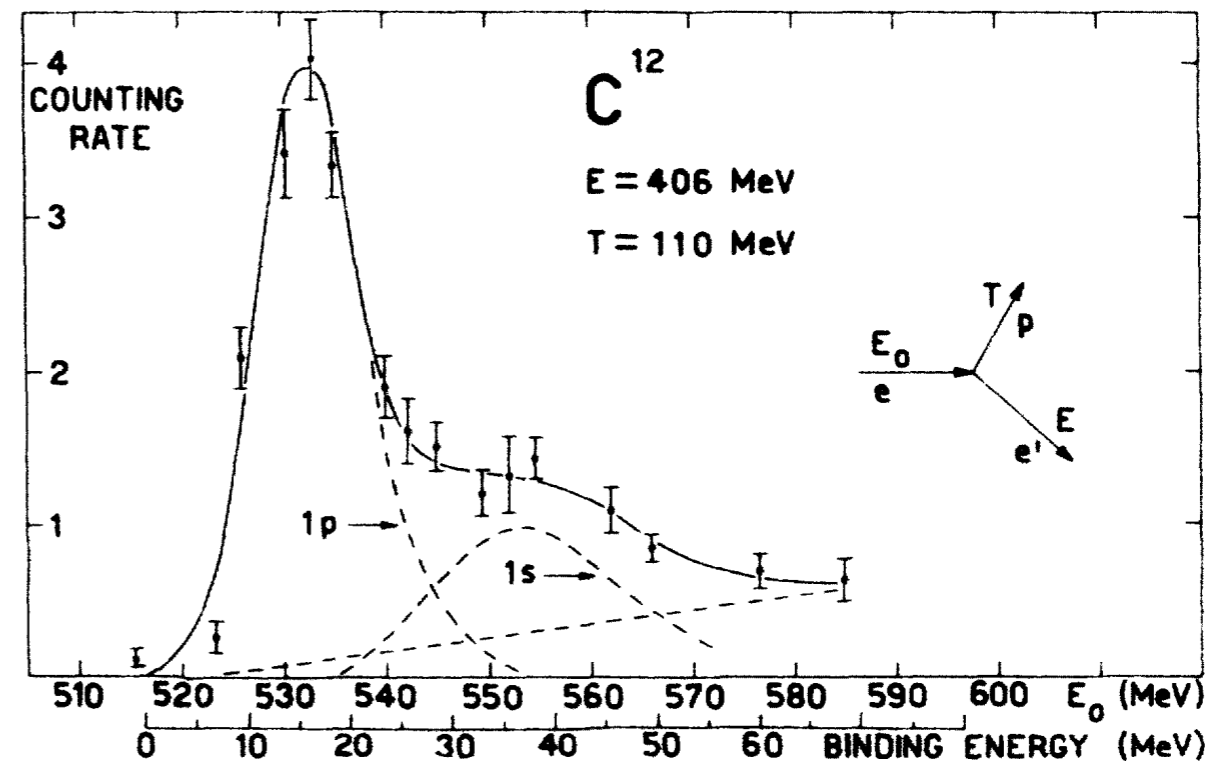
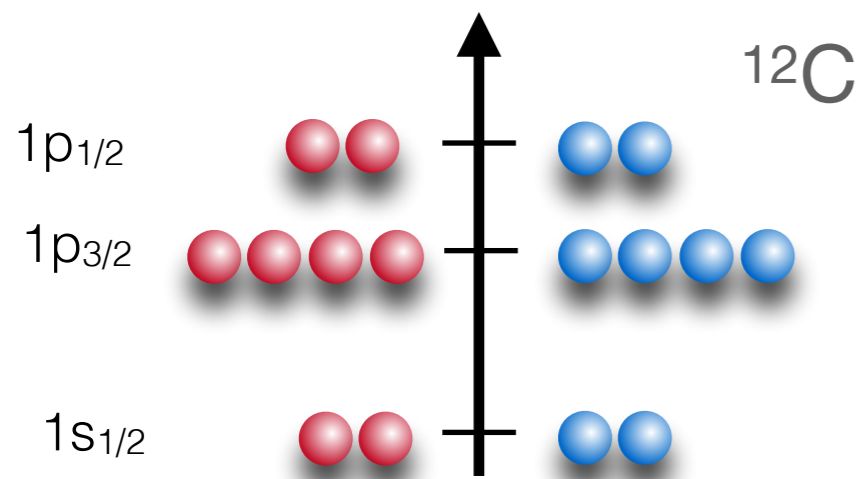
✎ Maria Goeppert Mayer poses with her colleagues in front of Argonne's Physics building.

(e,e'p) scattering experiments

- (e,e'p) experiments are extremely important to investigate the internal structure of the nucleus



- Assuming NO FSI the energy and momentum of the initial nucleon can be identified with the measured p_{miss} and E_{miss}

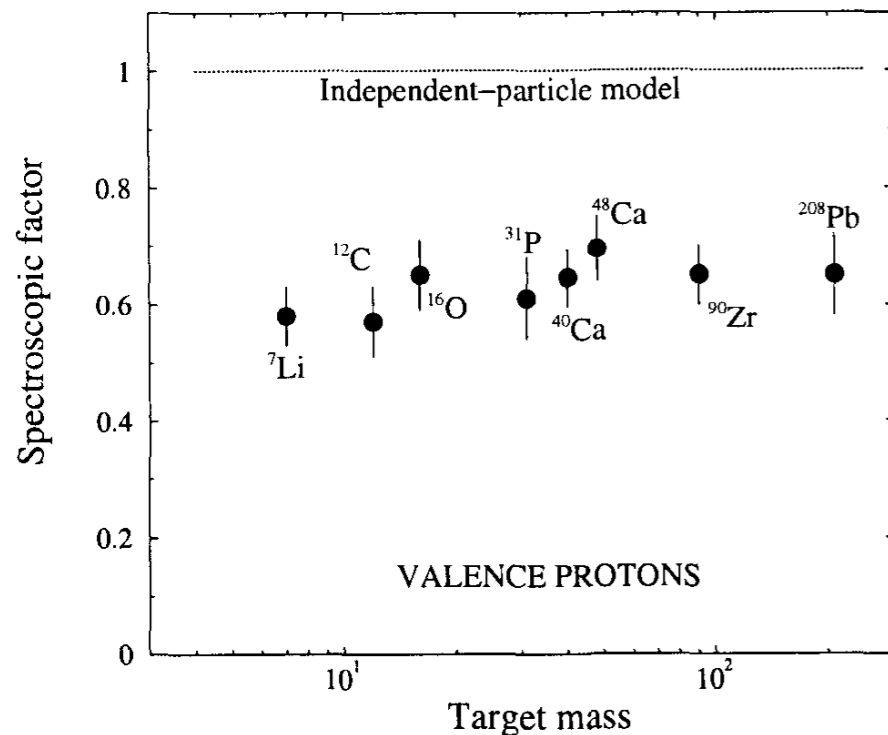


U. Amaldi et al, Phys. Rev. Lett. 13, 10 (1964)

- The peak coming from four 1p protons is visible
- The contribution of the two 1s protons is not clearly separated with this resolution

(e,e'p) scattering experiments

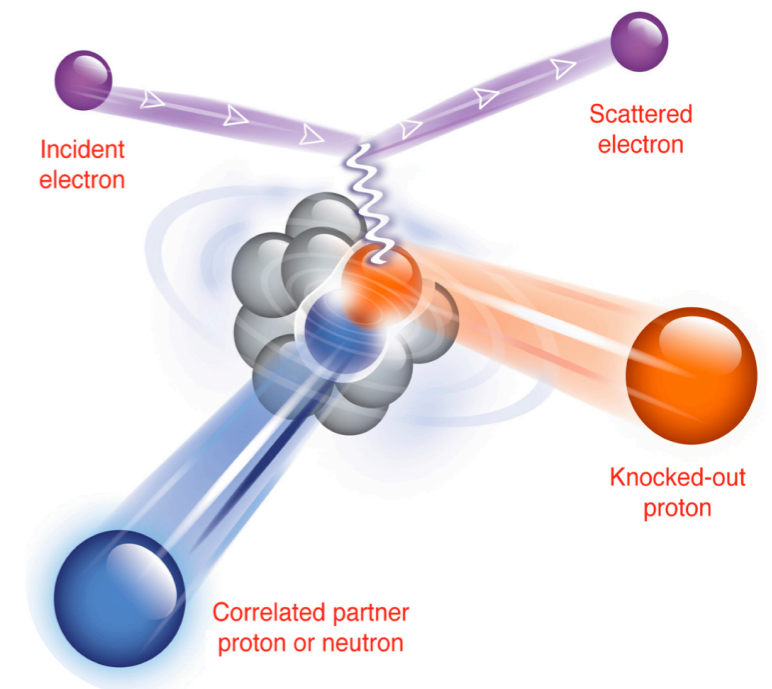
- Electron and proton experiments also pinned down the limitations of MF approaches



- Quenching of the spectroscopic factors of valence states has been confirmed by a number of high resolution (e,e'p) experiments

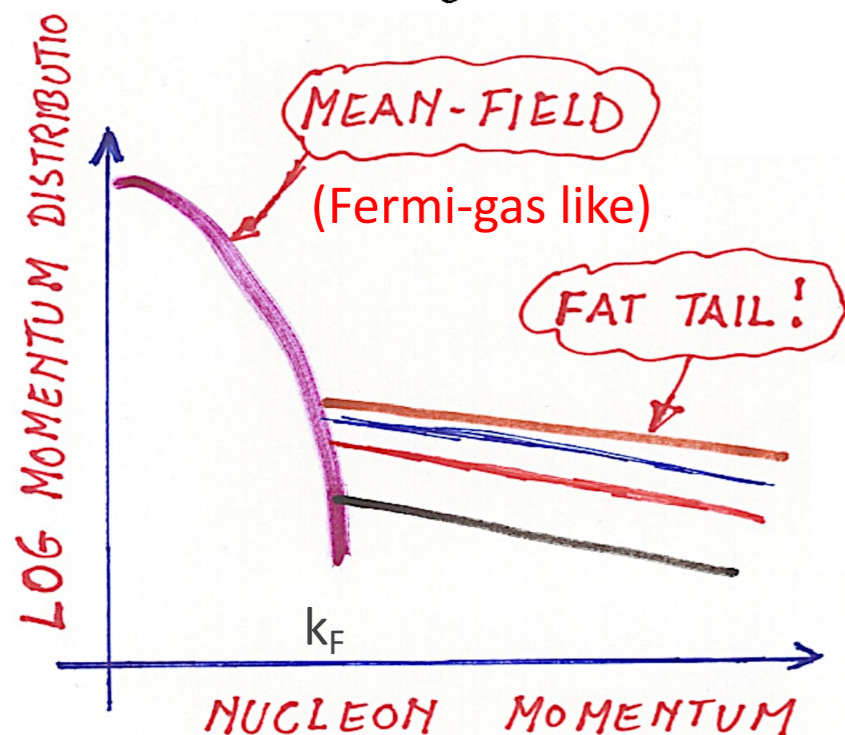
Subedi et al., Science 320, 1476 (2008)

- **Semi-exclusive 2N-SRC** experiments at $x > 1$ allows to detect both nucleons and reconstruct the initial state



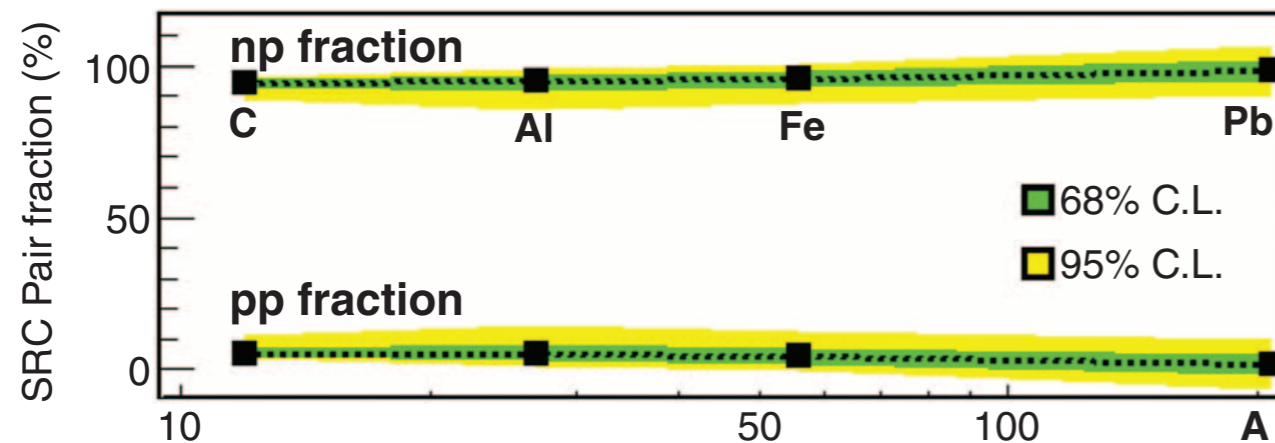
- Confirmed that the **high momentum tail** of the nuclear wave function consists mainly of 2N-SRC

- The large-momentum (short-range) component of the wave function is dominated by the presence of Short Range Correlated (SRC) pairs of nucleons



(e,e'p) scattering experiments

- Observed dominance of np-over-pp pairs for a variety of nuclei



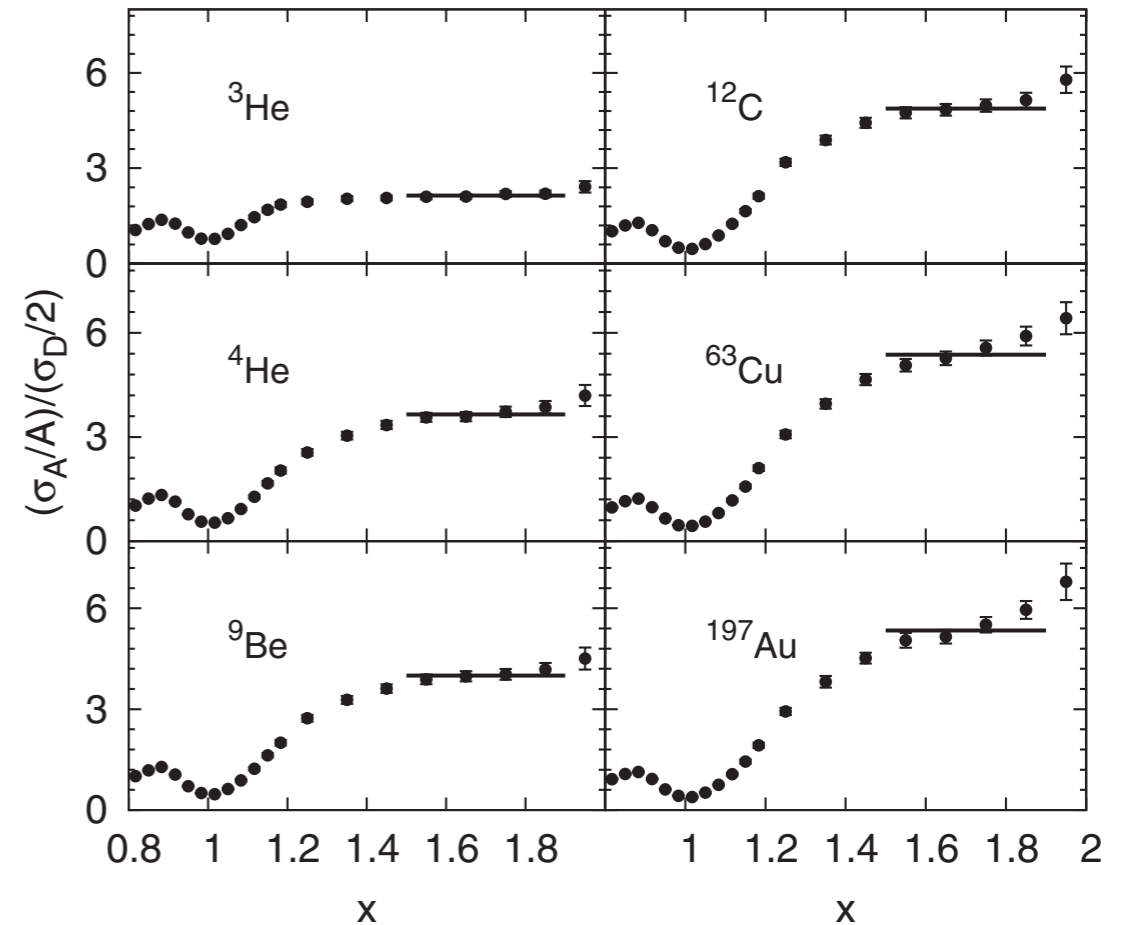
Subedi et al., Science 320, 1476 (2008)

- SRC pairs are in spin-triplet state, a consequence of the tensor part of the nucleon-nucleon interaction

Bottom Line

- Two-body Physics can not be neglected:
 - ~20% of the nucleons in nuclei
 - ~100% of the high k (>pF) nucleons
- Have large relative momentum and low center of mass momentum

- Universality of high-momentum component



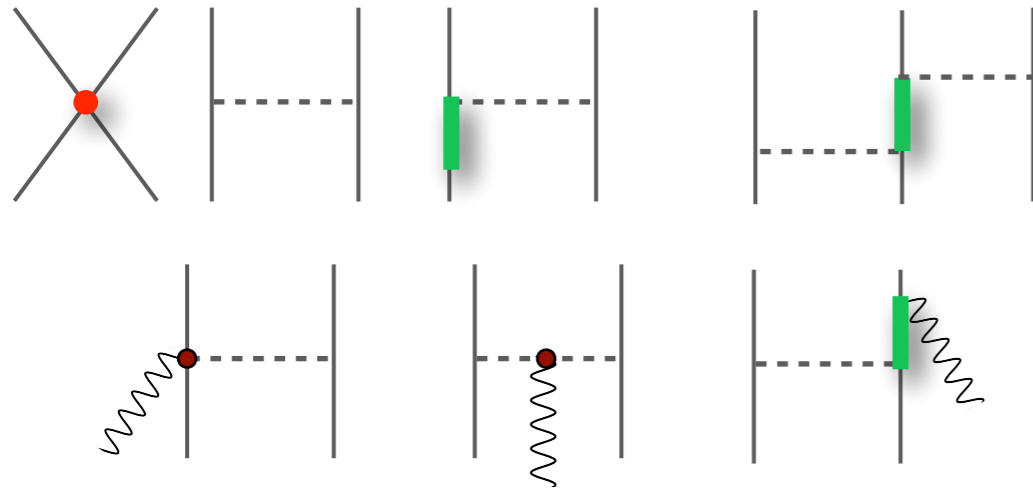
N. Fomin et al., PRL 108, 092502 (2012)

- The cross section ratio: A/d , sensitive to $n_A(k)/n_d(k)$
- Observed scaling for $x > 1.5$

$$n_A(k > p_F) = a_2(A) \times n_d(k)$$

The basic model of nuclear theory

Effective Hamiltonians and consistent currents

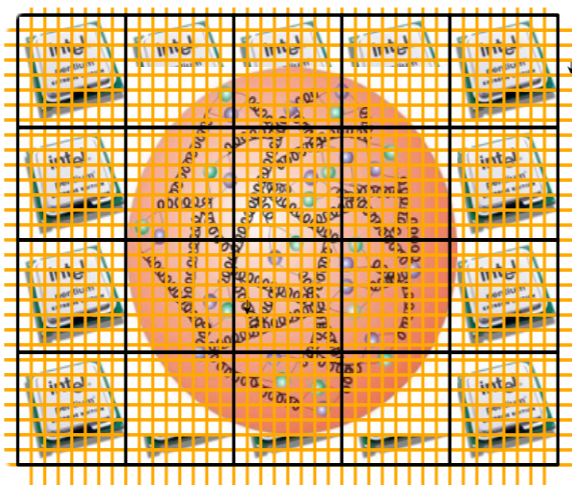


Accurate nuclear many-body methods

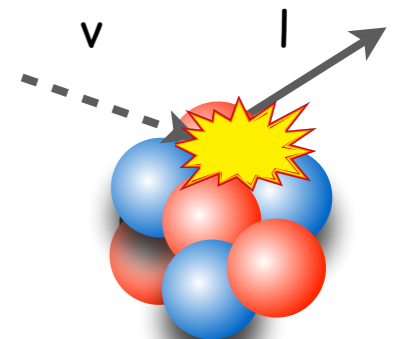
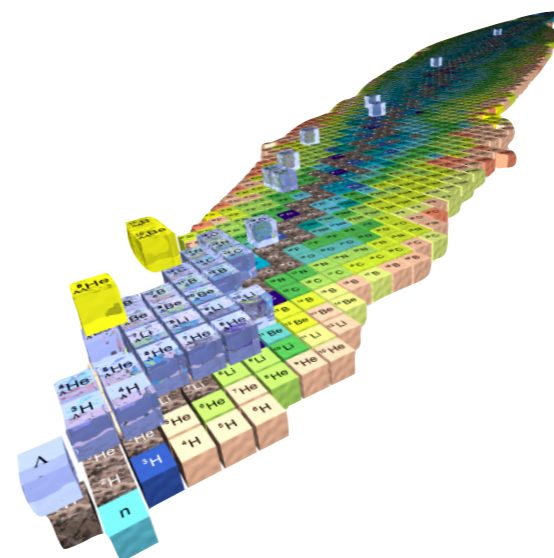


$$H|\Psi_n\rangle = E_n|\Psi_n\rangle$$
$$J_{mn} = \langle\Psi_m|J|\Psi_n\rangle$$

Quantum Chromodynamics



Nuclei and electroweak interactions



The basic model of nuclear theory

Effective field theories are the link between QCD and nuclear observables. At low energy, the effective degrees of freedom are pions and nucleons:

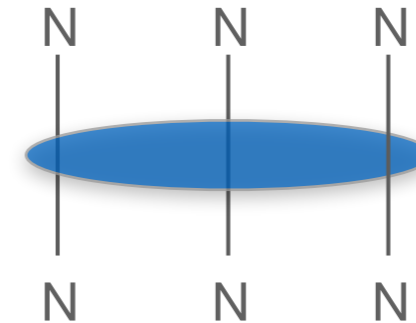
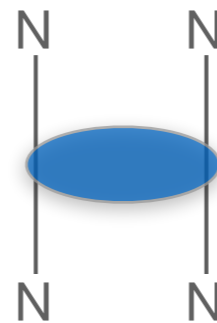
$$H = \sum_i \frac{\mathbf{p}_i^2}{2m} + \sum_{i < j} v_{ij} + \sum_{i < j < k} V_{ijk} + \dots$$

1-body 2-body 3-body



R. Machleidt, D. R. Entem,
Phys.Rept.503:1-75,2011

E. Epelbaum, (Lectures), arXiv:1001.3229

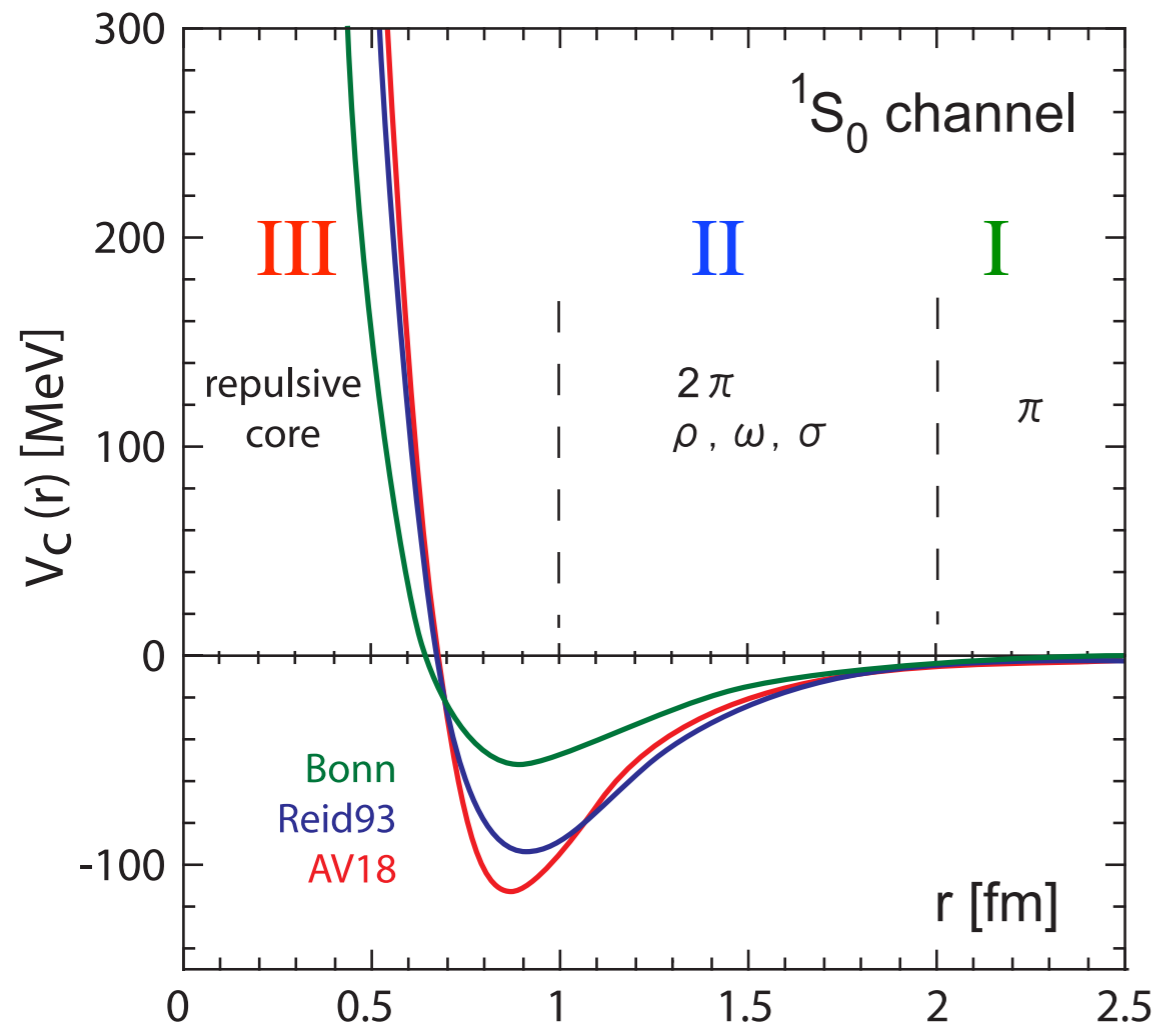


Different strategies to construct two- and three-body interactions

- ❖ Chiral Effective Field Theory interactions
- ❖ Phenomenological potentials

Nucleon-nucleon potential

Aoki et al. Comput.Sci.Disc.1(2008)015009



Long range part: One π exchange

$$\text{Range: } \frac{1}{m_\pi} \sim 1.4 \text{ fm}$$

Medium range part: Two π exchange

$$\text{Range: } \frac{1}{2m_\pi} \sim 0.7 \text{ fm}$$

Short range part: Repulsive core

Bonn PRC 63, 024001, 2001

Reid93 PRC 49, 2950, 1994

AV18: Wiringa PRC 51, 38, 1995

Phenomenological potential: av18 + IL7

Phenomenological potentials explicitly include the **long-range one-pion exchange interaction** and a set of **intermediate- and short-range phenomenological terms**

- **Argonne v₁₈** is a finite, local, configuration-space potential controlled by ~4300 np and pp scattering data below 350 MeV of the Nijmegen database

$$v_{ij} = \sum_{p=1}^{18} v^p(r_{ij}) O_{ij}^p \quad \longleftrightarrow \quad \begin{array}{c} N \quad N \\ | \quad | \\ \text{---} \pi \text{---} \\ | \quad | \\ N \quad N \end{array} \quad \begin{array}{c} N \quad N \\ | \quad | \\ \text{---} \pi \text{---} \text{---} \Delta \\ | \quad | \\ N \quad N \end{array} \quad \begin{array}{c} N \quad N \\ \diagdown \quad \diagup \\ \bullet \\ \diagup \quad \diagdown \\ N \quad N \end{array}$$

- Phenomenological three-nucleon interactions, like the **Illinois 7**, effectively include the lowest nucleon excitation, the $\Delta(1232)$ resonance, and other nuclear effects

$$V_{ijk}^{3N} = A_{2\pi}^{PW} O_{ijk}^{2\pi, PW} + A_{2\pi}^{SW} O_{ijk}^{2\pi, SW} + A_{3\pi}^{\Delta R} O_{ijk}^{3\pi, \Delta R} + A^R O_{ijk}^R \quad \longleftrightarrow \quad \begin{array}{c} N \quad N \quad N \\ | \quad | \quad | \\ \text{---} \pi \text{---} \bullet \text{---} \pi \text{---} \\ | \quad | \quad | \\ N \quad N \quad N \end{array} \quad \begin{array}{c} N \quad N \quad N \\ | \quad | \quad | \\ \text{---} \pi \text{---} \text{---} \Delta \text{---} \pi \text{---} \\ | \quad | \quad | \\ N \quad N \quad N \end{array}$$

The parameters of the AV18 + IL7 are fit to properties of **exactly solvable light nuclear systems**.

Chiral effective field theory

Chiral Hamiltonians exploits the (approximate) broken chiral symmetry of QCD

Identify the soft and hard scale of the problem $\mathcal{L}^{(n)} \sim \left(\frac{q}{\Lambda_b}\right)^n \sim \begin{matrix} \sim 100 \text{ MeV} & \text{soft scale} \\ \sim 1 \text{ GeV} & \text{hard scale} \end{matrix}$

Design an organizational scheme that can distinguish between more and less important terms:

$$\mathcal{L}_{\text{eff}} = \mathcal{L}^{(0)} + \mathcal{L}^{(1)} + \mathcal{L}^{(2)}$$

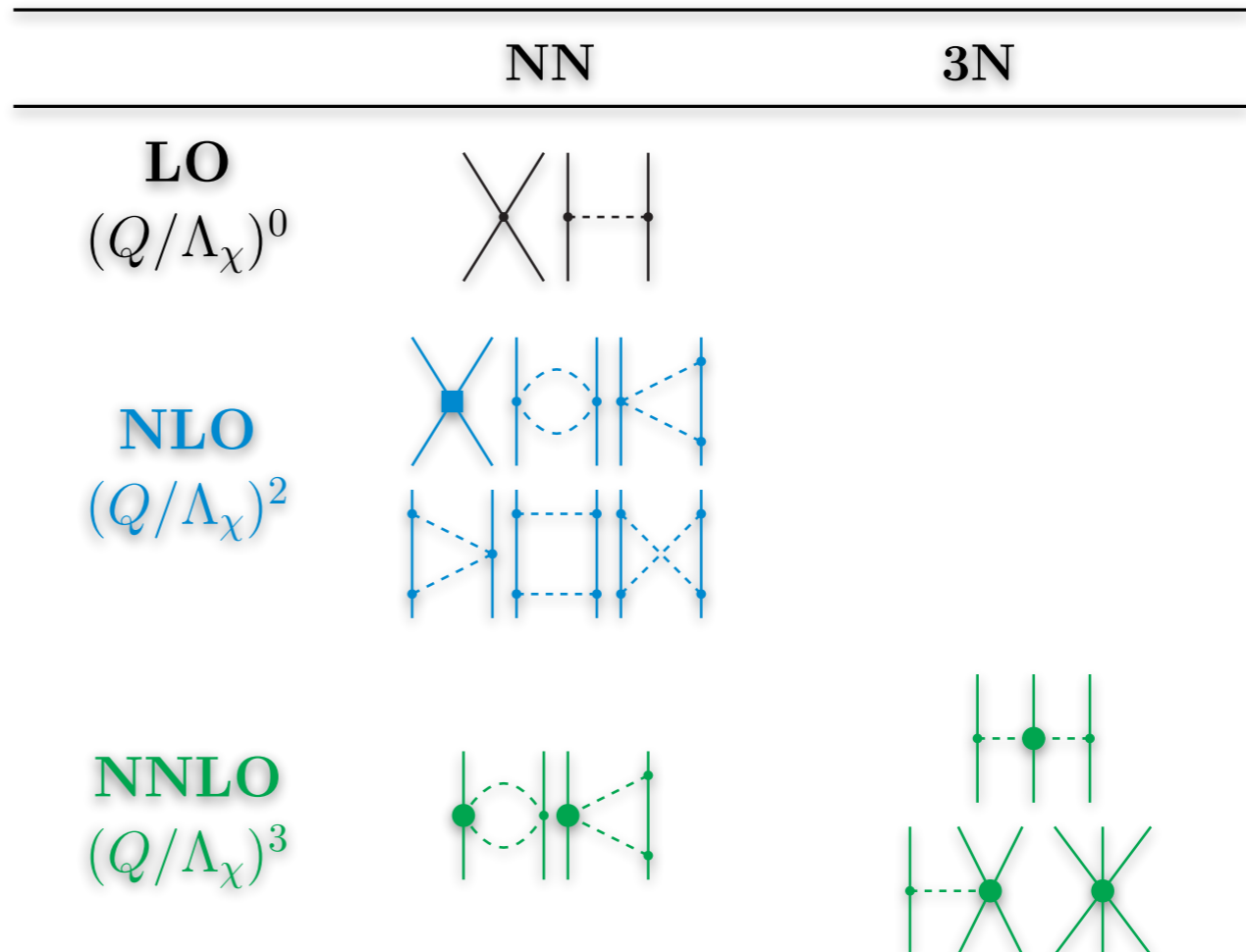
H. Hergert, *Front. in Phys.* **8**, 379 (2020)

Contact interactions lead to LEC:

Short range two-nucleon interaction
fit to deuteron and NN scattering

Three nucleon interactions fitted on
light nuclei

Long-range LEC are determined from
 π -nucleon scattering



Formulate statistical models for uncertainties: Bayesian estimates of EFT errors

S. Wesolowski, et al, *PRC* **104**, 064001 (2021)

The basic model of nuclear theory

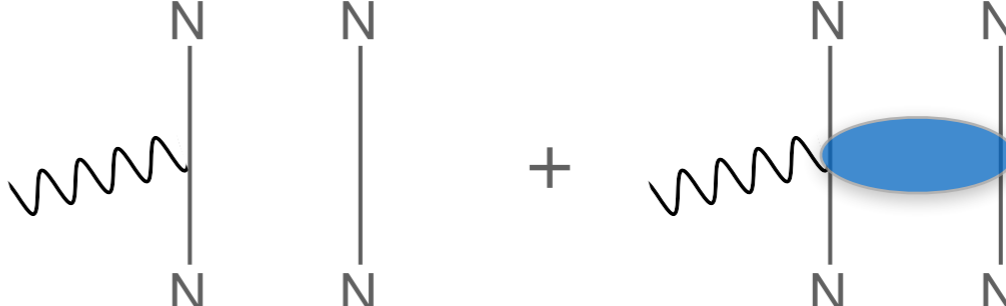
The current operator describes how the external probe interacts with nucleon, nucleons pairs, create new particles ...

The structure of the current operator is constrained by the Hamiltonian through the continuity equation

$$\nabla \cdot \mathbf{J}_{\text{EM}} + i[H, J_{\text{EM}}^0] = 0$$

$$[v_{ij}, j_i^0] \neq 0$$

The Hamiltonian structure implies that the current operator includes one and two-body contributions

$$J^\mu(q) = \sum_i j_i^\mu + \sum_{i < j} j_{ij}^\mu + \dots$$


The diagram illustrates the one and two-body contributions to the current operator. On the left, a wavy line (representing an external probe) connects to a single vertical line labeled 'N' at both ends, representing a one-body contribution. To the right of this is a plus sign, followed by another diagram. This second diagram shows a wavy line connecting to a vertical line labeled 'N' at both ends, which is then connected to a blue oval (representing a two-body interaction) that also connects to another vertical line labeled 'N' at both ends, representing a two-body contribution.

- ❖ Chiral Effective Field Theory Electroweak many-body currents
- ❖ “Phenomenological” Electroweak many-body currents

Variational Monte Carlo

In variational Monte Carlo, one **assumes a suitable form for the trial wave function**

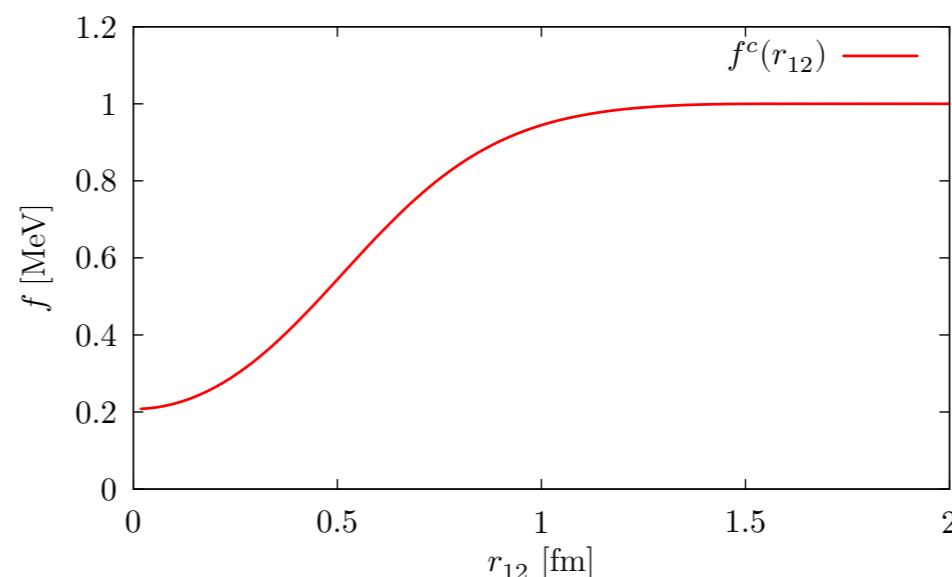
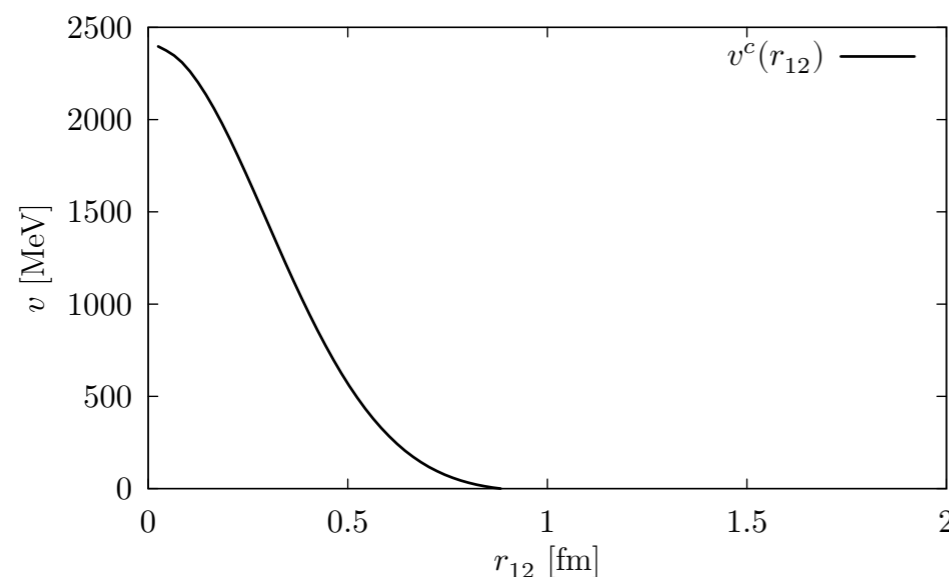
$$|\Psi_T\rangle = \mathcal{F}|\Phi\rangle \quad \left\{ \begin{array}{l} \Phi : \text{Mean field component; Slater determinant of single-particle orbitals} \\ \mathcal{F} : \text{correlations (2b \& 3b) induced by } H \end{array} \right.$$

The correlation operator reflects the spin-isospin dependence of the nuclear interaction

$$\mathcal{F} \equiv \left(\mathcal{S} \prod_{i < j} F_{ij} \right)$$

$$F_{ij} \equiv \sum_p f_{ij}^p O_{ij}^p$$

The best parameters are found by **optimizing the variational energy** $\frac{\langle \Psi_T | H | \Psi_T \rangle}{\langle \Psi_T | \Psi_T \rangle} = E_T \geq E_0$



Green's Function Monte Carlo

Any trial wave function can be expanded in the complete set of eigenstates of the the Hamiltonian according to

$$|\Psi_T\rangle = \sum_n c_n |\Psi_n\rangle \quad H|\Psi_n\rangle = E_n |\Psi_n\rangle$$

GFMC overcomes the limitations of the variational wave-function by using an imaginary-time projection technique to **projects out the exact lowest-energy state**

$$\lim_{\tau \rightarrow \infty} e^{-(H-E_0)\tau} |\Psi_T\rangle = \lim_{\tau \rightarrow \infty} \sum_n c_n e^{-(E_n-E_0)\tau} |\Psi_n\rangle = c_0 |\Psi_0\rangle$$

The direct calculation of the imaginary-time propagator for strongly-interacting systems involves prohibitive difficulties

J. Carlson , et al. Rev. Mod. Phys. 87 (2015) 1067

The imaginary-time evolution is broken into N small imaginary-time steps, and complete sets of states are inserted

$$e^{-(H-E_0)\tau} |\Psi_V\rangle = \int dR_1 \dots dR_N |R_N\rangle \langle R_N | e^{-(H-E_0)\Delta\tau} | R_{N-1} \rangle \dots \langle R_2 | e^{-(H-E_0)\Delta\tau} | R_1 \rangle \Psi_V(R_1)$$

Short Time Propagator

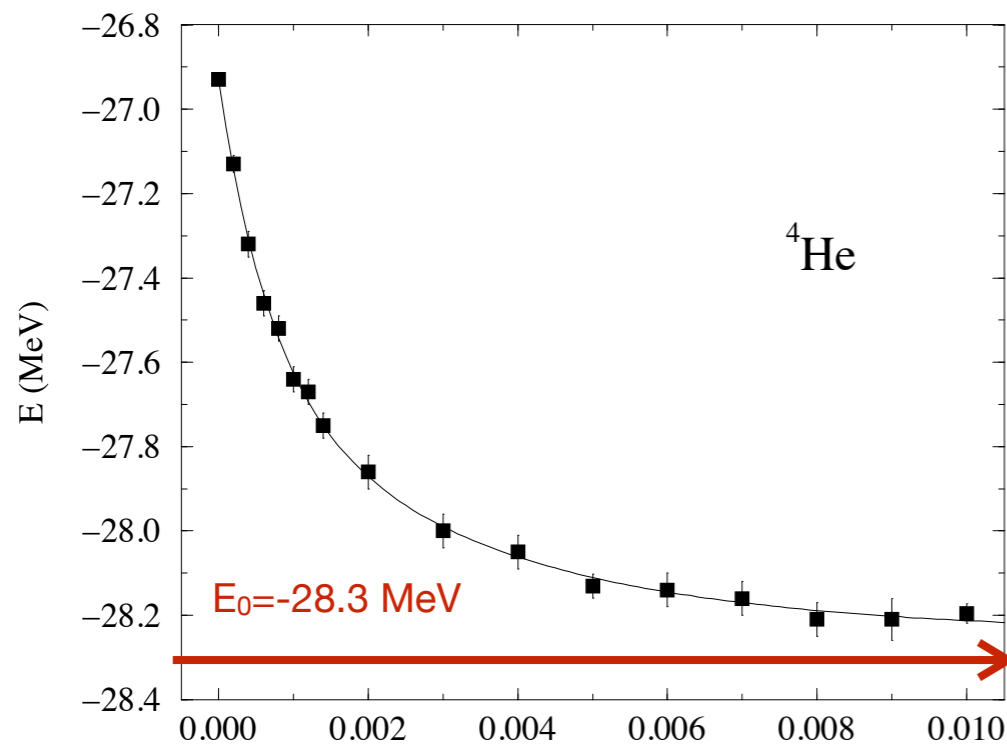
Green's Function Monte Carlo

Any trial wave function can be expanded in the complete set of eigenstates of the the Hamiltonian according to

$$|\Psi_T\rangle = \sum_n c_n |\Psi_n\rangle \quad H|\Psi_n\rangle = E_n |\Psi_n\rangle$$

GFMC overcomes the limitations of the variational wave-function by using an imaginary-time projection technique to **projects out the exact lowest-energy state**

$$\lim_{\tau \rightarrow \infty} e^{-(H-E_0)\tau} |\Psi_T\rangle = \lim_{\tau \rightarrow \infty} \sum_n c_n e^{-(E_n-E_0)\tau} |\Psi_n\rangle = c_0 |\Psi_0\rangle$$



B. Pudliner et al., PRC **56**, 1720 (1997)

The computational cost of the calculation is $2^A \times A!/(Z!(A-Z)!)$

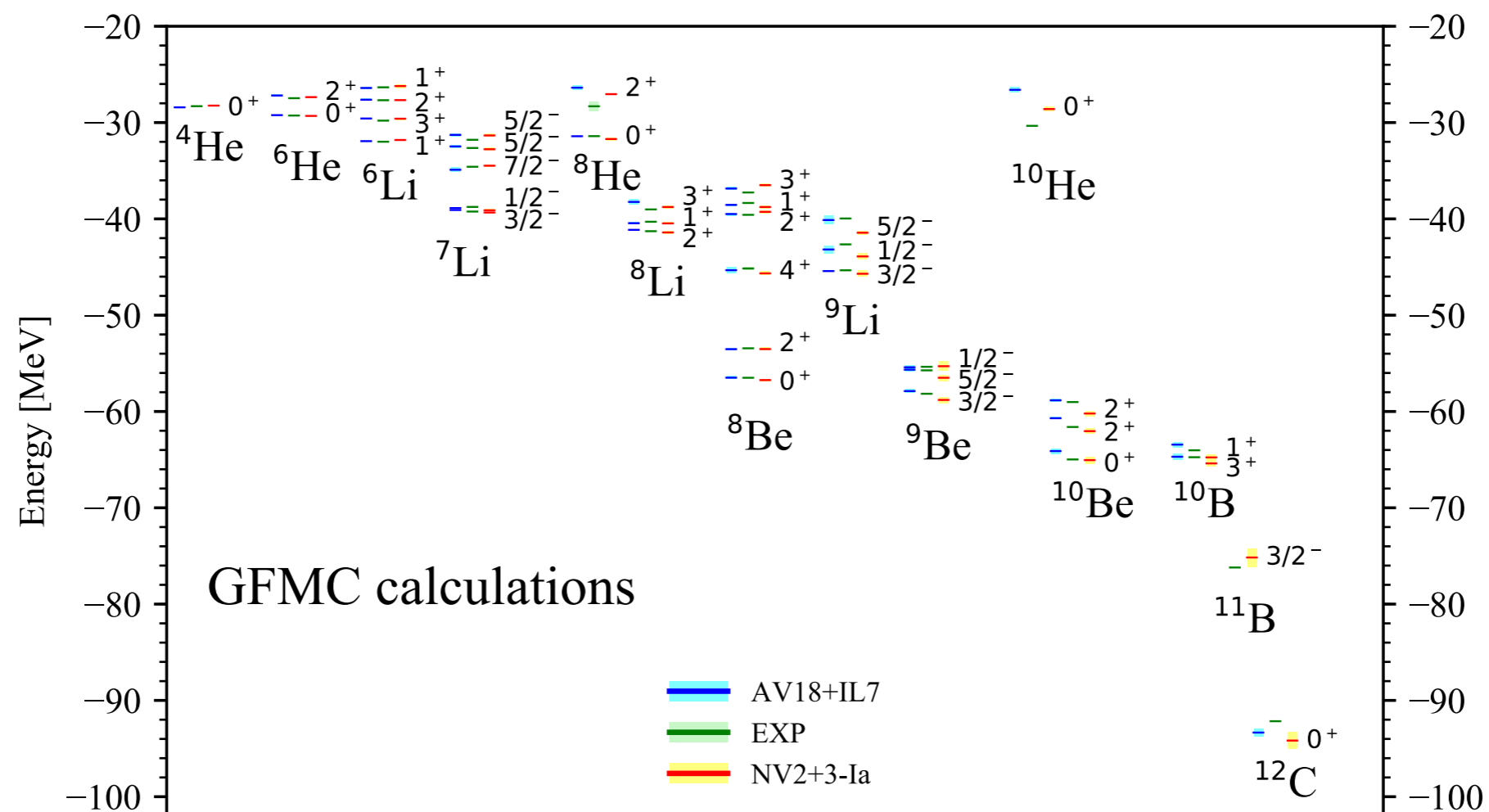
$$|S\rangle = \begin{pmatrix} s \uparrow \uparrow \uparrow \\ s \uparrow \uparrow \downarrow \\ s \uparrow \downarrow \uparrow \\ s \uparrow \downarrow \downarrow \\ s \downarrow \uparrow \uparrow \\ s \downarrow \uparrow \downarrow \\ s \downarrow \downarrow \uparrow \\ s \downarrow \downarrow \downarrow \end{pmatrix}$$

Solve the Many Body Nuclear problem

Develop Computational Methods to solve numerically

$$H\Psi(\mathbf{R}; s_1 \dots s_A, \tau_1 \dots \tau_A) = E\Psi(\mathbf{R}; s_1 \dots s_A, \tau_1 \dots \tau_A)$$

Quantum Monte Carlo techniques are suitable to solve the Schroedinger equation of medium nuclei

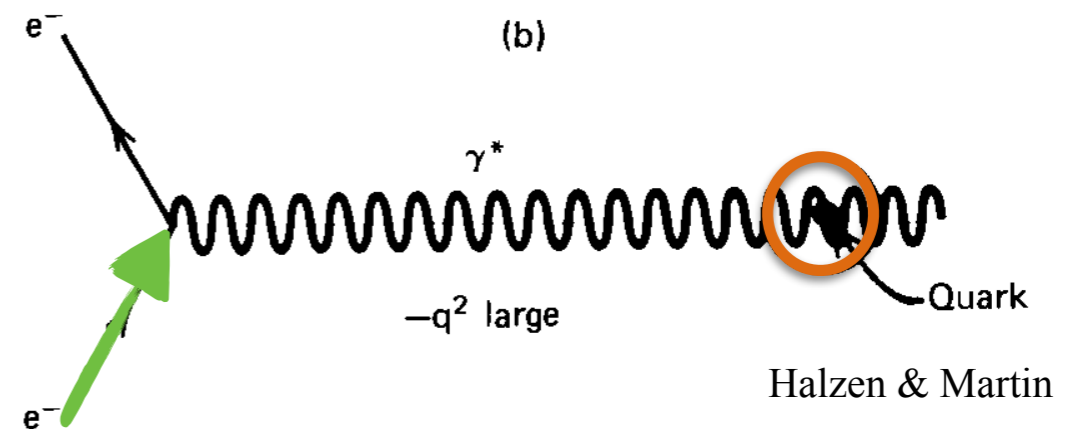
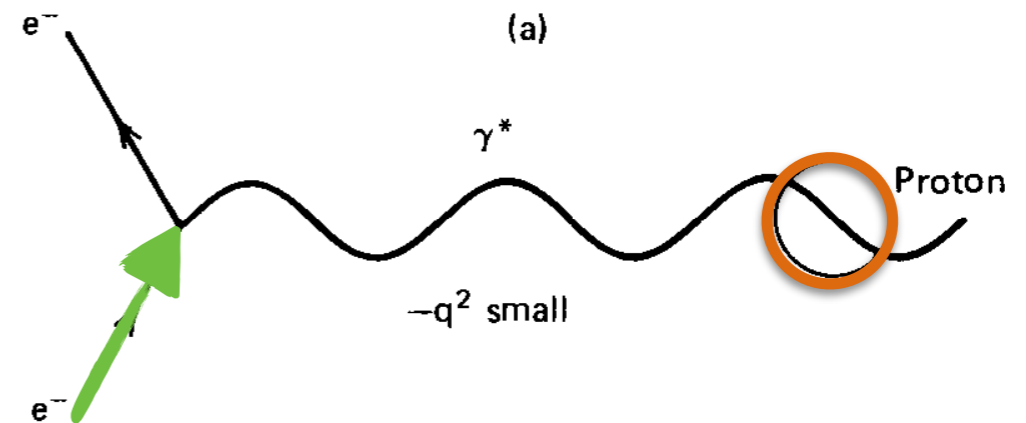


M. Piarulli, et al. Phys.Rev.Lett. 120 (2018) 5, 052503

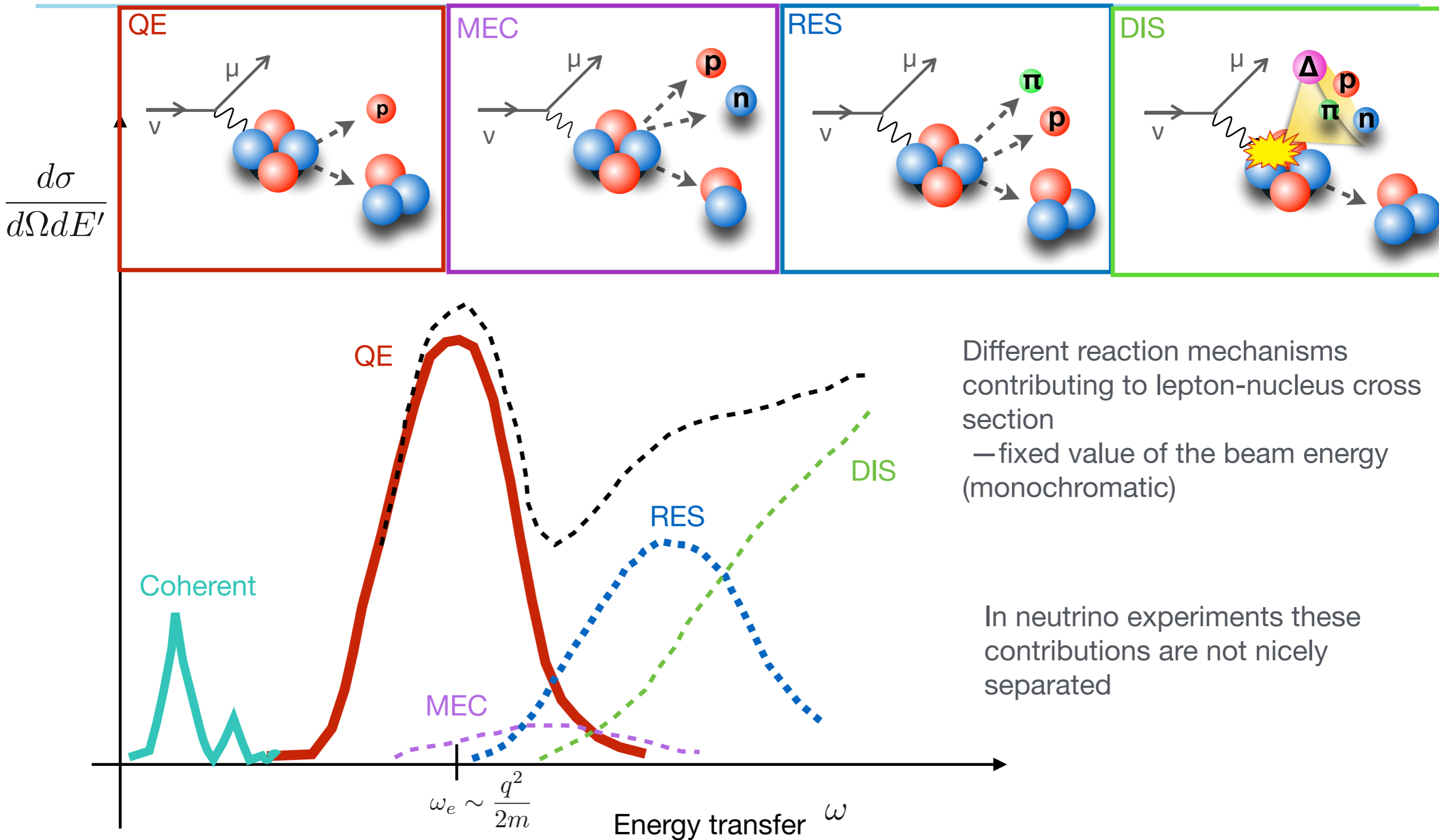
Probing the target structure

The interaction depends on the **mediator** energy (dubbed as energy transfer ω)

Higher energy transfer = smaller de Broglie wavelength = the probe can resolve the structure inside the nucleon

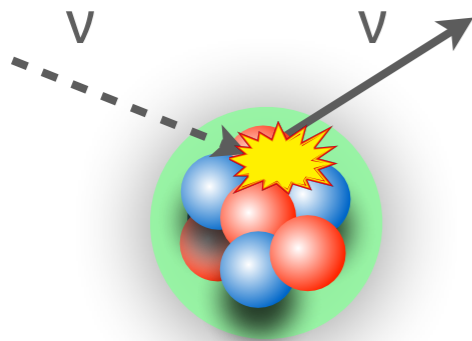


Lepton-nucleus cross section



Coherent elastic ν -Nucleus scattering (CEvNS)

- The first detection of CEvNS was published by the COHERENT collaboration in 2017, and opened an exciting chapter of using CEvNS to test the Standard Model and search for new physics
- Neutral-current process that arises when the momentum transfer in the neutrino-nucleus interaction is less than the inverse of the size of the nucleus $E_\nu \sim 50$ MeV.
- The interaction is mediated by the Z-boson, with its vector component leading to the coherent enhancement



CEvNS Cross Section:

$$\frac{d\sigma}{dT} = \frac{G_F^2}{\pi} M_A \left[1 - \frac{T}{E_i} - \frac{M_A T}{2E_i^2} \right] \frac{Q_W^2}{4} F_W^2(q)$$

Nuclear recoil:

$$T \in \left[0, \frac{2E_i^2}{(M_A + 2E_i)} \right]$$

- Final state nucleus stays in its ground state
- Tiny recoil energy, large cross section
- Signal: keV energy nuclear recoil

Weak nuclear charge:

$$Q_W^2 = [g_n^V N + g_p^V Z]^2 = [N - (1 - 4 \sin^2 \theta_W) Z]^2$$

The proton contribution is suppressed with respect to the neutron one

Coherent elastic ν -Nucleus scattering (CEvNS)

- Due to the suppression of the proton weak charge, main contribution comes from the neutron $d\sigma \propto N^2$

Weak Form Factor:
$$F_W(q^2) = \frac{1}{Q_W} \left[ZQ_W^p F_p(q^2) + NQ_W^n F_n(q^2) \right]$$

$$F_p(q^2) = \frac{4\pi}{Z} \int dr \, r^2 \frac{\sin(qr)}{qr} \rho_p(r)$$

$$F_n(q^2) = \frac{4\pi}{N} \int dr \, r^2 \frac{\sin(qr)}{qr} \rho_n(r)$$

- $\rho_{p(n)}(r)$ is the proton (neutron) density distribution for a given nucleus

- Helm phenomenological parametrization:
$$F_{\text{Helm}}(q^2) = \frac{3j_1(qR_0)}{qR_0} e^{-q^2 s^2/2}$$

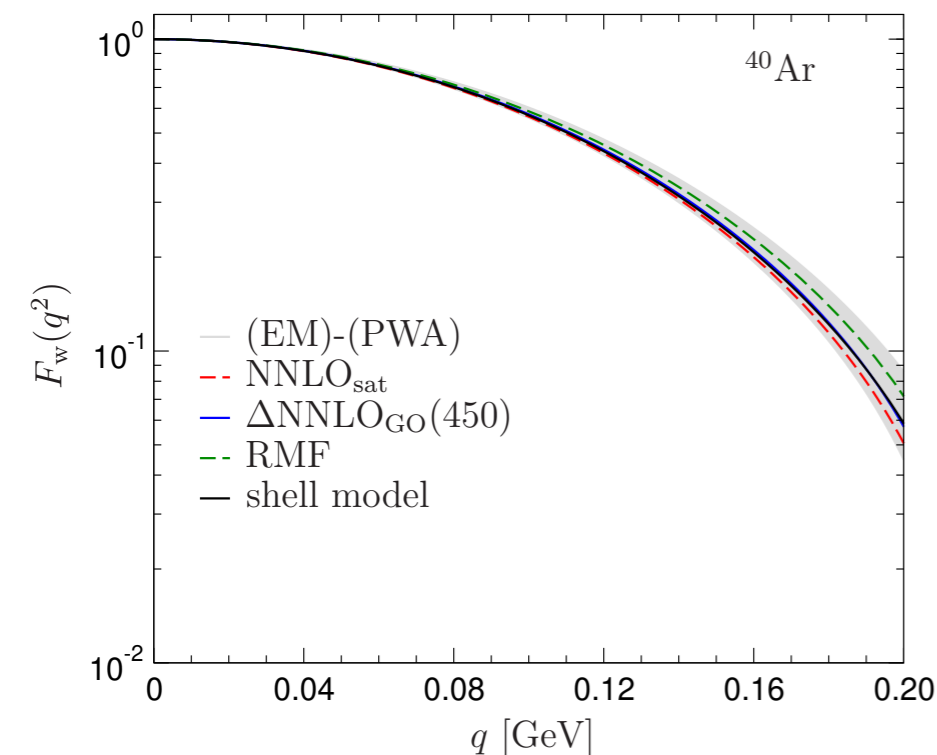
The nucleon distribution is given by the convolution of a uniform density with radius R_0 and a Gaussian profile with width s , the surface thickness.

This parameterization needs to assume a value for the neutron radius, related to R_0 and only try to capture the leading nuclear responses, with the neutron distribution largely unconstrained

Coherent elastic ν -Nucleus scattering (CEvNS)



Theoretical tools for neutrino scattering,
Contribution to: 2022 Snowmass Summer Study

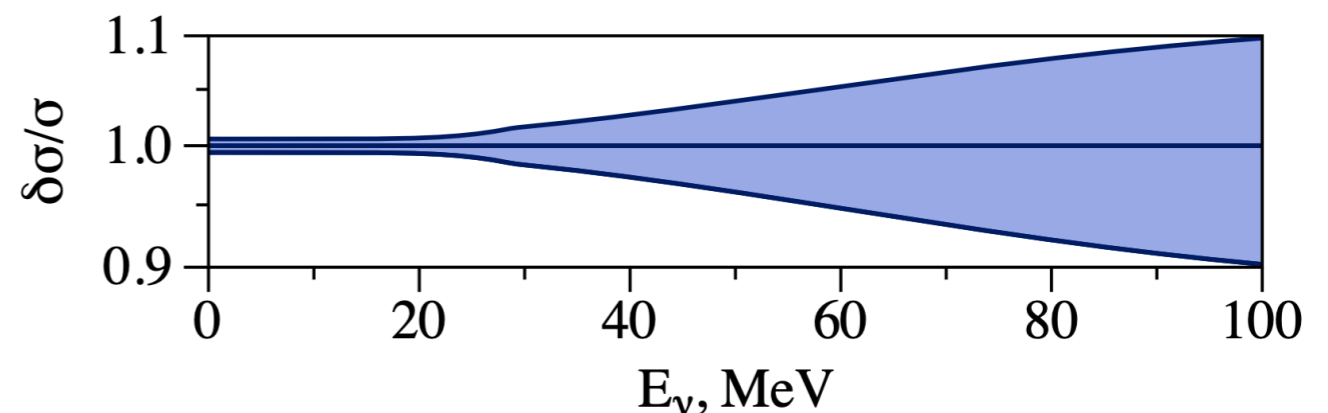


CEvNS cross section needs to be known at percent level precision to allow resolving degeneracies in the standard and non-standard physics observables in CEvNS experiments.

Retaining all responses that at least display coherent enhancement, $F_W(q^2)$ also receives the contribution of **spin-orbit corrections**, which add coherently for nucleons with spin aligned with the orbital angular momentum.

Theoretical predictions for the weak form factor of ^{40}Ar from Relativistic Mean Field, coupled-cluster, and shell-model [20] calculations.

O. Tomalak, P. Machado, V. Pandey, R. Plestid, JHEP 02, 097 (2021)

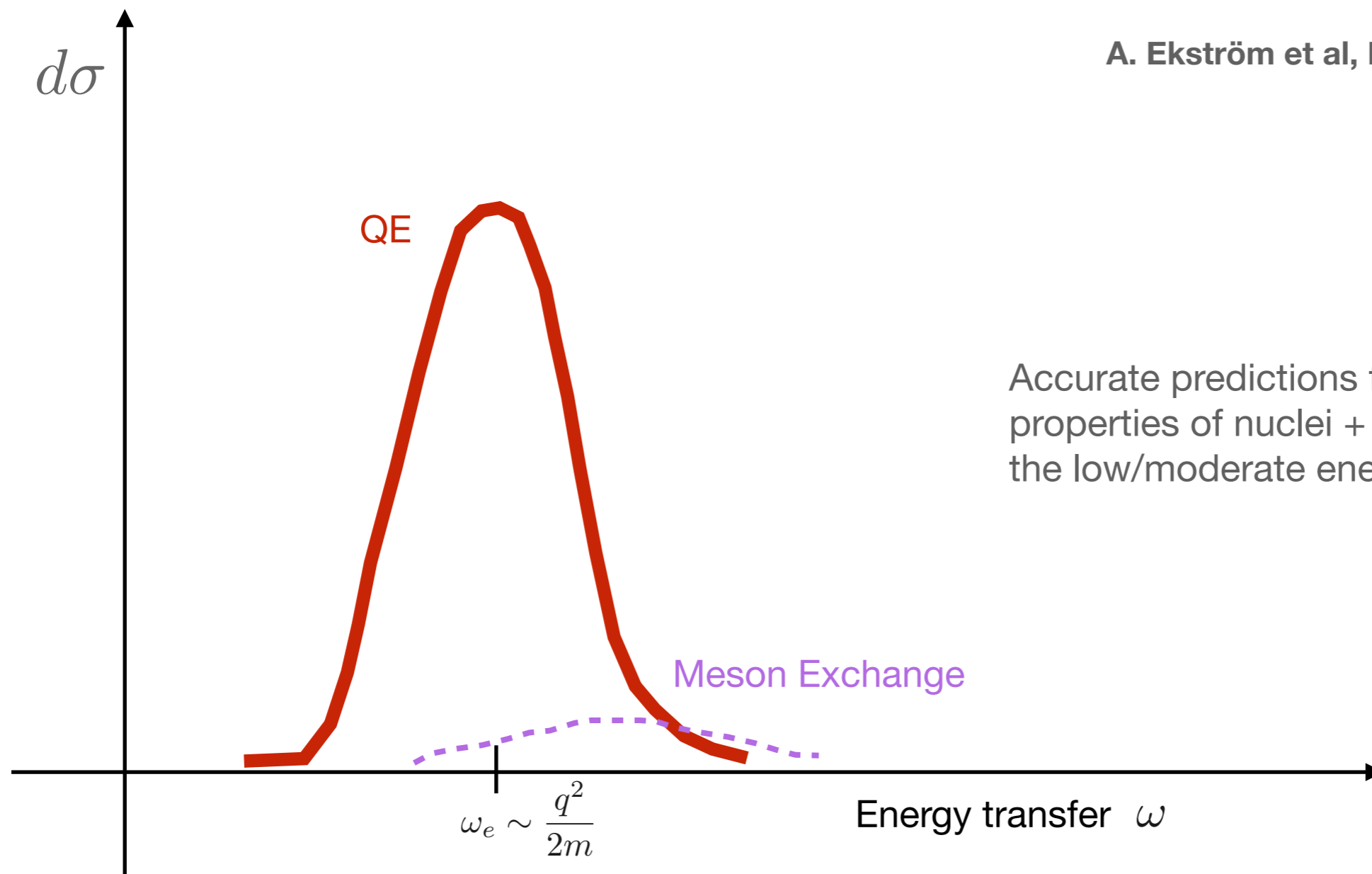


Relative CEvNS cross section theoretical uncertainty

Ab initio Methods

Ab-initio methods (CC, IMSRG, SCGF, QMC, etc) are systematically improvable many-body approaches.

A. Ekström et al, Front. Phys.11 (2023) 29094



Accurate predictions for ground state properties of nuclei + response functions in the low/moderate energy region

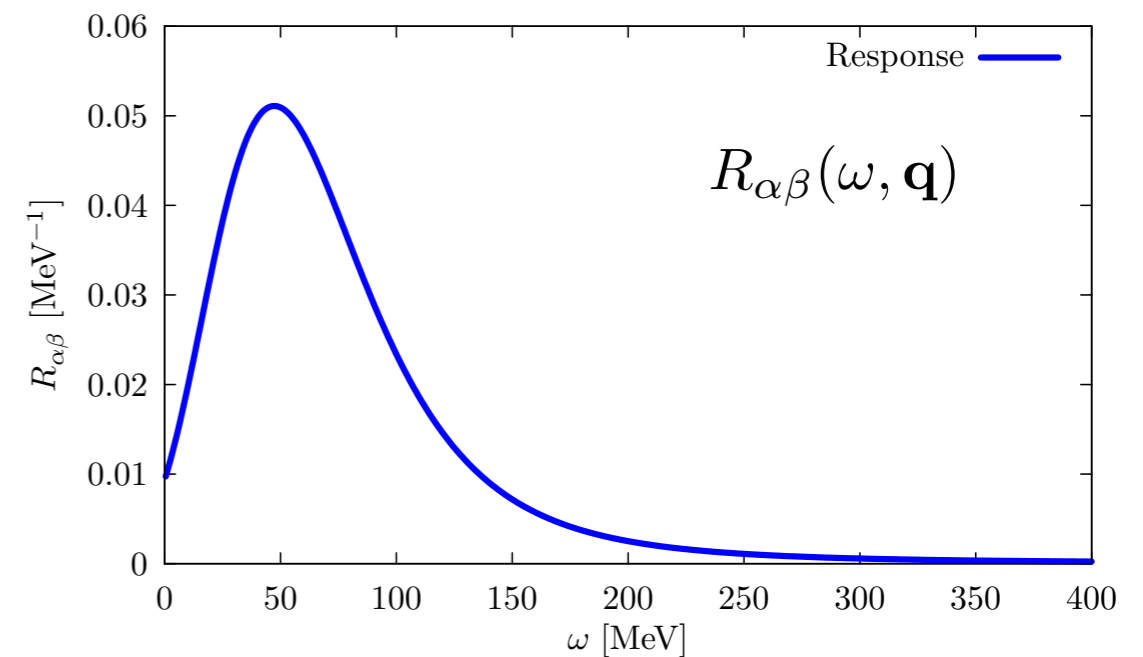
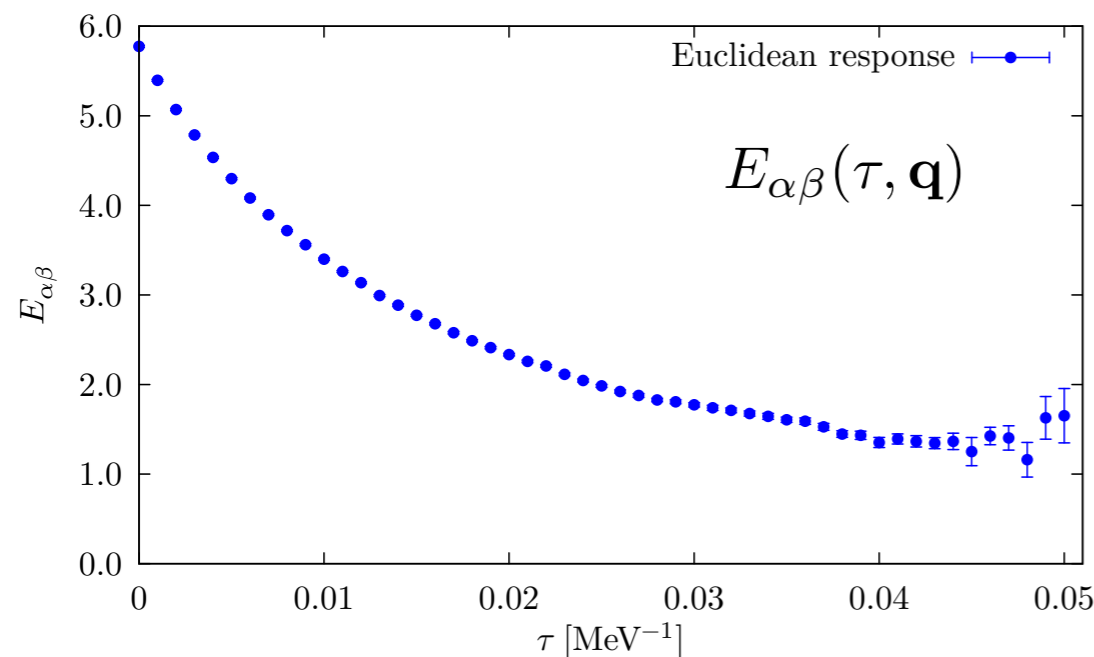


Nuclear response function involves evaluating a number of transition amplitudes.
Valuable information can be obtained from the **integral transform of the response function**

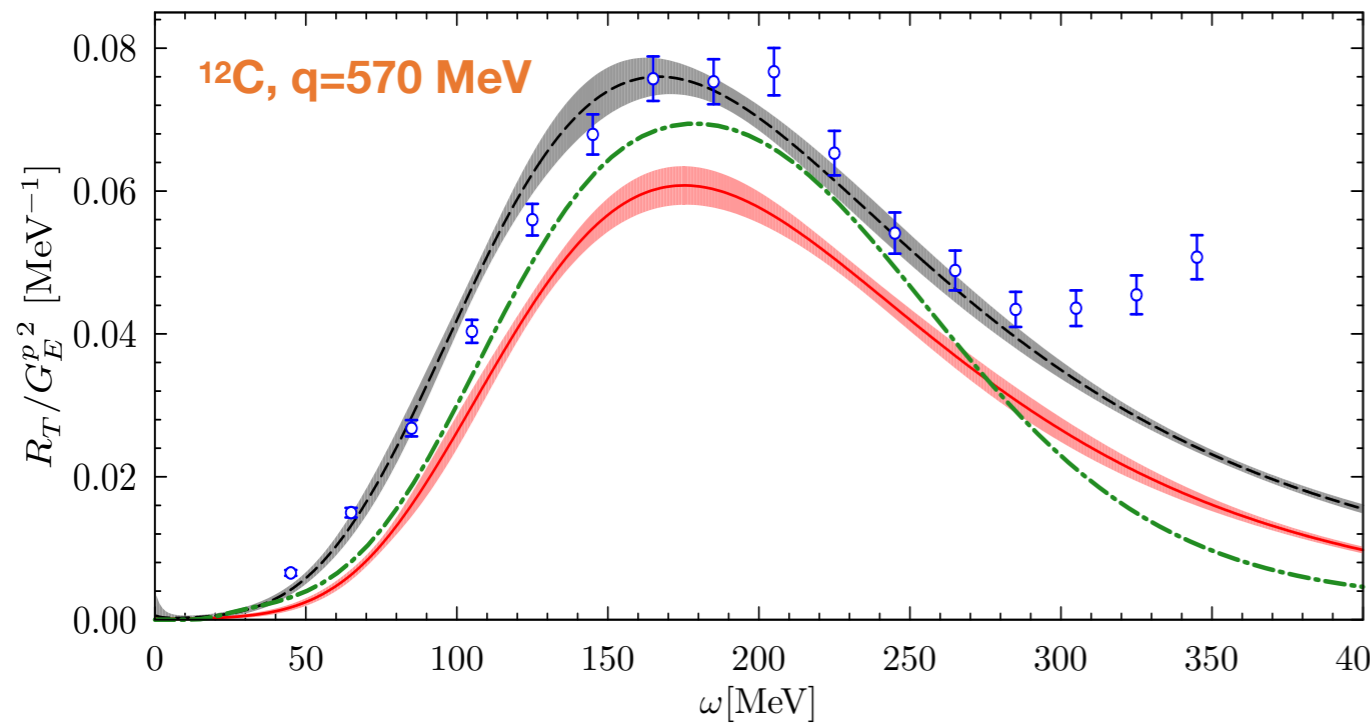
$$E_{\alpha\beta}(\sigma, \mathbf{q}) = \int d\omega K(\sigma, \omega) R_{\alpha\beta}(\omega, \mathbf{q}) = \langle \psi_0 | J_{\alpha}^{\dagger}(\mathbf{q}) K(\sigma, H - E_0) J_{\beta}(\mathbf{q}) | \psi_0 \rangle$$

Inverting the integral transform is a complicated problem

A. Lovato et al, PRL117 (2016), 082501,
PRC97 (2018), 022502



Same problem applies to different realm physics for example lattice QCD



Legend:

- GPMC O_{1b}
- GPMC O_{1b+2b}
- .- PWIA
- World data

Alessandro Lovato et al. PRL 117 082501 (2016)

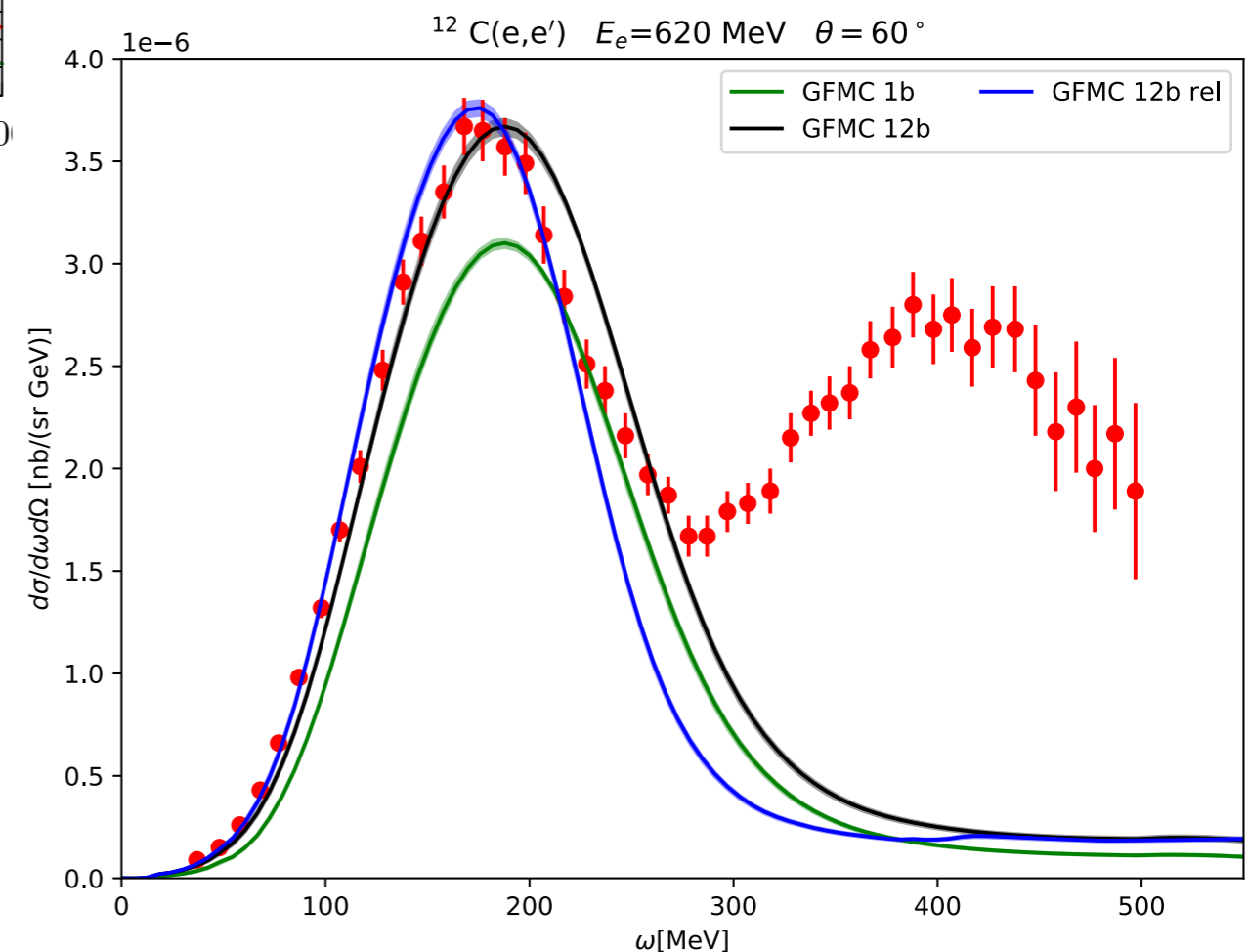
Limitations:

Medium mass nuclei $A < 13$

Inclusive results which are virtually correct in the QE

Relies on non-relativistic treatment of the kinematics

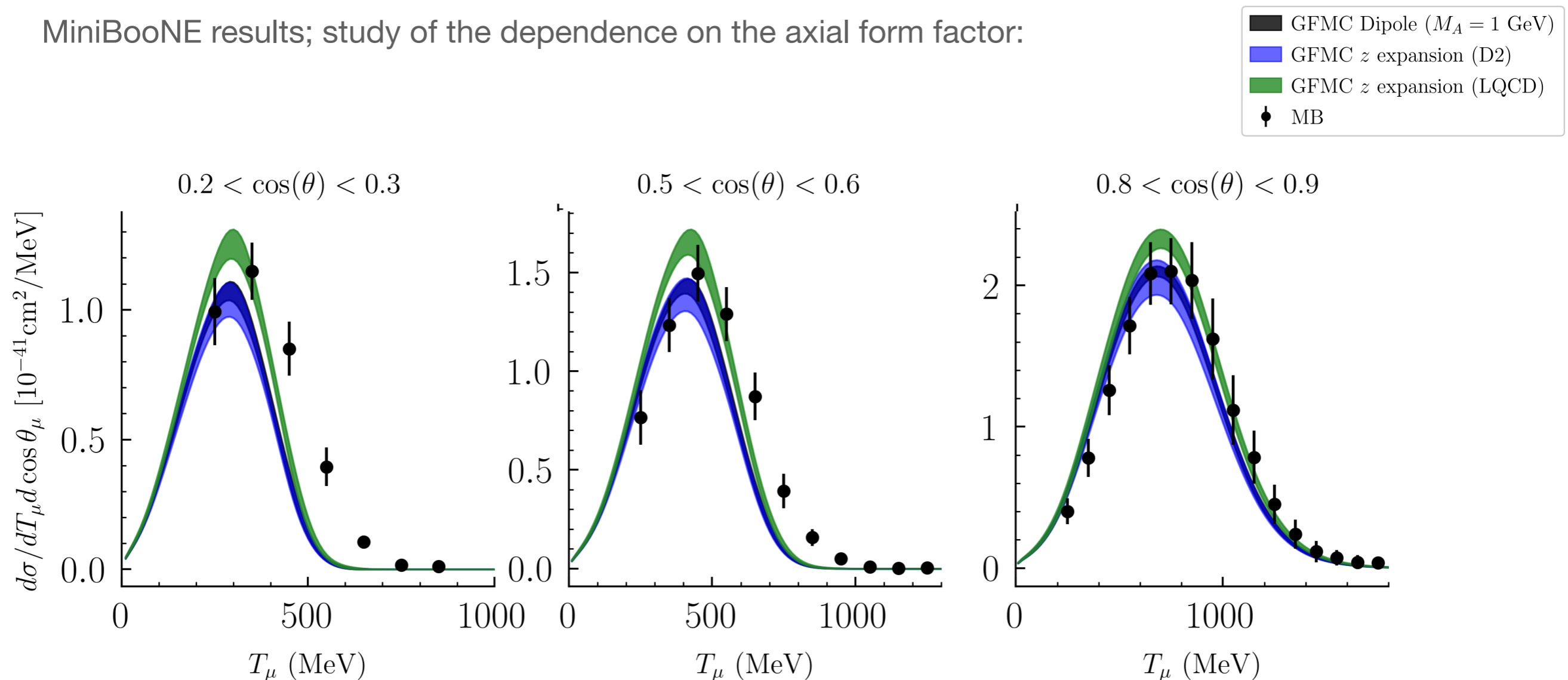
Can not handle explicit pion degrees of freedom



A.Lovato, NR, et al, submitted to Universe

Study of model dependence in neutrino predictions

MiniBooNE results; study of the dependence on the axial form factor:

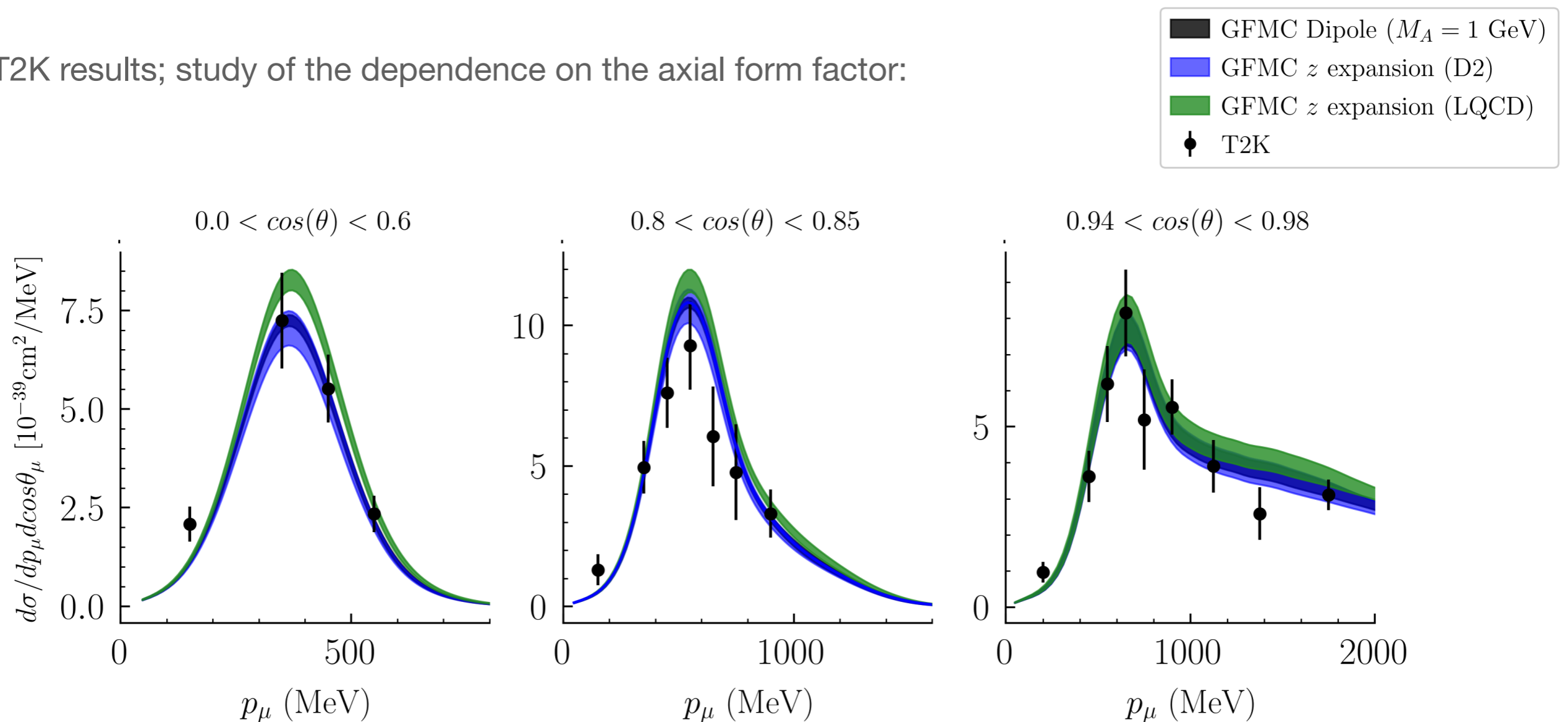


D.Simons, N. Steinberg et al, 2210.02455

MiniBooNE	$0.2 < \cos \theta_\mu < 0.3$	$0.5 < \cos \theta_\mu < 0.6$	$0.8 < \cos \theta_\mu < 0.9$
GFMC Difference in $d\sigma_{\text{peak}}$ (%)	18.6	17.1	12.2

Study of model dependence in neutrino predictions

T2K results; study of the dependence on the axial form factor:



D.Simons, N. Steinberg et al, 2210.02455

T2K	$0.0 < \cos \theta_\mu < 0.6$	$0.80 < \cos \theta_\mu < 0.85$	$0.94 < \cos \theta_\mu < 0.98$
GPMC difference in $d\sigma_{\text{peak}}$ (%)	15.8	8.0	4.6

Coupled Cluster Method

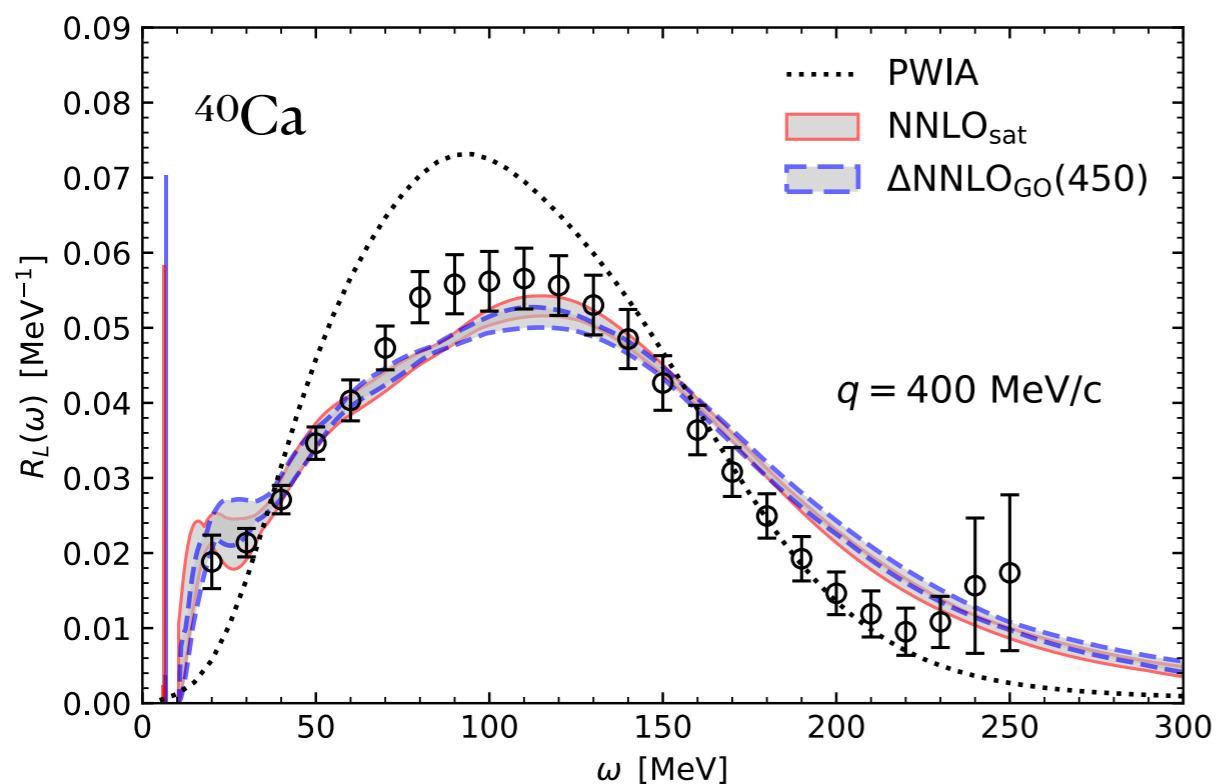
Reference state Hartree Fock: $|\Psi\rangle$

Include correlations through e^T operator

Similarity transformed Hamiltonian $e^{-T} H e^T |\Psi\rangle = \bar{H} |\Psi\rangle = E |\Psi\rangle$

Expansion in second quantization single + doubles:

$$T = \sum t_a^i a_a^\dagger a_i + \sum t_{ab}^{ij} a_a^\dagger a_b^\dagger a_i a_j + \dots$$



Polynomial scaling with the number of nucleons (predictions for ¹³²Sn and ²⁰⁸Pb)

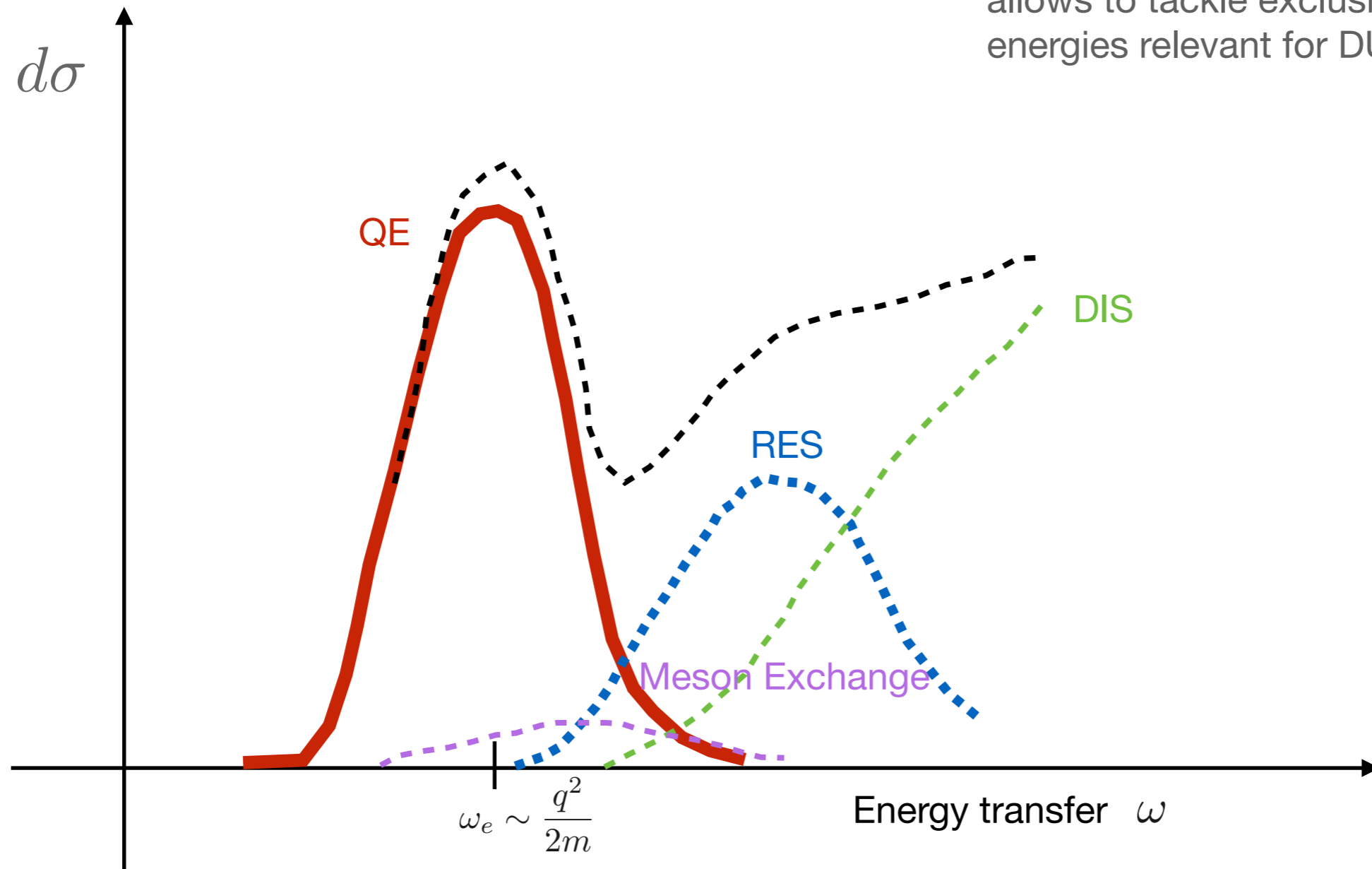
Electroweak response functions obtained using **LIT**

$$K_\Gamma(\omega, \sigma) = \frac{1}{\pi} \frac{\Gamma}{\Gamma^2 + (\omega - \sigma)^2}$$

JES, B. Acharya, S. Bacca, G. Hagen; PRL 127 (2021) 7, 072501

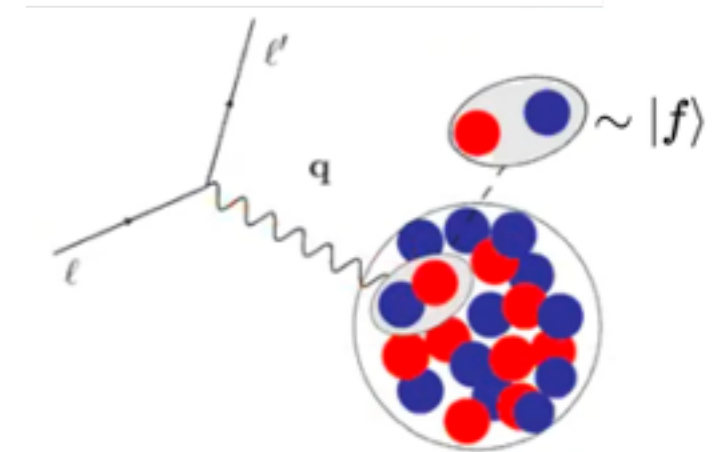
Factorization Based Approaches

Factorization of the hadronic final states:
allows to tackle exclusive channels + higher
energies relevant for DUNE





- ❖ Based on Factorization
- ❖ Retains two-body physics
- ❖ Response functions are given by the scattering from pairs of fully interacting nucleons that propagate into a correlated pair of nucleons
- ❖ Allows to retain both two-body correlations and currents at the vertex
- ❖ Provides “more” exclusive information in terms of nucleon-pair kinematics via the Response Densities



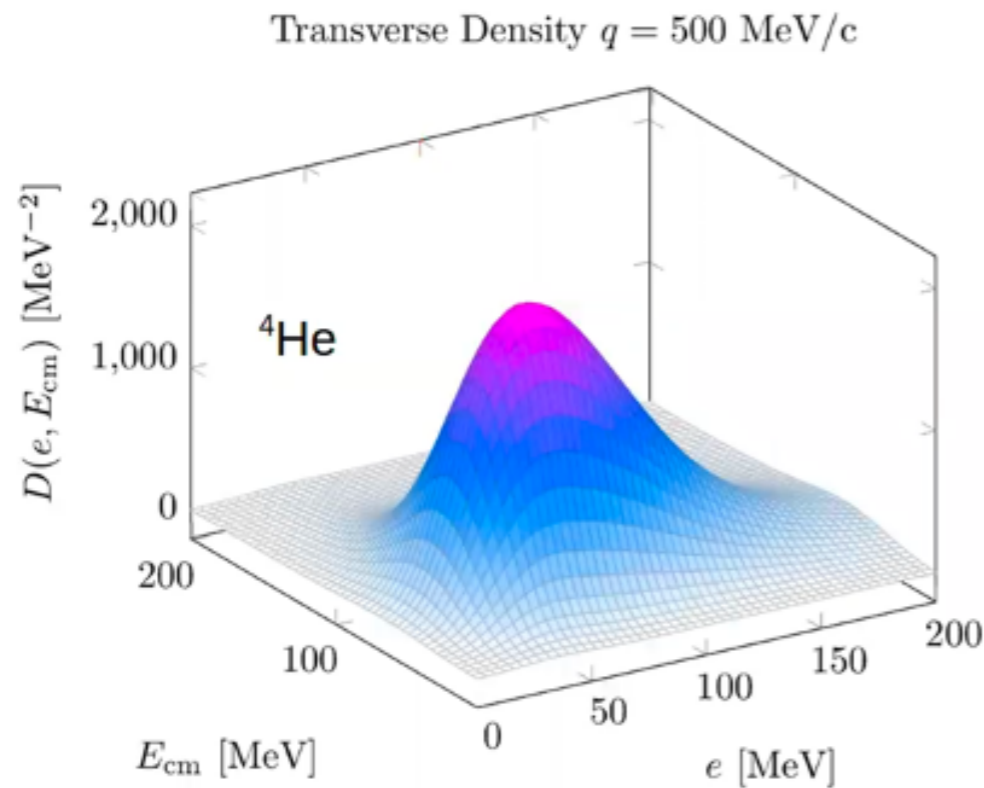
The sum over all final states is replaced by a two nucleon propagator

$$R_{\alpha}(q, \omega) = \int_{-\infty}^{\infty} \frac{dt}{2\pi} e^{i(\omega + E_i)t} \langle \Psi_i | O_{\alpha}^{\dagger}(\mathbf{q}) e^{-iHt} O_{\alpha}(\mathbf{q}) | \Psi_i \rangle$$

The STA restricts the propagation to two active nucleons and allows to compute density functions of the CoM and relative momentum of the pair

$$R^{\text{STA}}(q, \omega) \sim \int \delta(\omega + E_0 - E_f) de dE_{cm} \mathcal{D}(e, E_{cm}; q)$$

Short-Time Approximation



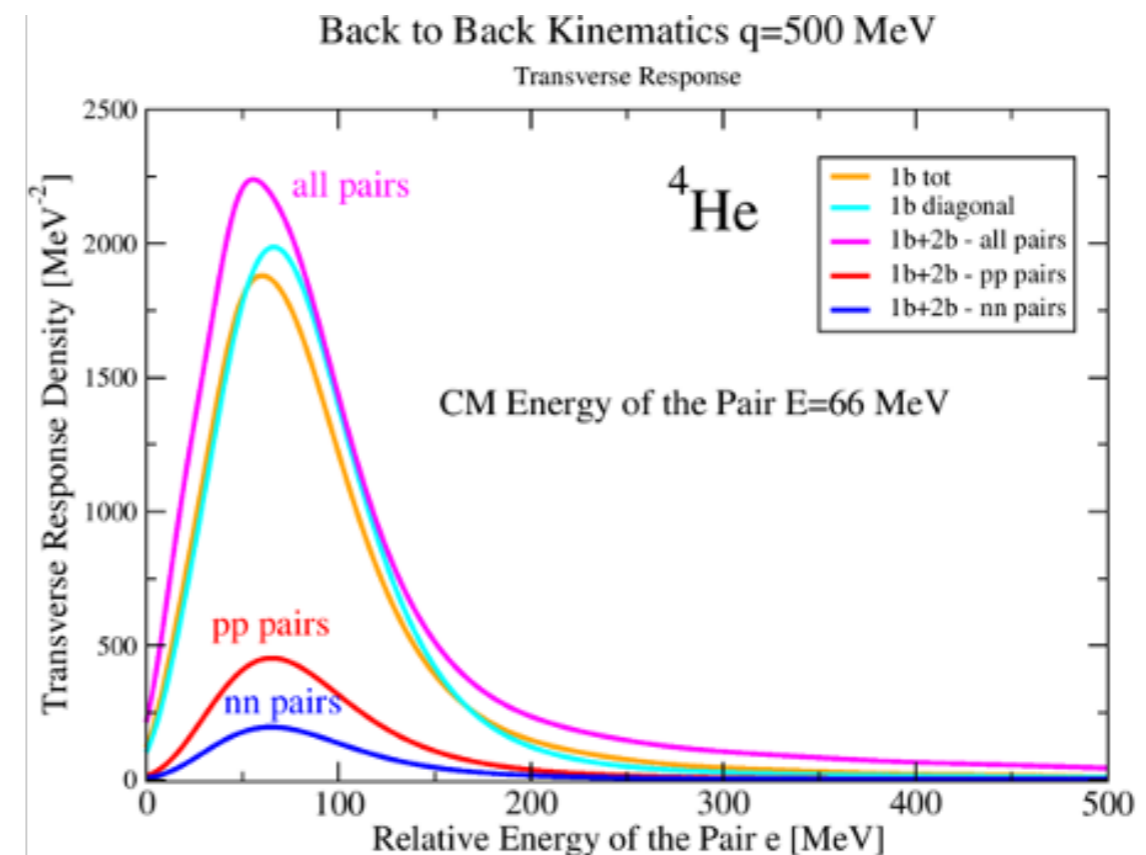
Pastore et al. PRC101(2020)044612

- pp pairs
- nn pairs
- 1 body tot
- all pairs tot

$$R^{\text{STA}}(q, \omega) \sim \int \delta(\omega + E_0 - E_f) de dE_{cm} \mathcal{D}(e, E_{cm}; q)$$

Electron scattering from ^4He :

- ❖ Response density as a function of (E, e)
- ❖ Give access to particular kinematics for the struck nucleon pair



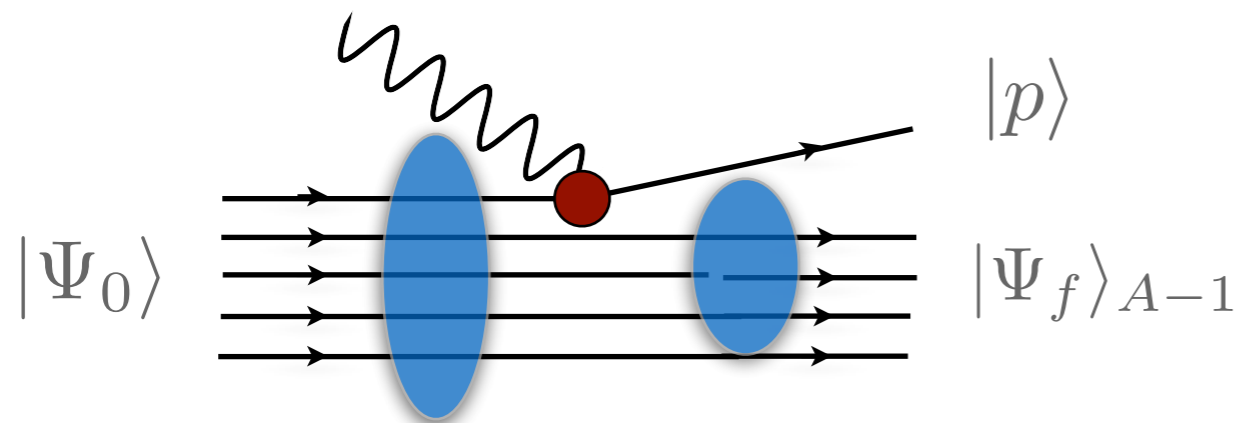
Spectral function approach

At large momentum transfer, the scattering reduces to the sum of individual terms

$$J_\alpha = \sum_i j_\alpha^i \qquad |\Psi_f\rangle \rightarrow |p\rangle \otimes |\Psi_f\rangle_{A-1}$$

The incoherent contribution of the one-body response reads

$$R_{\alpha\beta} \simeq \int \frac{d^3k}{(2\pi)^3} dE P_h(\mathbf{k}, E) \sum_i \langle k | j_\alpha^{i\dagger} | k + q \rangle \langle k + q | j_\beta^i | k \rangle \delta(\omega + E - e(\mathbf{k} + \mathbf{q}))$$



The Spectral Function is the imaginary part of the two point Green's Function

Different many-body methods can be adopted to determine it

I. Korover, et al Phys.Rev.C 107 (2023) 6, L061301

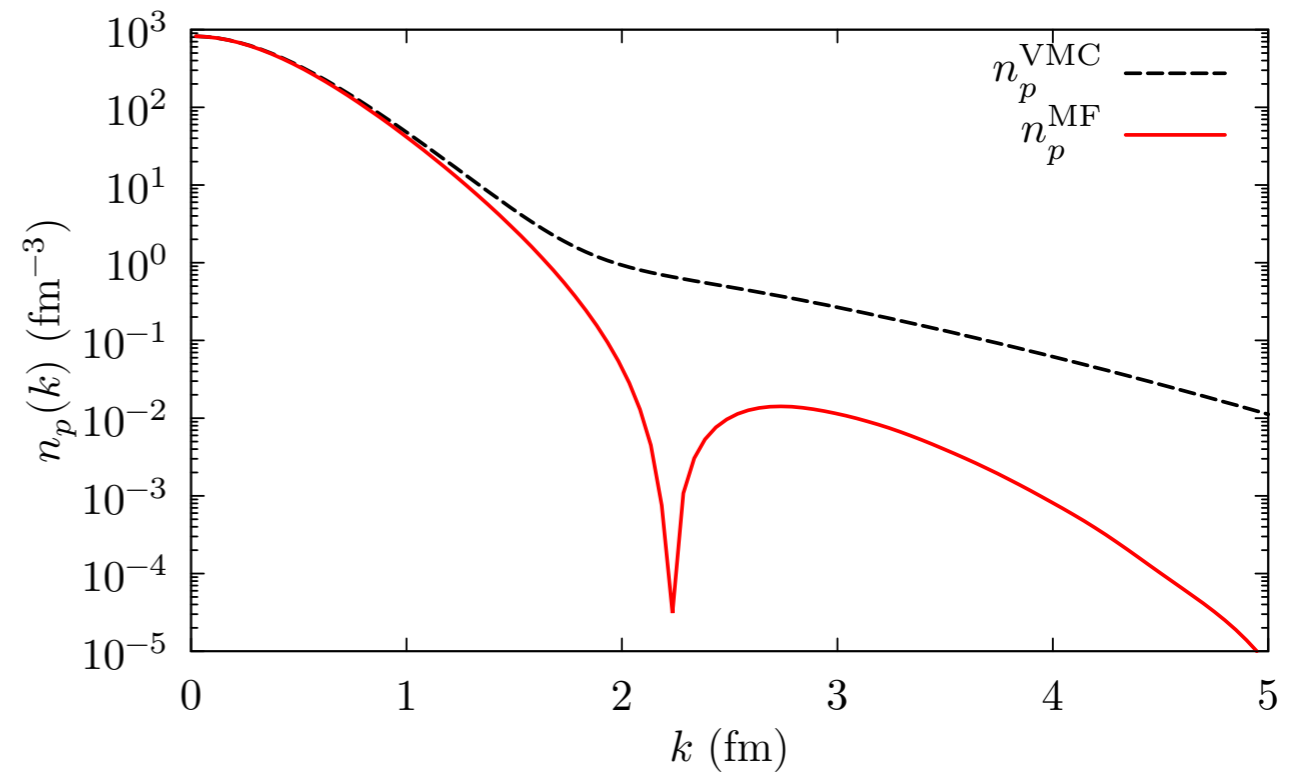
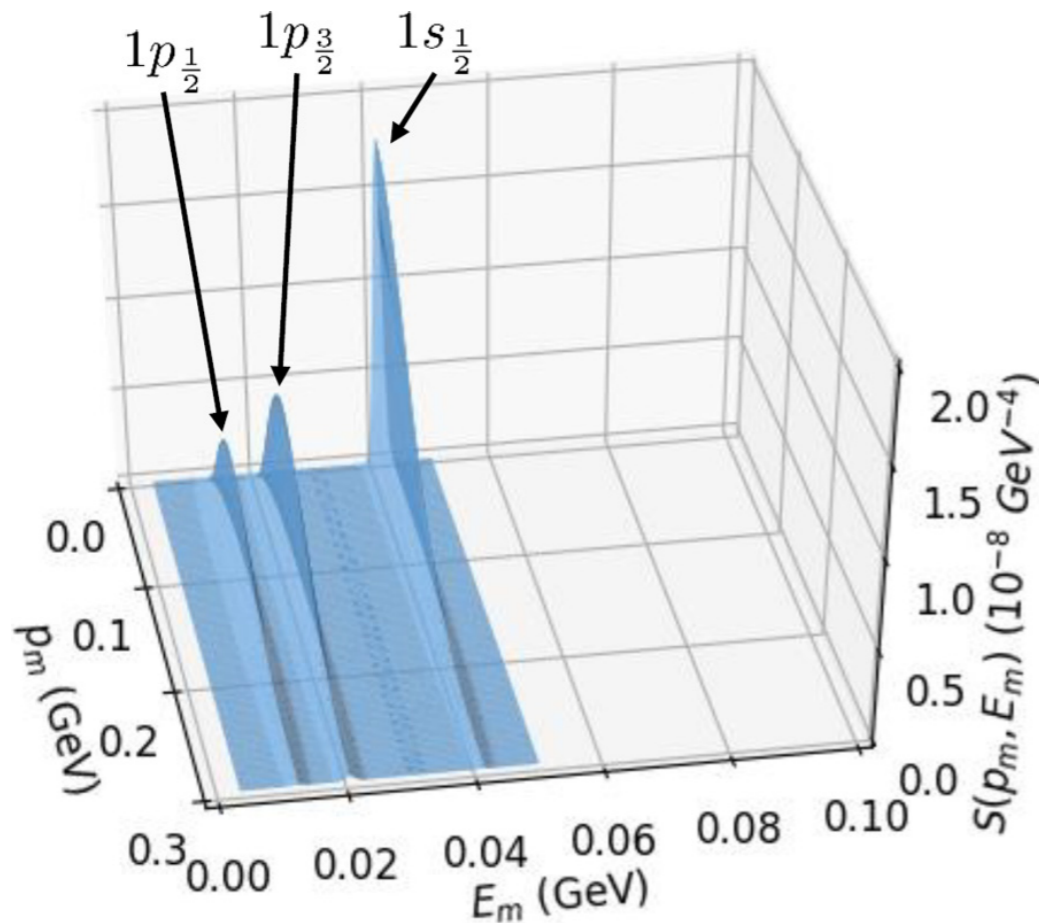
L. Andreoli, AL, et al. PRC 105, 014002 (2022)

NR, Frontiers in Phys. 8 (2020) 116

Spectral function approach

- Single-nucleon spectral function:

$$P_h(\mathbf{k}, E) = P_{\text{MF}}(\mathbf{k}, E) + P_{\text{corr}}(\mathbf{k}, E)$$



$$P_{\text{MF}}(\mathbf{k}, E) = \left| \langle \Psi_0^A | \left[|k\rangle \otimes |\Psi^{A-1}\rangle \right] \right|^2 \times \delta \left(E - B_0^A + B_0^{A-1} - \frac{k^2}{2M_{A-1}} \right)$$

- Can be derived from IPSM calculations + experiments or computed using ab-initio

QMC Spectral Function of ^{12}C

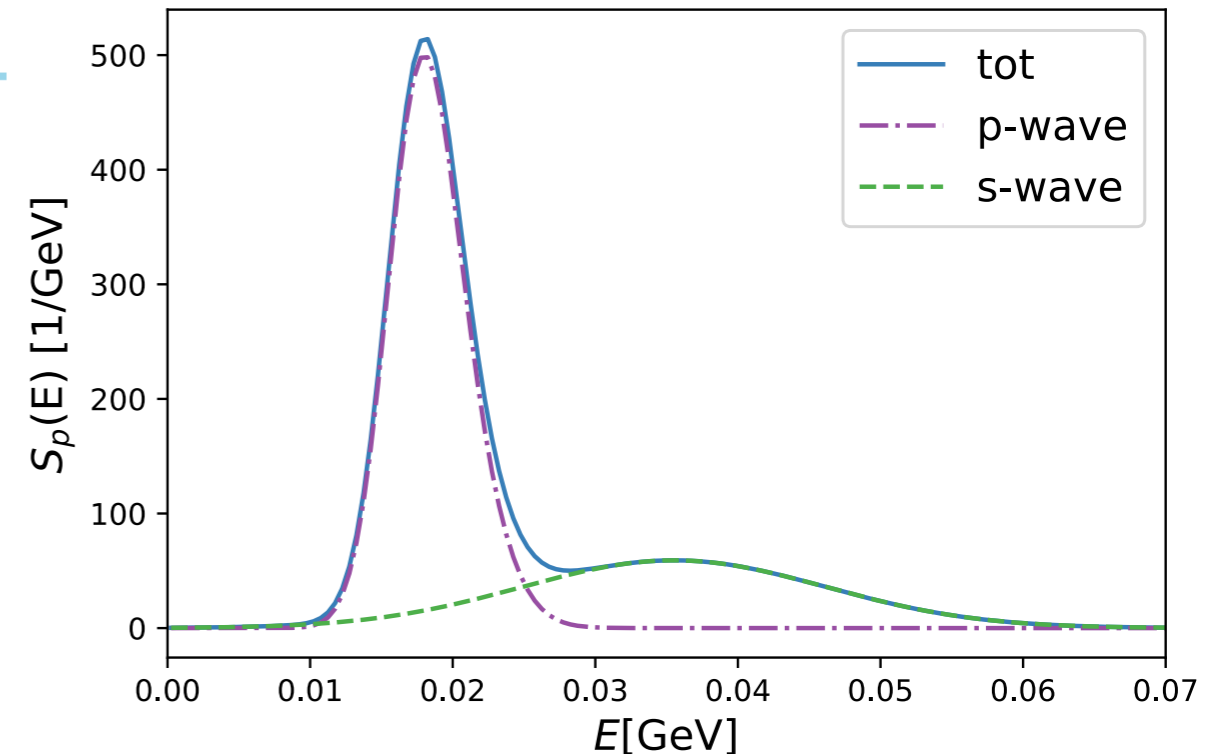
- The p-shell contribution has been obtained by FT the radial overlaps:

$$^{12}\text{C}(0^+) \rightarrow ^{11}\text{B}(3/2^-) + p$$

$$^{12}\text{C}(0^+) \rightarrow ^{11}\text{B}(1/2^-) + p$$

$$^{12}\text{C}(0^+) \rightarrow ^{11}\text{B}(3/2^-)^* + p.$$

R. Crespo, et al, Phys.Lett.B 803 (2020) 135355

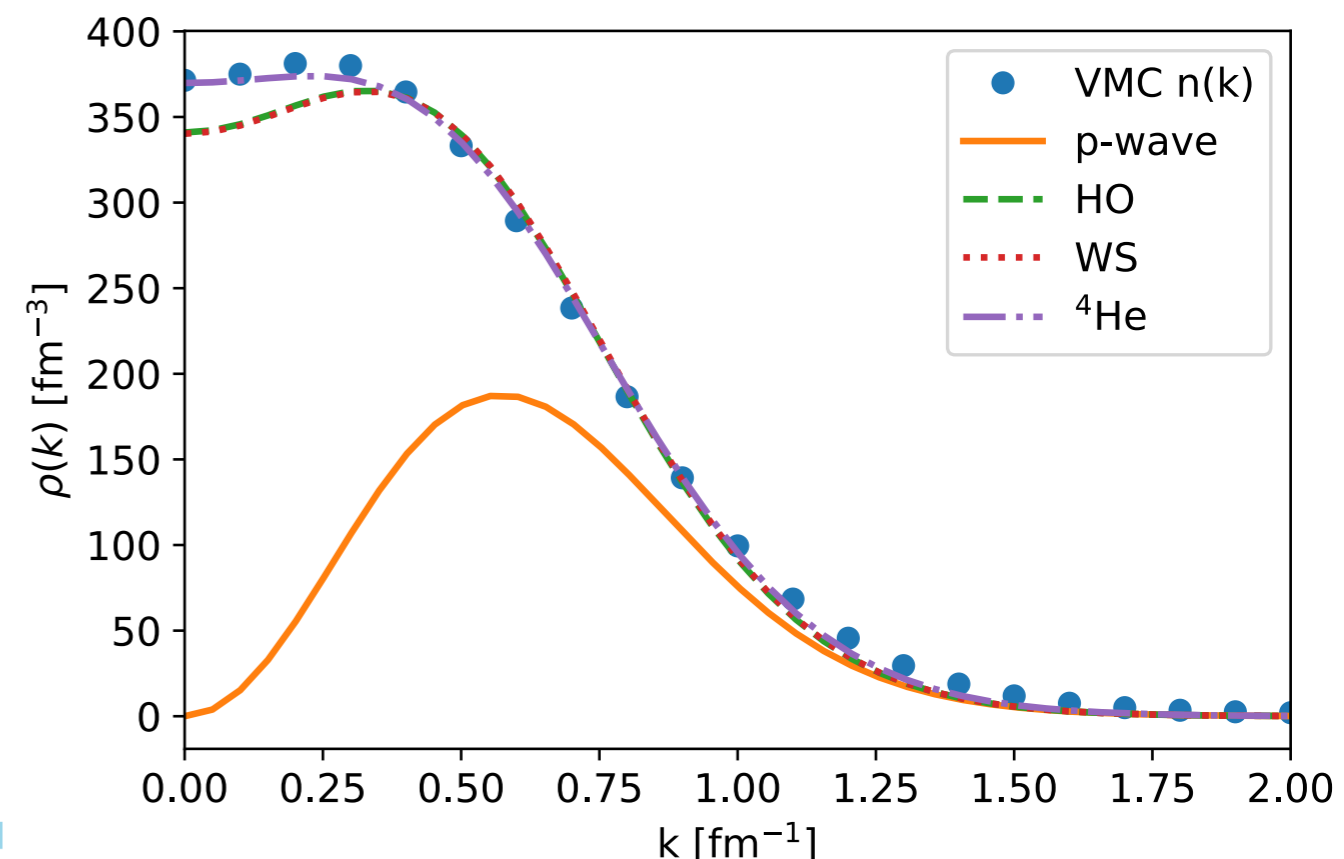


- The quenching of the spectroscopic factors automatically emerges from the VMC calculations

Computing the s-shell contribution is non trivial within VMC. We explored different alternatives:

- Quenched Harmonic Oscillator
- Quenched Wood Saxon
- VMC overlap associated for the $^4\text{He}(0^+) \rightarrow ^3\text{H}(1/2^+) + p$ transition

Korover, et al, CLAS collaboration submitted (2021)



Spectral function approach

$$P_p^{\text{corr}}(\mathbf{k}, E) = \sum_n \int \frac{d^3 k'}{(2\pi)^3} |\langle \Psi_0^A | [|\mathbf{k}\rangle |\mathbf{k}'\rangle | \Psi_n^{A-2} \rangle|^2 \delta(E + E_0^A - e(\mathbf{k}') - E_n^{A-2})$$

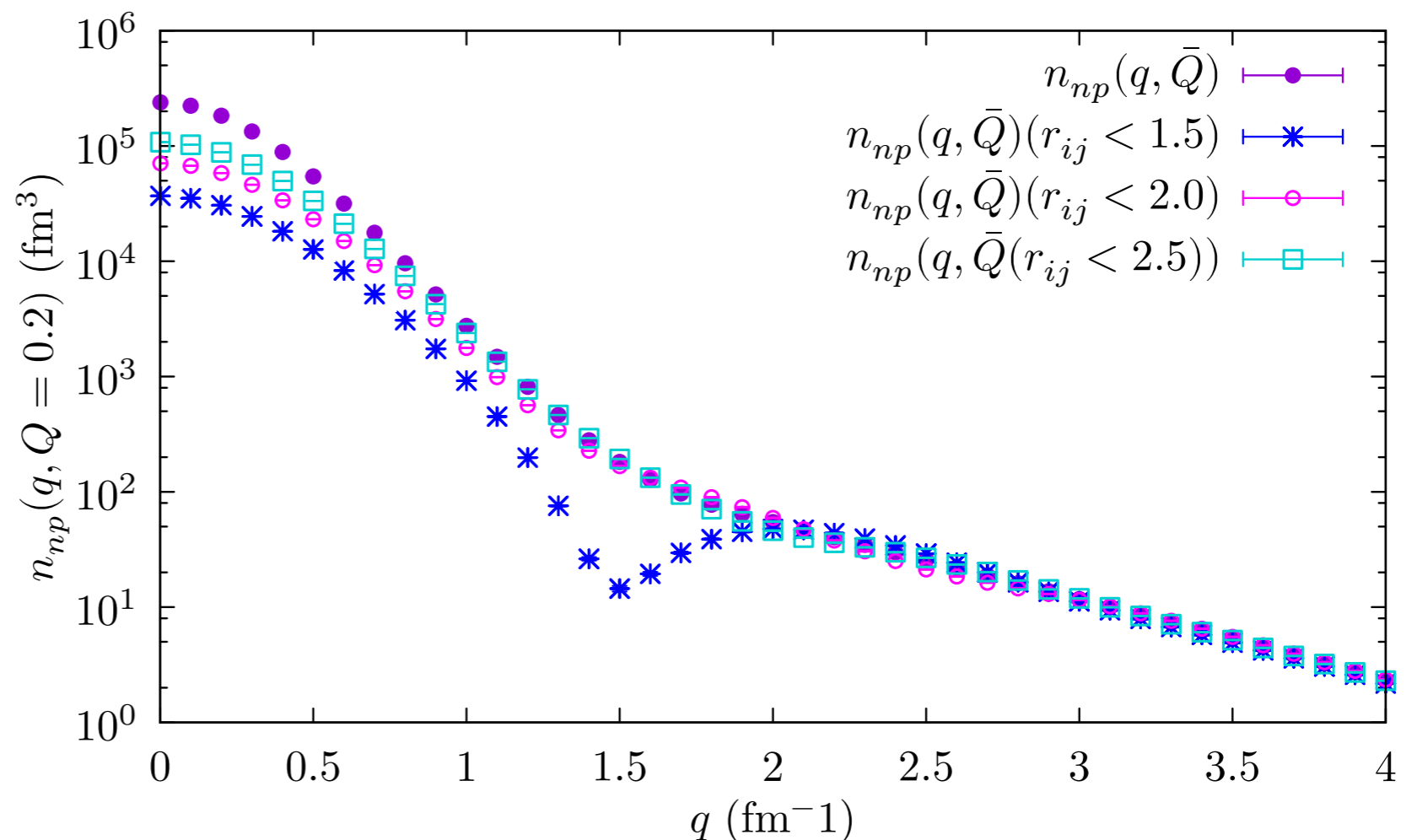


Using QMC techniques

$$\sum_{\tau_{k'}=p,n} n_{p,\tau_{k'}}(\mathbf{k}, \mathbf{k}') \delta\left(E - B_A - e(\mathbf{k}') + B_{A-2} - \frac{(\mathbf{k} + \mathbf{k}')^2}{2m_{A-2}}\right)$$

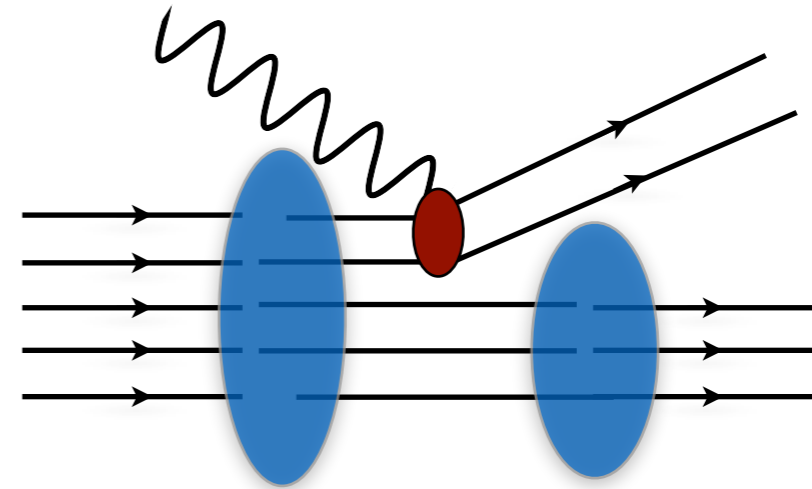
Only SRC pairs should be considered: $|\Psi_0^{A-1}\rangle$ and $|\mathbf{k}'\rangle |\psi_n^{A-2}\rangle$ be orthogonalized

One can introduce **cuts** on the **relative distance** between the particles in the two-body momentum distribution



Two-body currents

$$|f\rangle \rightarrow |pp'\rangle_a \otimes |f_{A-2}\rangle \rightarrow$$

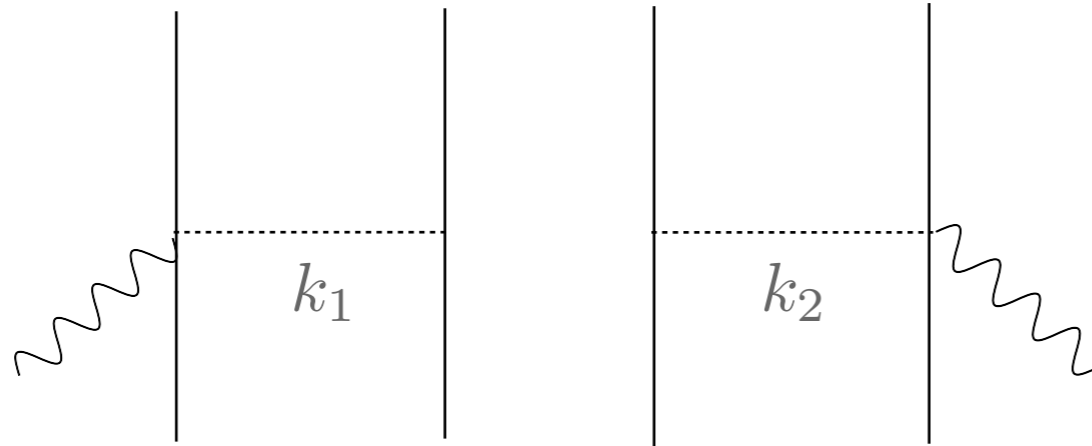


$$R_{2b}^{\mu\nu}(\mathbf{q}, \omega) = \frac{V}{4} \int dE d^3k d^3k' d^3p d^3p' P_{2b}(\mathbf{k}, \mathbf{k}', E) 2 \langle kk' | j_{2b}^{\mu} | pp' \rangle_a \langle pp' | j_{2b}^{\nu \dagger} | kk' \rangle \\ \times \delta(\omega - E + 2m - e(\mathbf{p}) - e(\mathbf{p}')) \delta^{(3)}(\mathbf{p} + \mathbf{q} - \mathbf{p}')$$

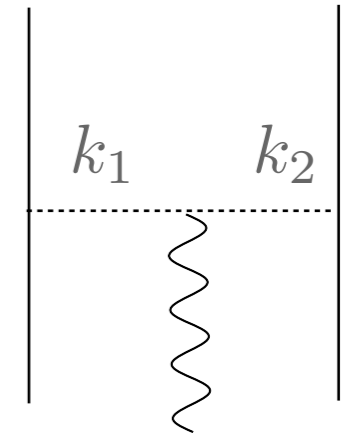
The normalization volume for the nuclear wave functions $V = \rho/A$ with $\rho = 3\pi^2 k_F^3/2$ depends on the Fermi momentum of the nucleus

Factor 1/4 accounts for the fact that we sum over indistinguishable pairs of particles, while the factor 2 stems from the equality of the product of the direct terms and the product of the two exchange terms after interchange of indices

Two-body currents - pion contribution



Seagull



Pion in flight

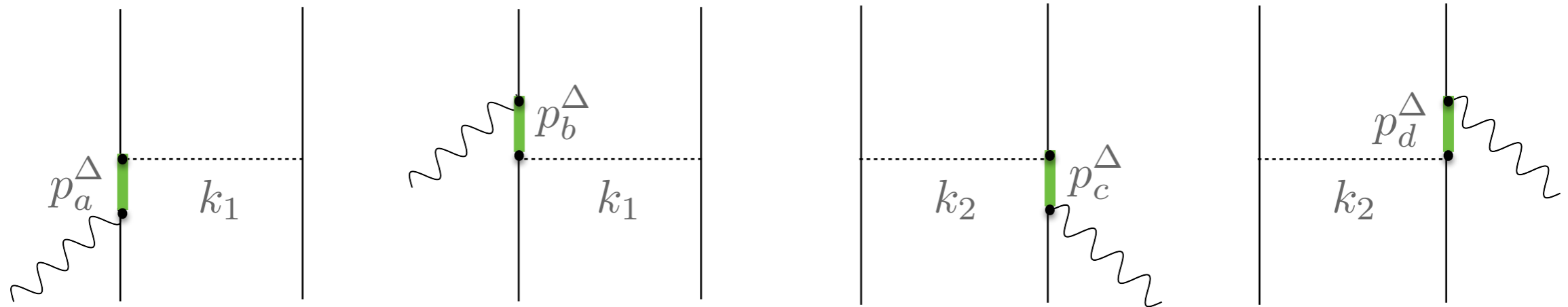
$$(J_{\text{sea}}^\mu) = (I_V)_z \frac{f_{\pi NN}^2}{m_\pi^2} F_1^V(q) F_{\pi NN}^2(k_1) \Pi(k_1)_{(1)} (\gamma_5 \gamma^\mu)_{(2)} - (1 \leftrightarrow 2)$$

Isospin structure: $(I_V)_z = (\tau^{(1)} \times \tau^{(2)})_z$

$$J_{\text{pif}}^\mu = \frac{f_{\pi NN}^2}{m_\pi^2} F_1^V(q) F_{\pi NN}(k_1) F_{\pi NN}(k_2) \Pi(k_1)_{(1)} \Pi(k_2)_{(2)} (k_1^\mu - k_2^\mu)$$

Pion propagation and absorption: $\Pi(k) = \frac{\gamma_5 \not{k}}{k^2 - m_\pi^2}$

Two-body currents - Delta contribution



$$j_{\Delta}^{\mu} = \frac{3}{2} \frac{f_{\pi NN} f^{*}}{m_{\pi}^2} \left\{ \Pi(k_2)_{(2)} \left[\left(-\frac{2}{3} \tau^{(2)} + \frac{I_V}{3} \right)_z F_{\pi NN}(k_2) F_{\pi N\Delta}(k_2) (J_a^{\mu})_{(1)} \right. \right. \\ \left. \left. - \left(\frac{2}{3} \tau^{(2)} + \frac{I_V}{3} \right)_z F_{\pi NN}(k_2) F_{\pi N\Delta}(k_2) (J_b^{\mu})_{(1)} \right] + (1 \leftrightarrow 2) \right\}$$

where

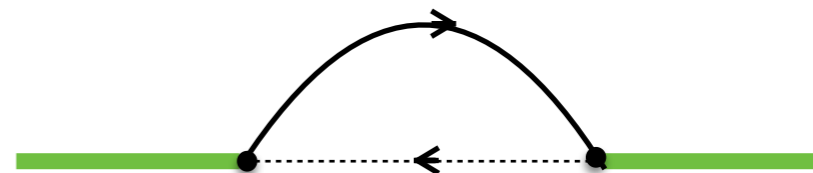
Rarita Schwinger propagator

$$(J_a^{\mu})_V = (k_1)^{\alpha} G_{\alpha\beta}(p_{\Delta}) \left[\frac{C_3^V}{m_N} \left(g^{\beta\mu} \not{q} - q^{\beta} \gamma^{\mu} \right) + \frac{C_4^V}{m_N^2} \left(g^{\beta\mu} q \cdot p_{\Delta} - q^{\beta} p_{\Delta}^{\mu} \right) \right. \\ \left. + \frac{C_5^V}{m_N^2} \left(g^{\beta\mu} q \cdot k - q^{\beta} k^{\mu} + C_6^V g^{\beta\mu} \right) \right] \gamma_5$$

Two-body currents - Delta contribution

Rarita-Schwinger propagator

$$G^{\alpha\beta}(p_\Delta) = \frac{P^{\alpha\beta}(p_\Delta)}{p_\Delta^2 - M_\Delta^2}$$



The spin 3/2 projection operator reads

$$P^{\alpha\beta}(p_\Delta) = (\not{p}_\Delta + M_\Delta) \left[g^{\alpha\beta} - \frac{1}{3} \gamma^\alpha \gamma^\beta - \frac{2}{3} \frac{p_\Delta^\alpha p_\Delta^\beta}{M_\Delta^2} + \frac{1}{3} \frac{p_\Delta^\alpha \gamma^\beta - p_\Delta^\beta \gamma^\alpha}{M_\Delta} \right].$$

To account for the resonant behavior of the Δ : $M_\Delta \rightarrow M_\Delta - i\Gamma(p_\Delta)/2$

$$\Gamma(p_\Delta) = -2\text{Im}\Sigma_{\pi N}(s) = \frac{(4f_{\pi N\Delta})^2}{12\pi m_\pi^2} \frac{|\mathbf{d}|^3}{\sqrt{s}} (m_N + E_d) R(r^2)$$

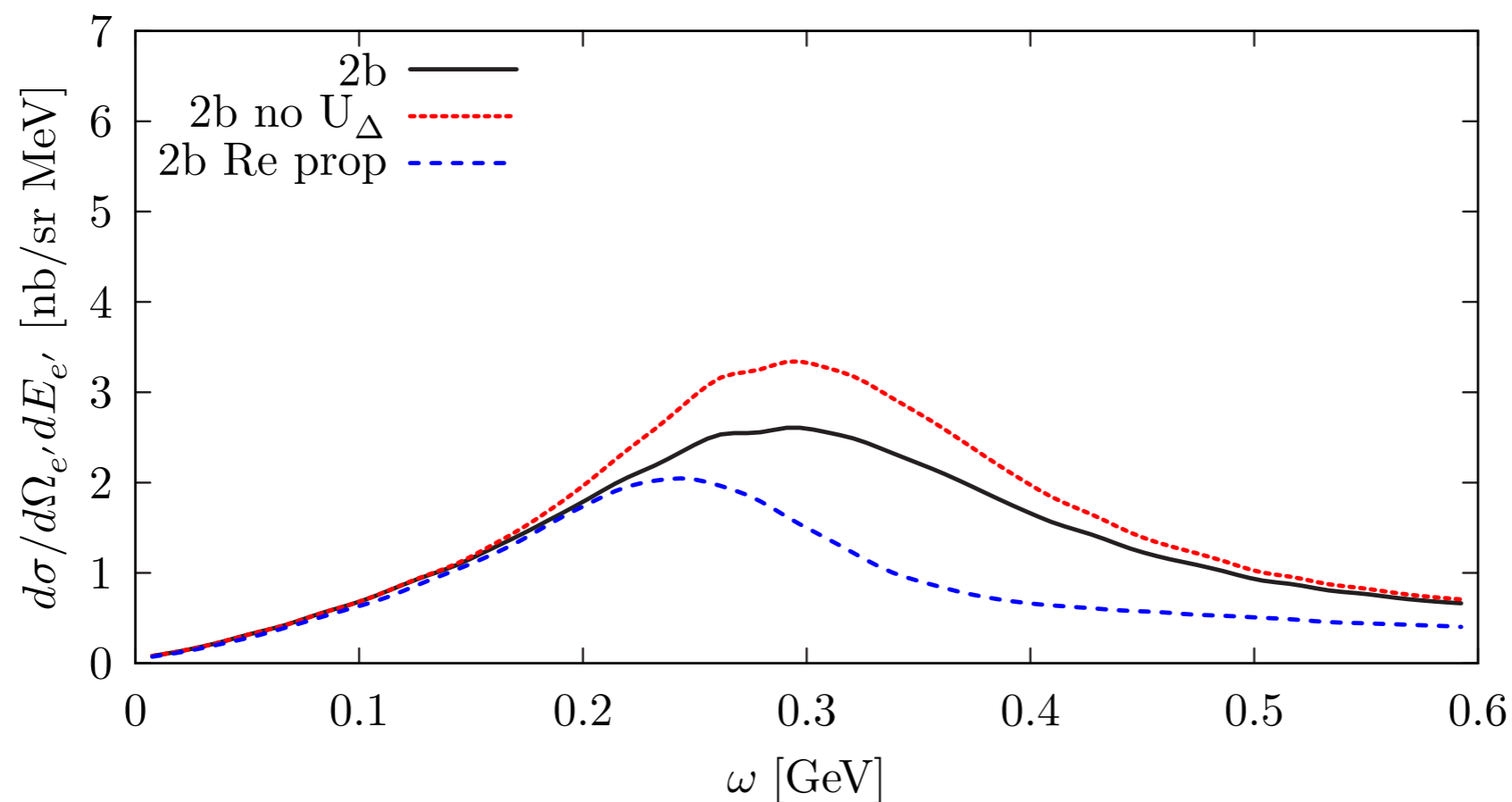
\mathbf{d} is the decay three-momentum in the πN center of mass frame

In medium effects of the Δ $\Gamma_\Delta(p_\Delta) \rightarrow \Gamma_\Delta(p_\Delta) - 2\text{Im}[U_\Delta(p_\Delta, \rho = \rho_0)]$

Two-body currents - Delta contribution

$E_e=730 \text{ MeV}, \theta_e=37.0^\circ$

NR, et al, PRC 100 045503, 2019



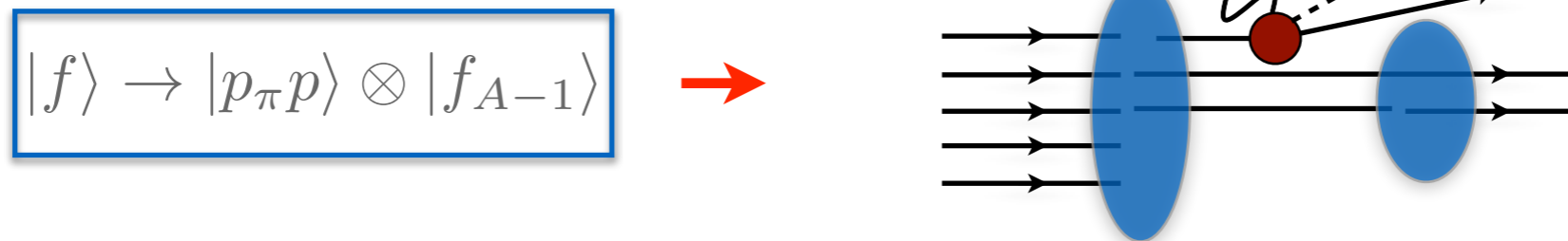
$$\Gamma(p_\Delta) = -2\text{Im}\Sigma_{\pi N}(s) = \frac{(4f_{\pi N\Delta})^2}{12\pi m_\pi^2} \frac{|\mathbf{d}|^3}{\sqrt{s}} (m_N + E_d) R(r^2)$$

\mathbf{d} is the decay three-momentum in the πN center of mass frame

In medium effects of the Δ

$$\Gamma_\Delta(p_\Delta) \rightarrow \Gamma_\Delta(p_\Delta) - 2\text{Im}[U_\Delta(p_\Delta, \rho = \rho_0)]$$

Spectral function approach



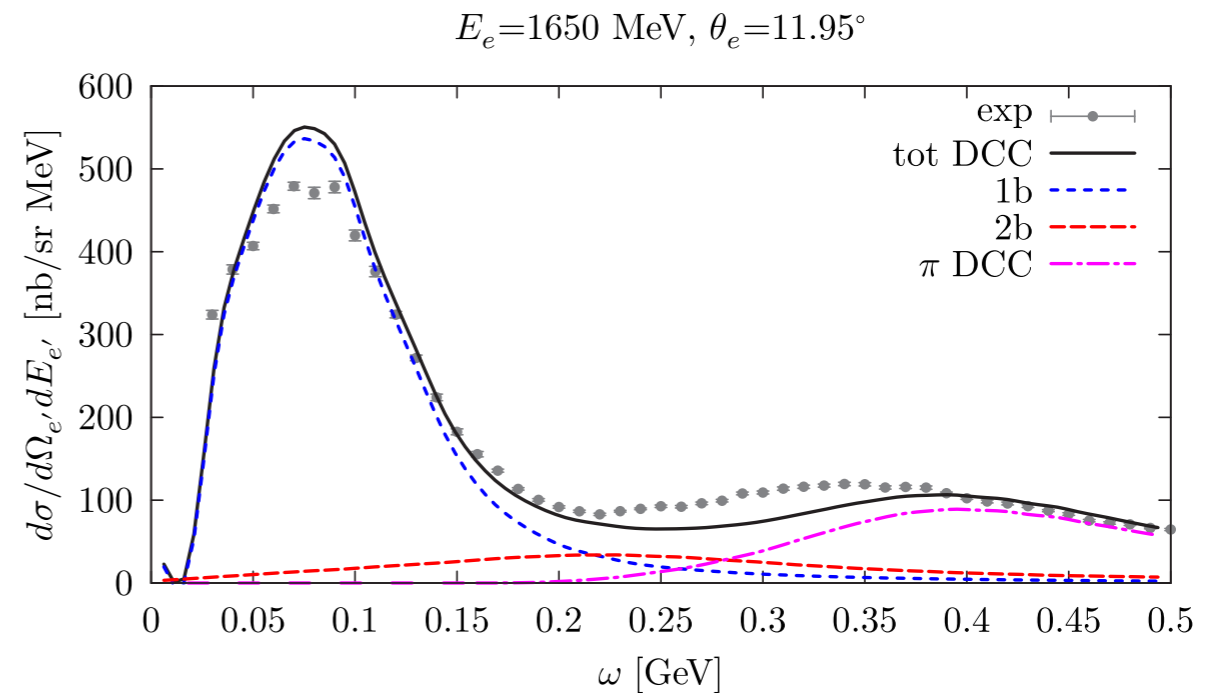
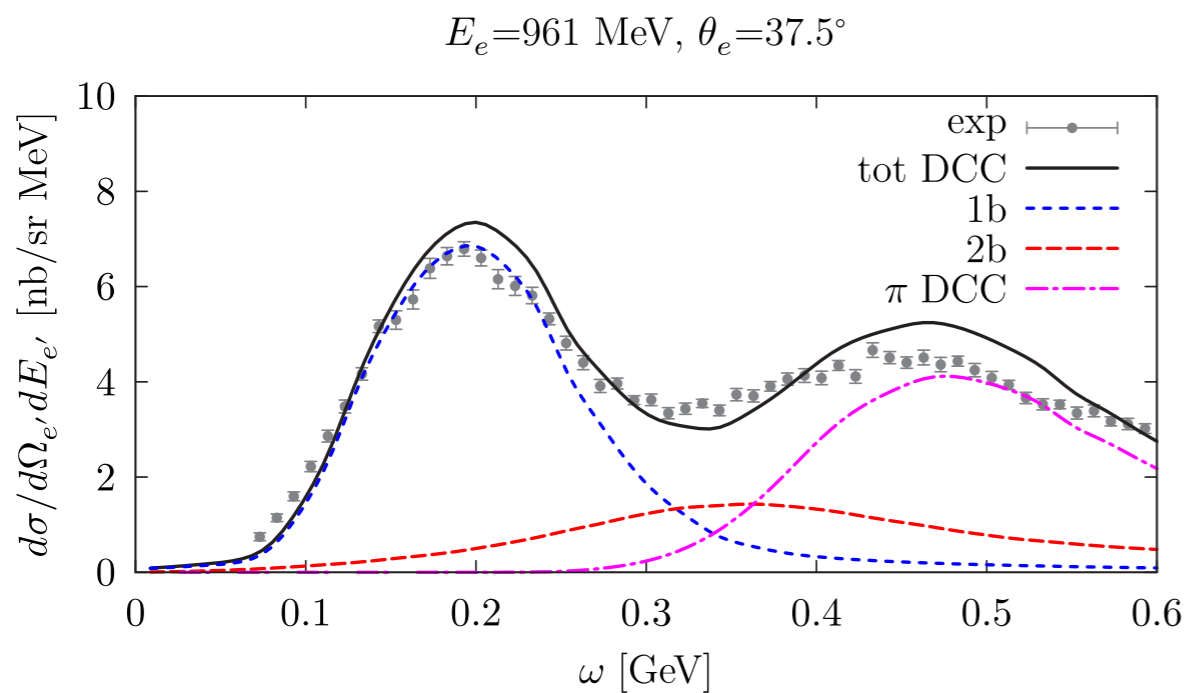
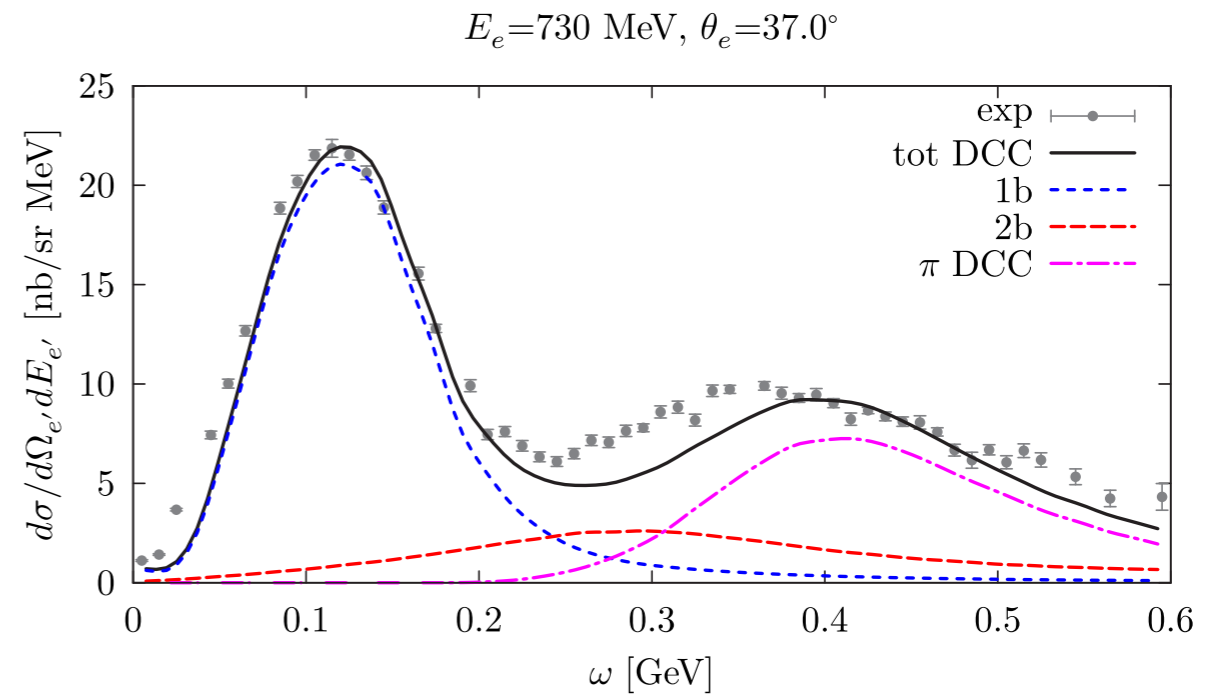
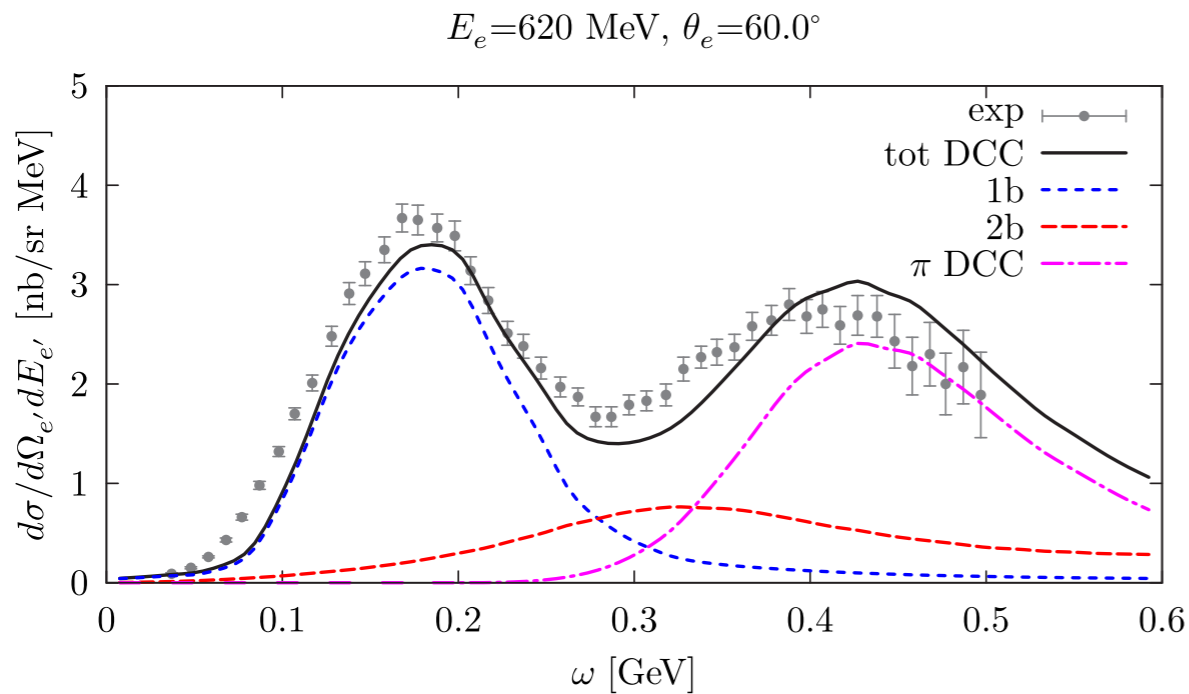
Production of real π in the final state:

$$R_{1b1\pi}^{\mu\nu}(\mathbf{q}, \omega) = \int \frac{d^3 k}{(2\pi)^3} dE P_h(\mathbf{k}, E) \frac{d^3 p_\pi}{(2\pi)^3} \sum_I \langle k | j_I^{\mu\dagger} | p_\pi p \rangle \langle p_\pi p | j_I^\nu | k \rangle \Big|_{\mathbf{p}=\mathbf{k}+\mathbf{q}-\mathbf{p}_\pi} \\ \times \delta(\omega - E + m_N - e(\mathbf{k} + \mathbf{q} - \mathbf{p}_\pi) - e_\pi(\mathbf{p}_\pi)) ,$$

* Pion production elementary amplitudes currently derived within the **Dynamic Couple Chanel approach**;

Spectral function approach

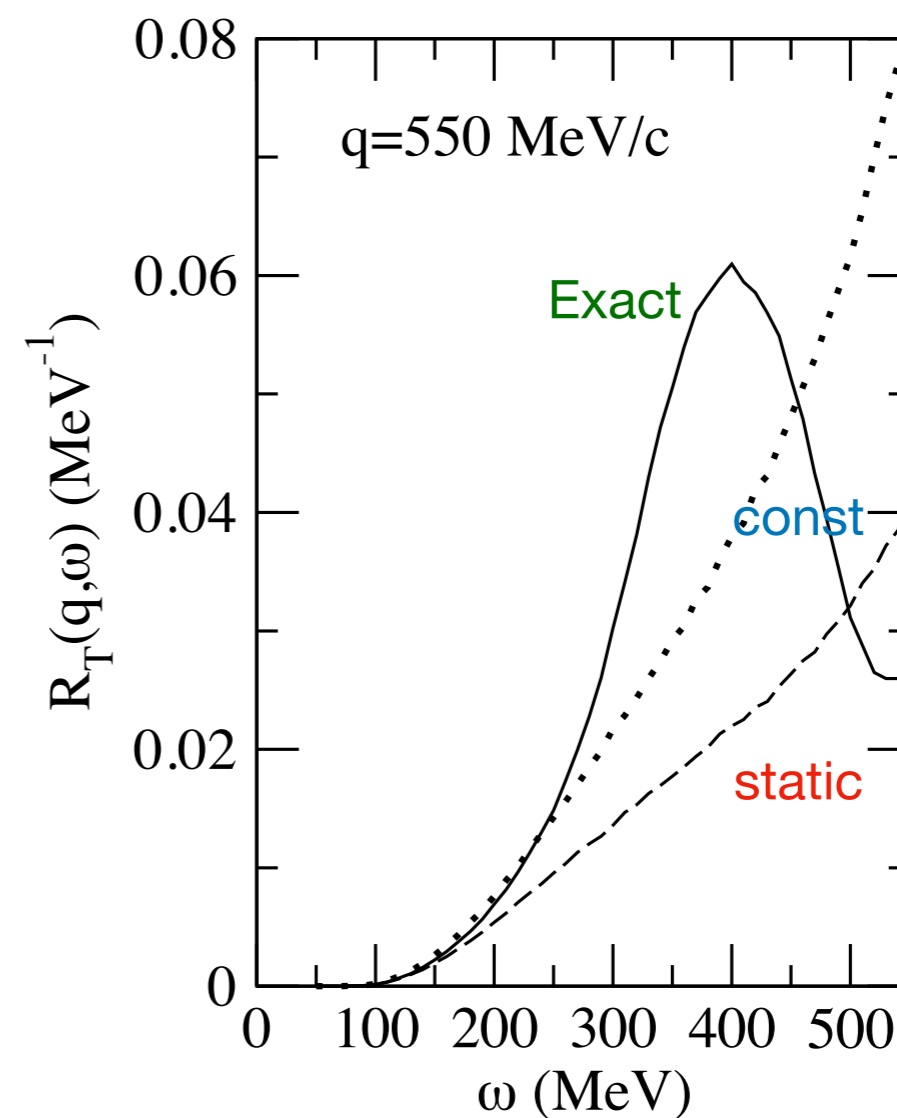
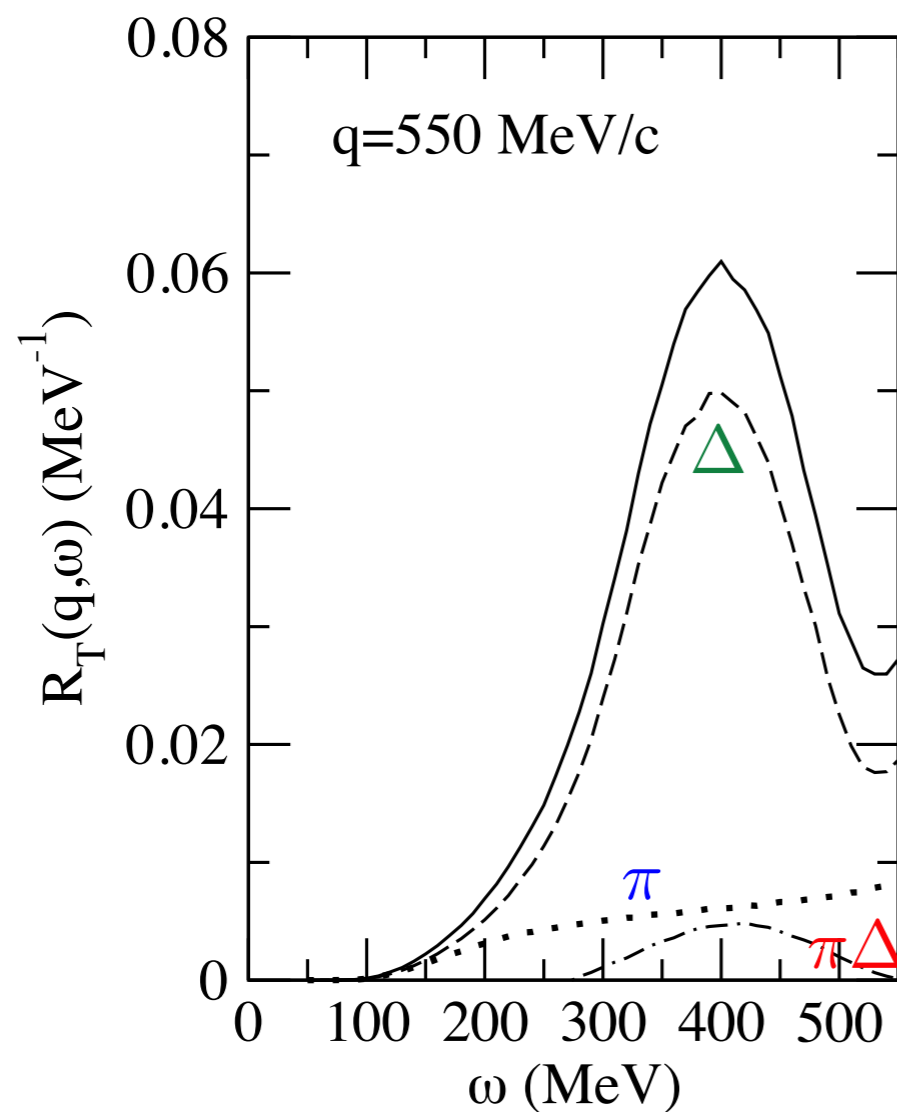
NR, et al, PRC 100 045503, 2019



Electron scattering results

Two-body currents - Delta contribution

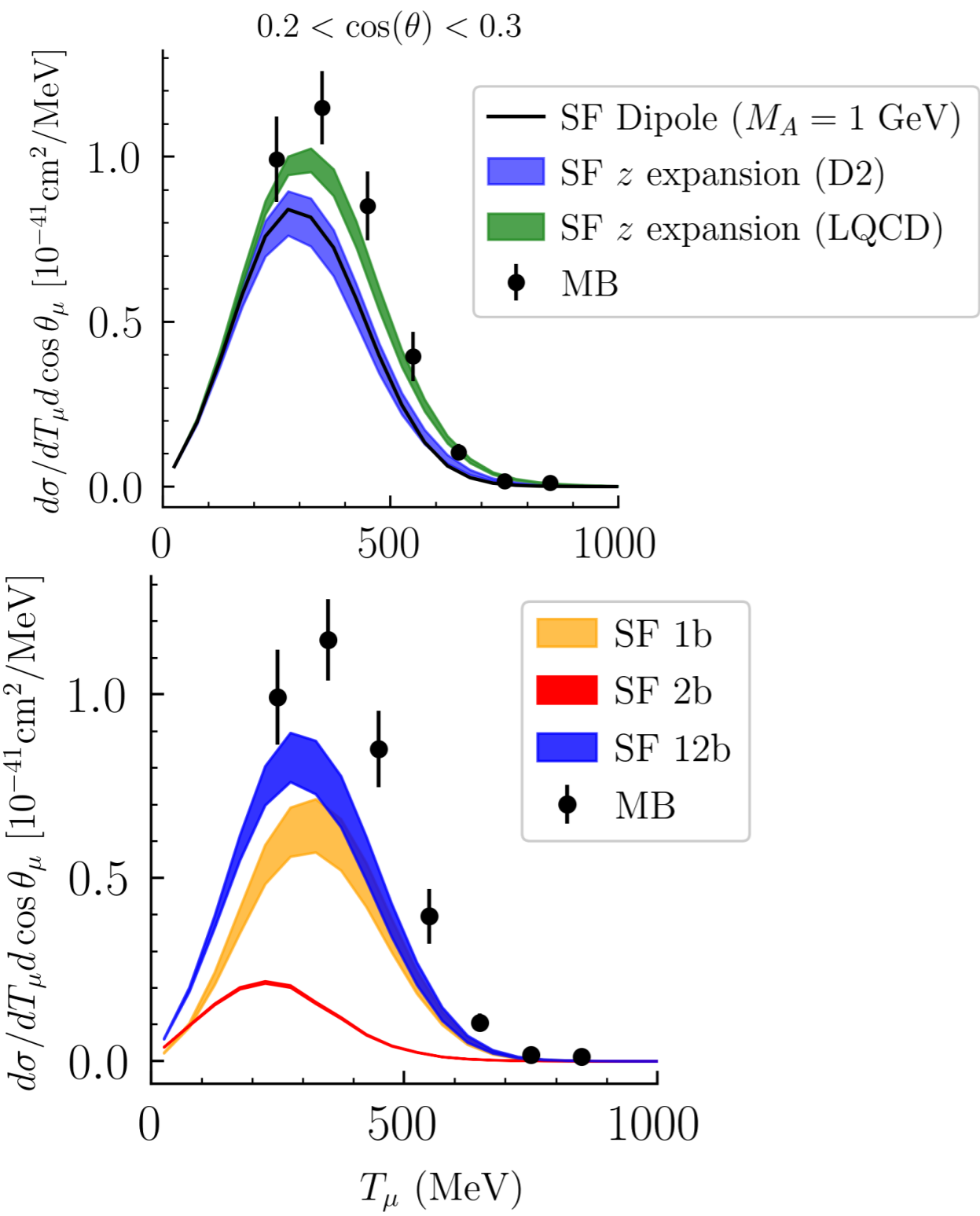
A. De Pace, et al, Nucl.Phys.A 726 (2003) 303-326



RGFG — electromagnetic response of $A=56$ $k_F=1.3$ fm⁻¹

Axial Form Factors Uncertainty needs

D.Simons, N. Steinberg et al, 2210.02455



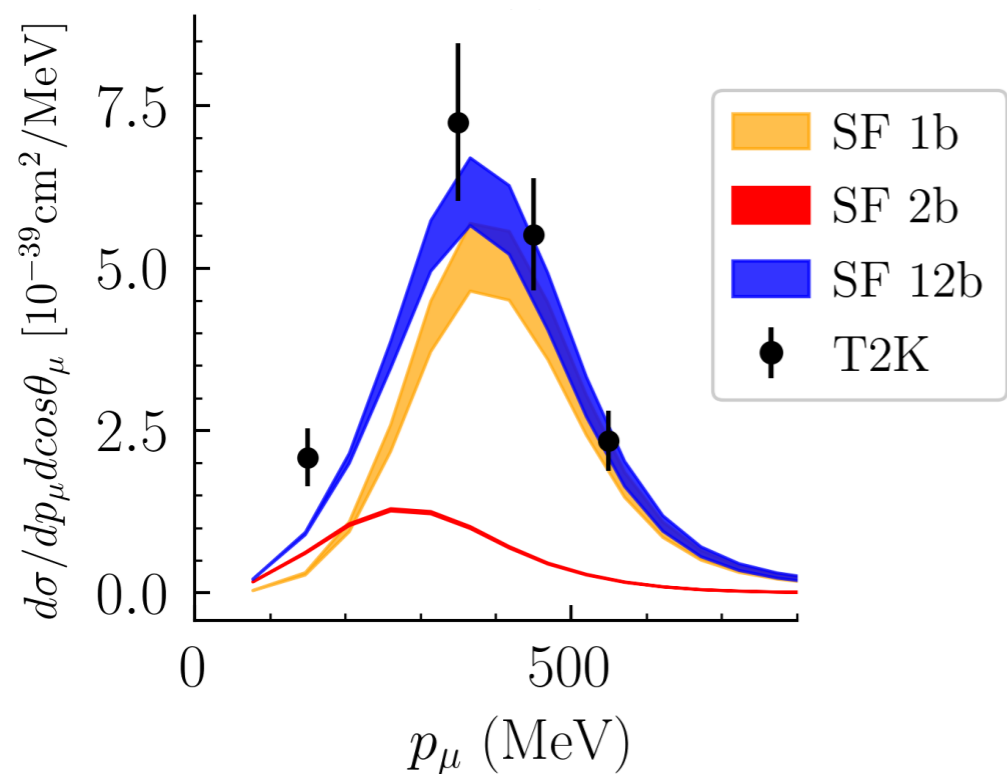
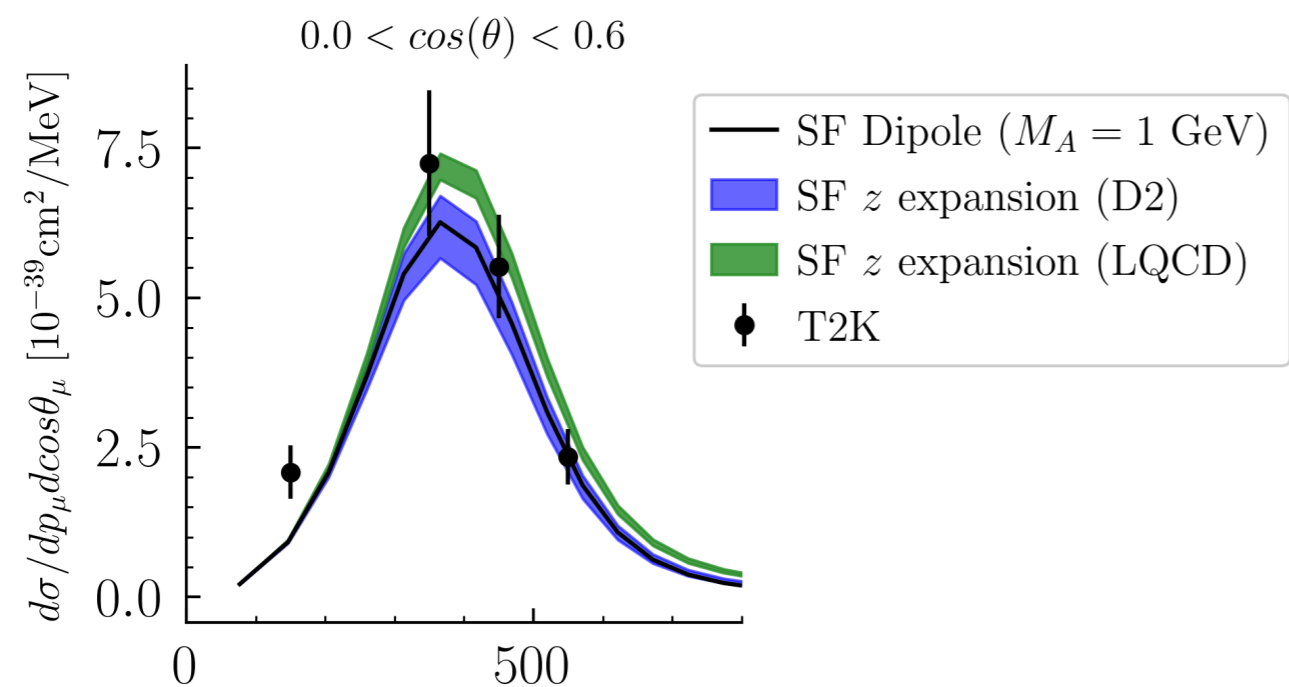
* Axial form factor dependence:

MiniBooNE	0.2 < cos θ_μ < 0.3
SF Difference in $d\sigma_{\text{peak}}$ (%)	16.3

* Many-body method dependence:

MiniBooNE	0.2 < cos θ_μ < 0.3
GFMC/SF difference in $d\sigma_{\text{peak}}$ (%)	22.8

Axial Form Factors Uncertainty needs



D.Simons, N. Steinberg et al, 2210.02455

* Axial form factor dependence:

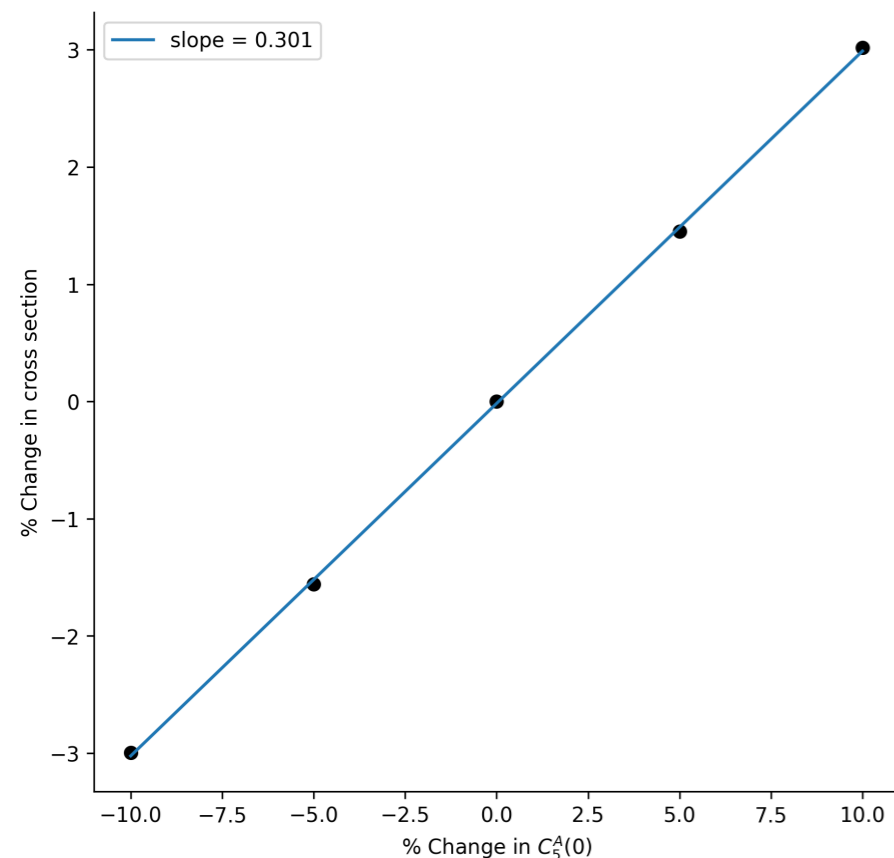
T2K	0.0 < cos θ_μ < 0.6
SF difference in $d\sigma_{\text{peak}}$ (%)	15.3

* Many-body method dependence:

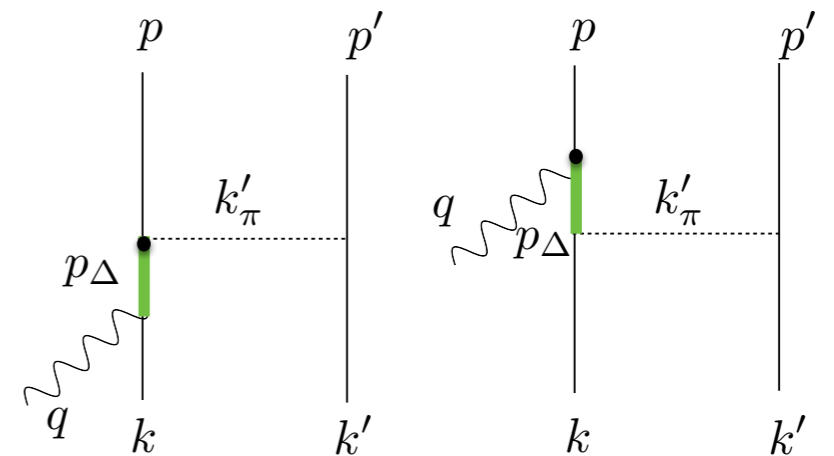
T2K	0.0 < cos θ_μ < 0.6
GFMC/SF difference in $d\sigma_{\text{peak}}$ (%)	13.4

Resonance Uncertainty needs

The largest contributions to two-body currents arise from resonant $N \rightarrow \Delta$ transitions yielding pion production



D.Simons, N. Steinberg et al, 2210.02455



The normalization of the dominant $N \rightarrow \Delta$ transition form factor needs be known to 3% precision to achieve 1% cross-section precision for MiniBooNE kinematics

State-of-the-art determinations of this form factor from experimental data on pion electroproduction achieve 10-15% precision (under some assumptions)

Hernandez et al, PRD 81 (2010)

Further constraints on $N \rightarrow \Delta$ transition relevant for two-body currents and π production will be necessary to achieve few-percent cross-section precision

Scaling in the Fermi gas model

- Scaling of the first kind: the nuclear electromagnetic responses divided by an appropriate function describing the single-nucleon physics no longer depend on two variables ω and \mathbf{q} , but only upon $\psi(\mathbf{q}, \omega)$

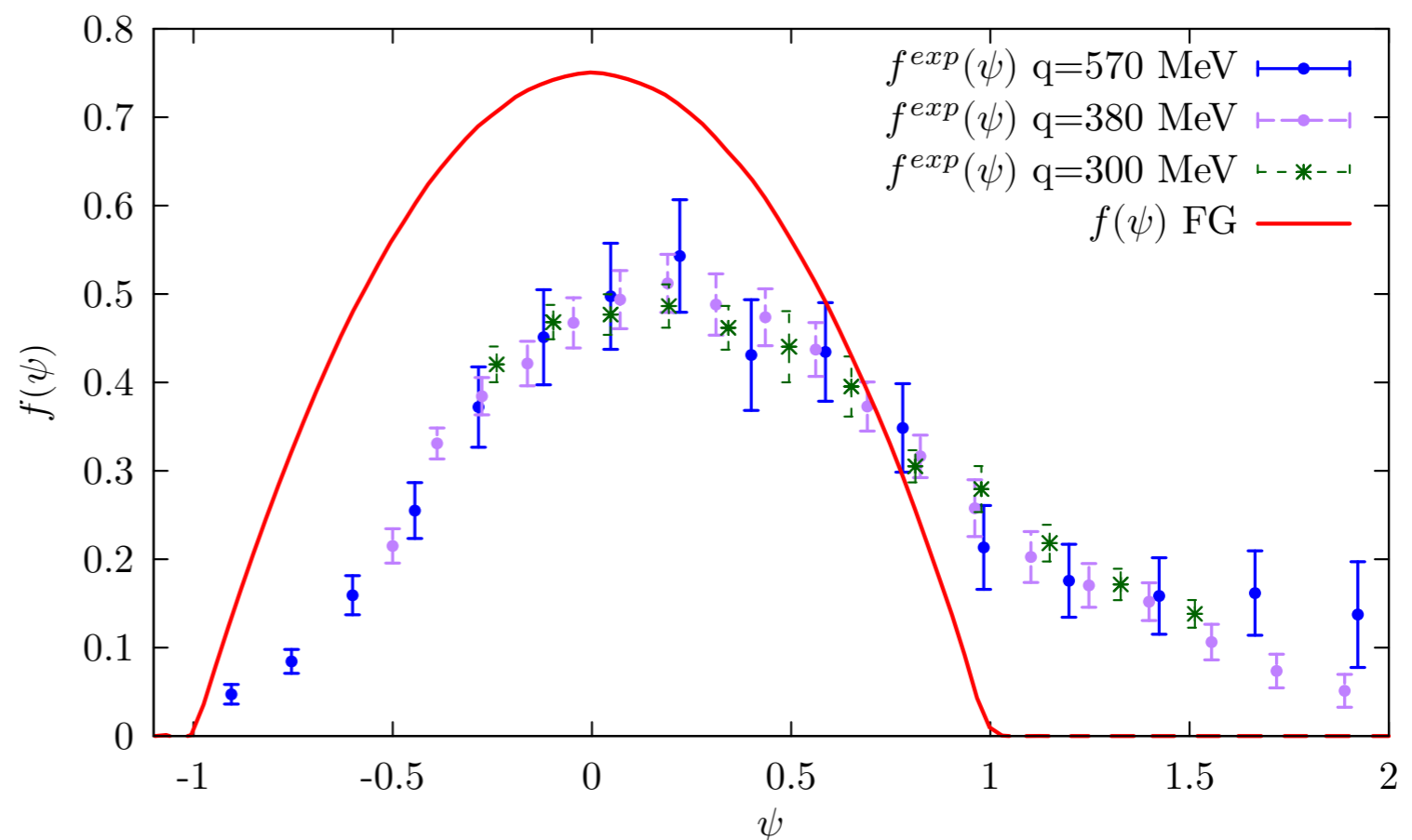
$$f_{L,T}(\mathbf{q}, \omega) = p_F \frac{R_{L,T}}{G_{L,T}} = \frac{\text{nuclear response function}}{\text{elem single nucleon function}}$$

- For sufficiently large values of \mathbf{q}

$$f(\mathbf{q}, \omega) \rightarrow f(\psi)$$

- Within the Relativistic Fermi gas scaling of the first kind is exactly fulfilled

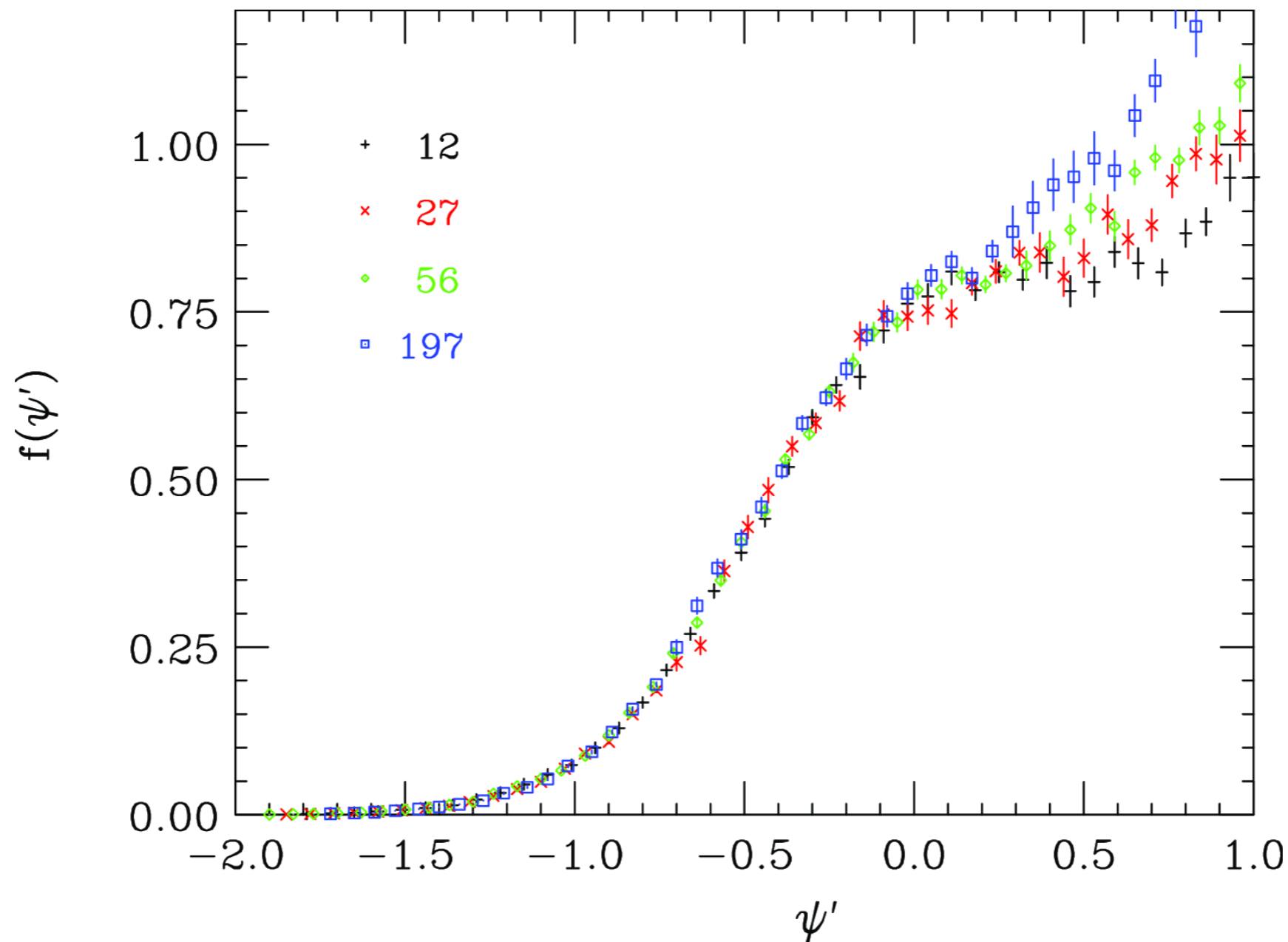
$$f_{\text{RFG}} = \frac{3}{4}(1 - \psi^2)$$



- Scaling function of ^{12}C , obtained dividing the R_L by the single nucleon functions for different \mathbf{q}

Scaling in the Fermi gas model

- Scaling of the second kind: independence of the nuclear species A

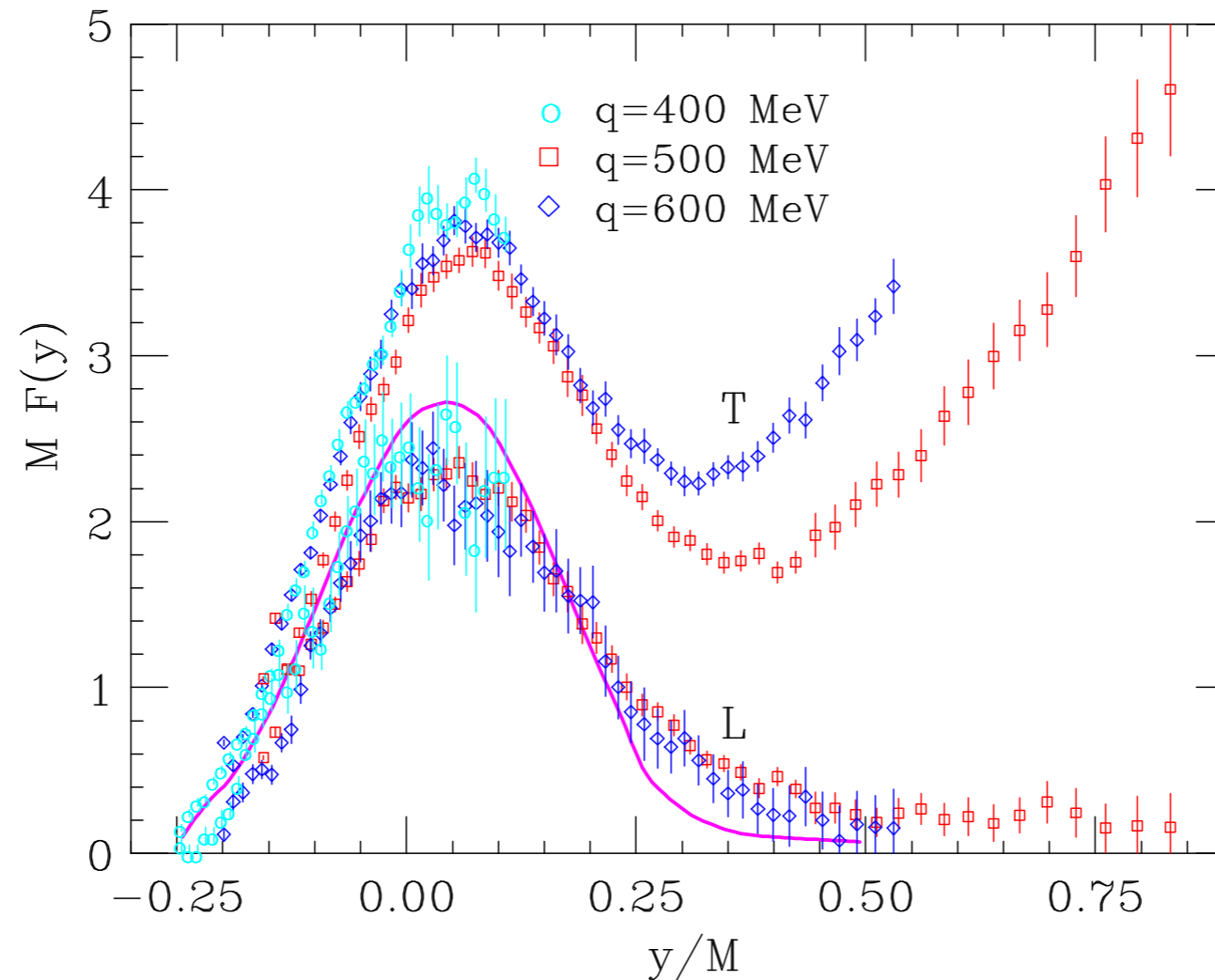


Two-body currents violate scaling

- Within the FG model we have this simple expression:

$$R_{L,T} = (1 - \psi^2)\theta(1 - \psi^2) \times G_{L,T}$$

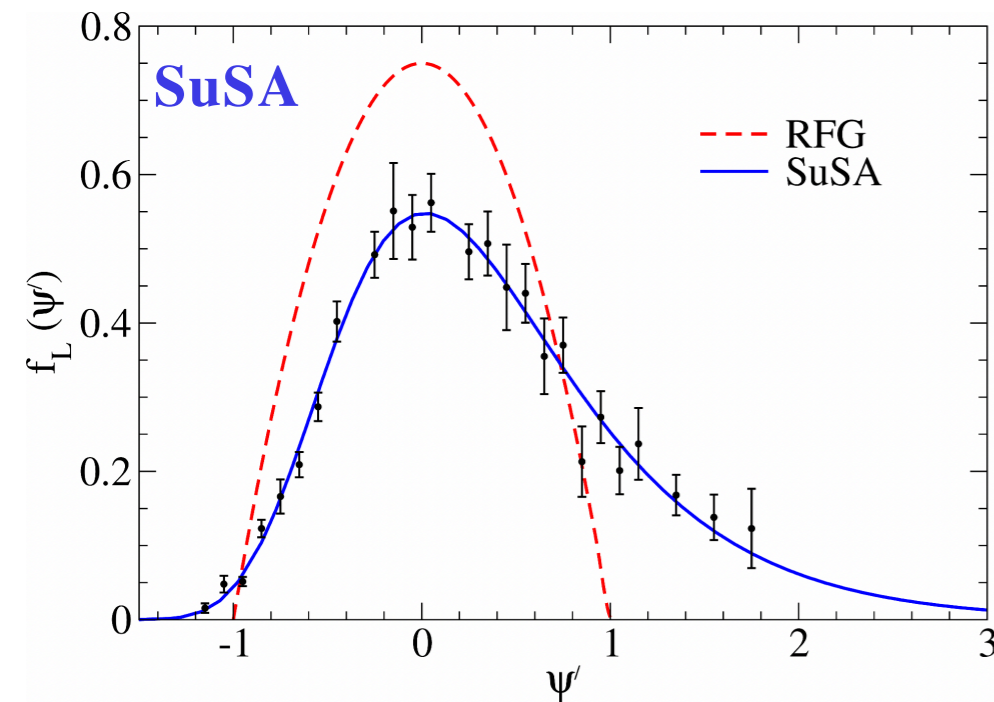
- Scaling functions associated with the longitudinal (L) and transverse (T) response of Carbon,



- The onset of scaling is clearly visible in the quasi-elastic peak
- Large scaling violations appear in $F_T(y)$ at $y > 0$

Super-Scaling (SuSA) model

Amaro *et al.*, PRC71 (2005)

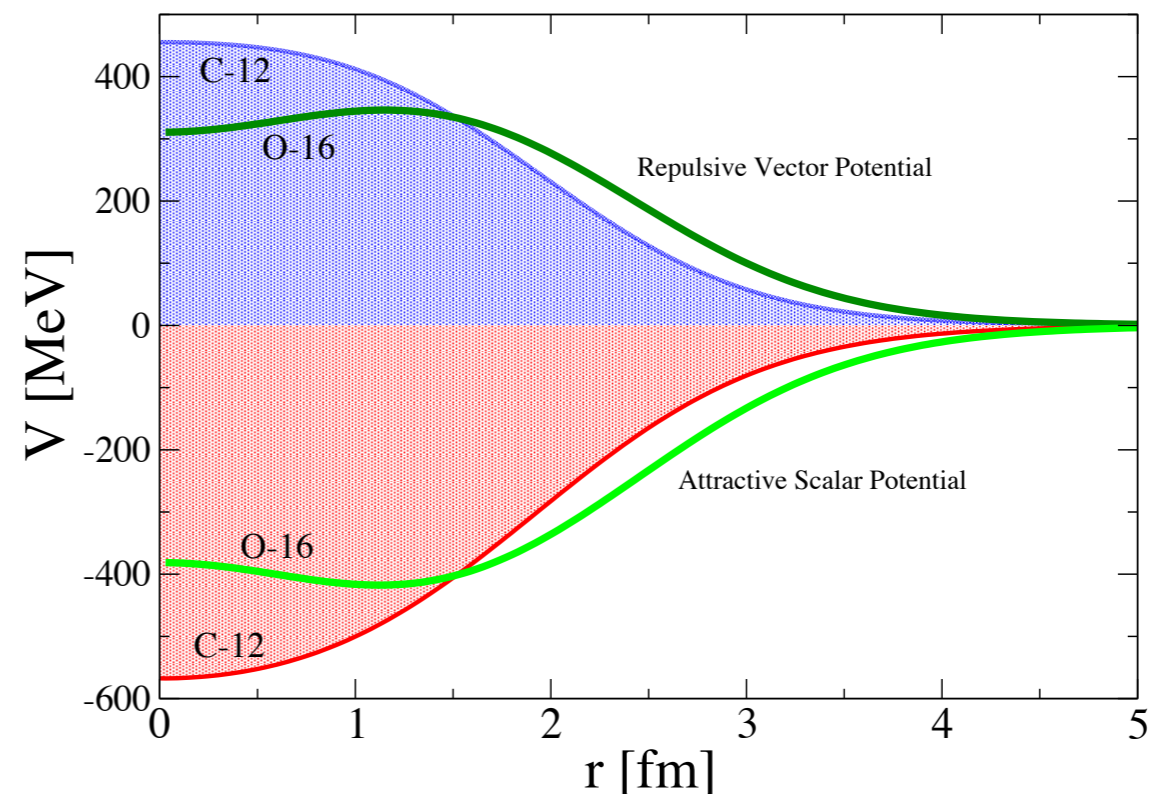


The nucleon wave functions are solutions of the Dirac equation with phenomenological relativistic scalar and vector mean field potentials

$$(i\gamma^\mu \partial_\mu - M - S + V) \psi(\vec{r}, t) = 0$$

Basic idea is to use the scaling function extracted from longitudinal (e,e') data to predict ν -scattering cross sections

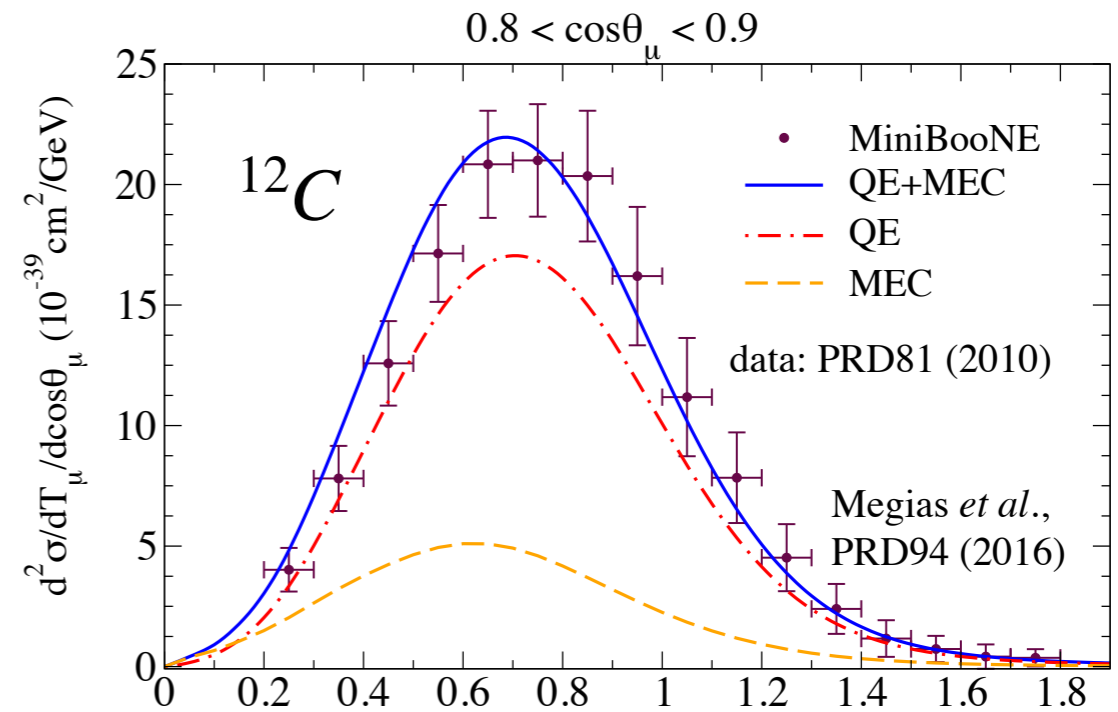
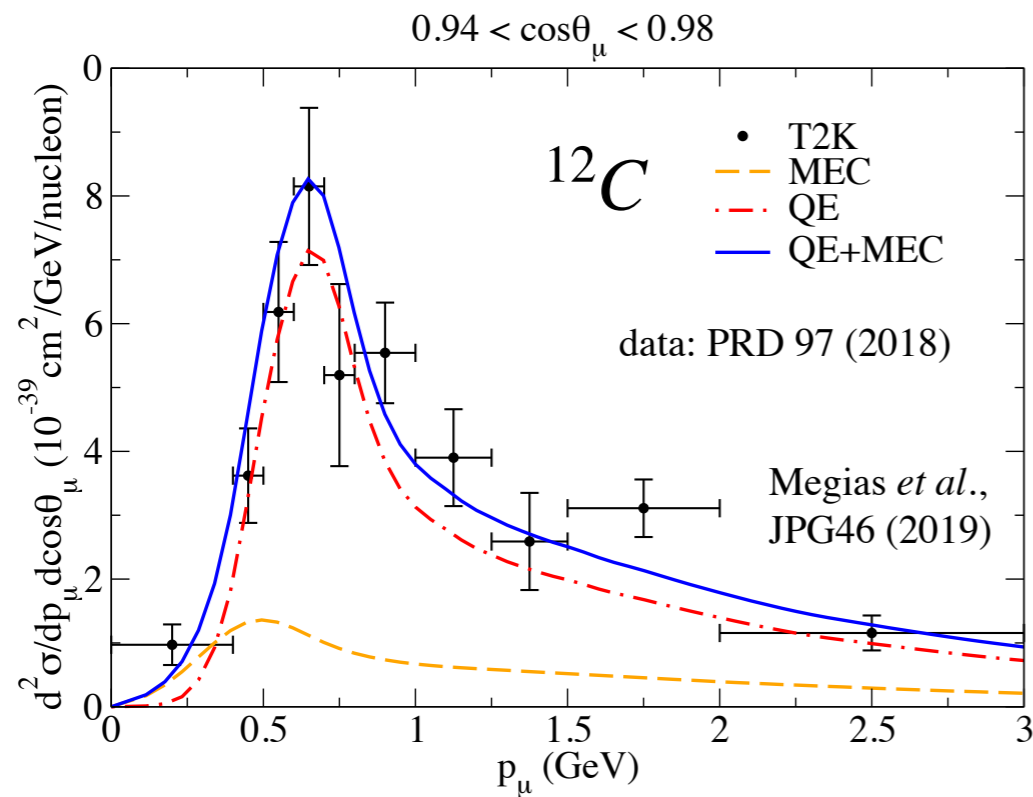
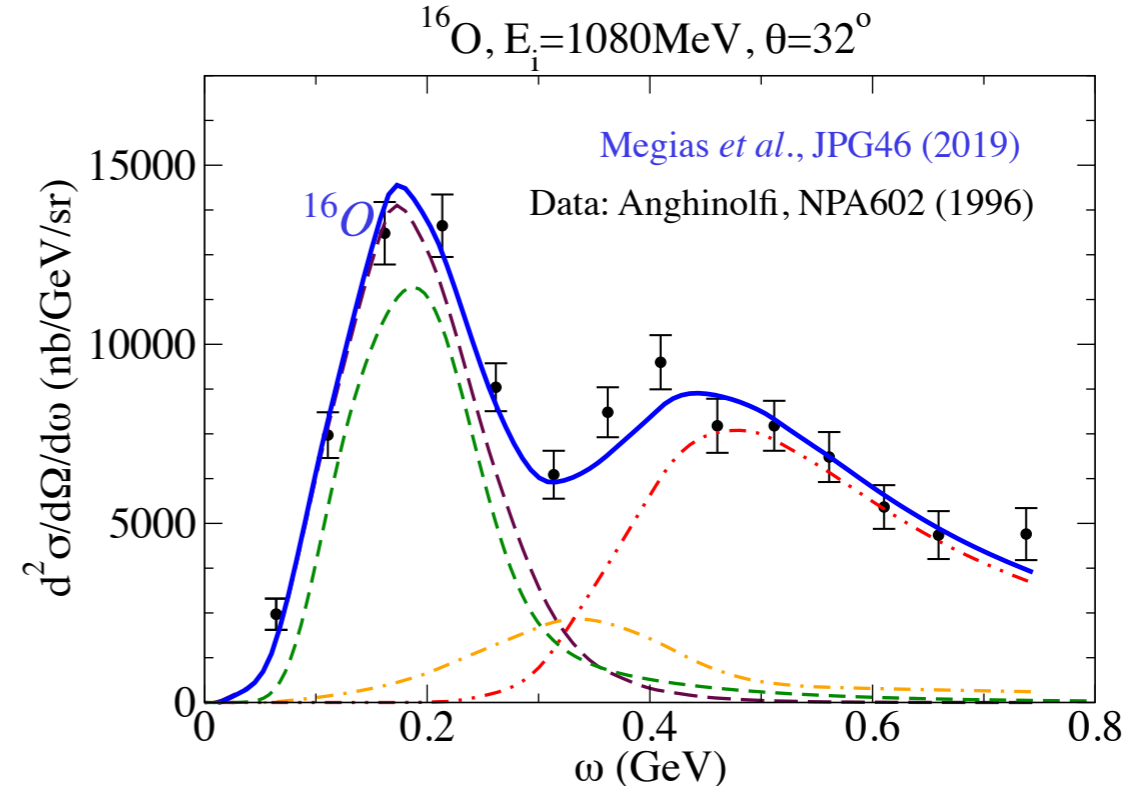
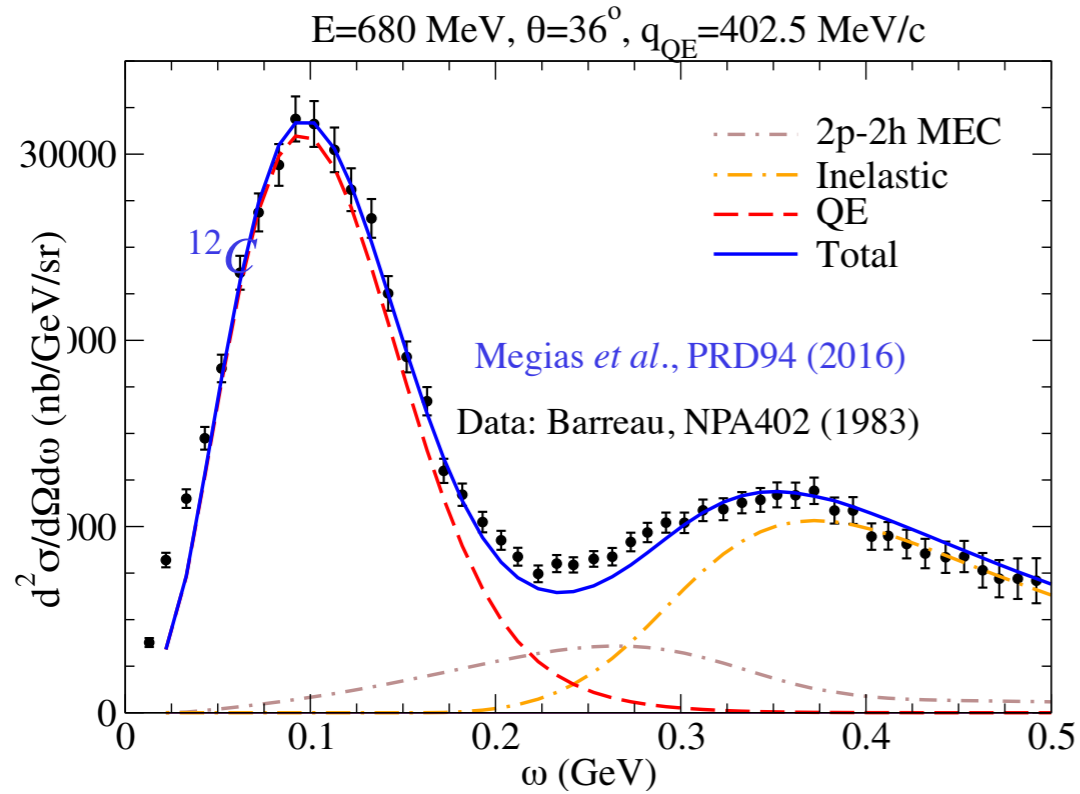
Gonzalez-Jimenez *et al.*, PRC90(2014)



SuSAv2 : uses scaling functions extracted from Relativistic Mean Field calculations.

$f_T > f_L$ in agreement with L/T separated (e,e') data

SuSAv2 predictions

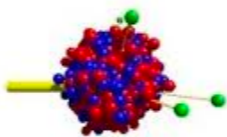


Different **Monte Carlo event generators** on the market

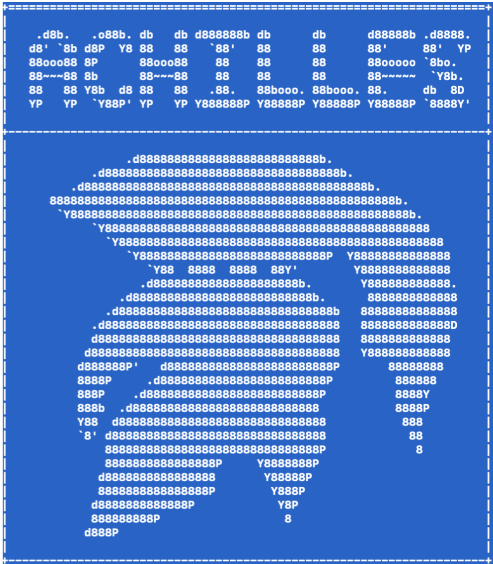
Event generators also used to predict **backgrounds** and **efficiency**

Using a factorization scheme

Many generators also tune theoretical models to data



Institut für Theoretische Physik, JLU Giessen
GiBUU
The Giessen Boltzmann-Uehling-Uhlenbeck Project



From neutrino-nucleon to neutrino-nucleus

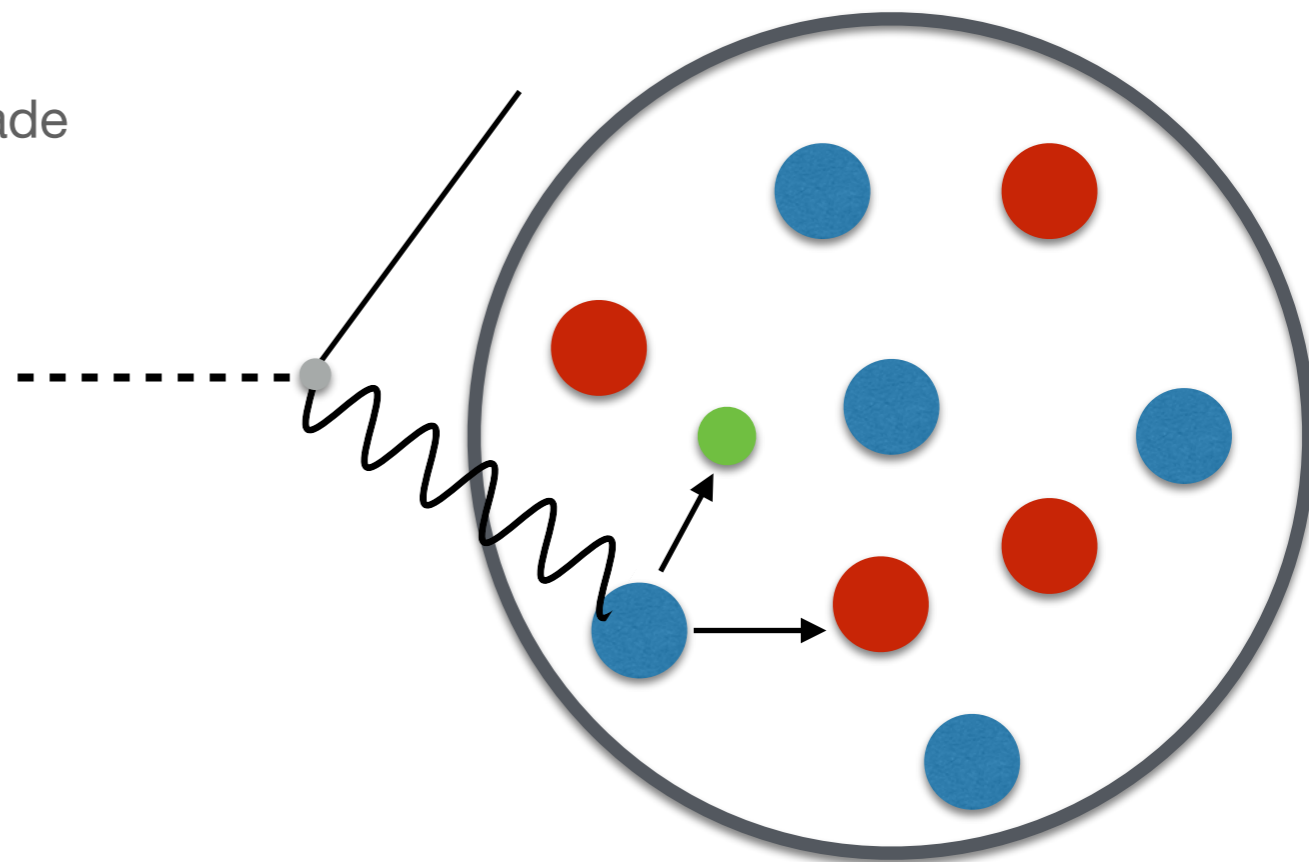
Factorization Scheme:

$$|\mathcal{M}(\{k\} \rightarrow \{p\})|^2 \simeq \sum_{p'} |\mathcal{V}(\{k\} \rightarrow \{p'\})|^2 \times |\mathcal{P}(\{p'\} \rightarrow \{p\})|^2$$

- Nuclear Model
- Primary Interaction
- Evolution out of the nucleus (intra-nuclear) cascade

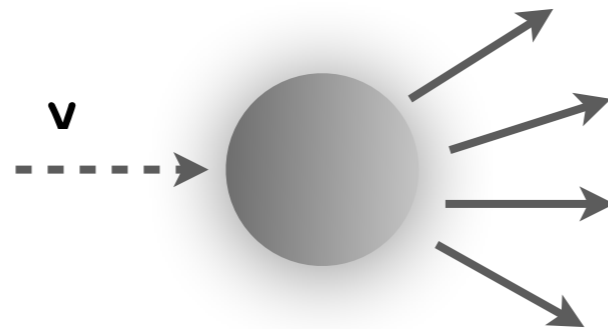
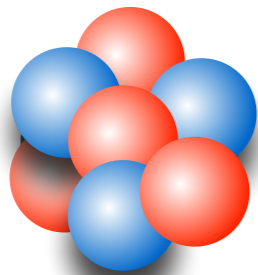
The propagation of **nucleons** through the **nuclear medium** is crucial in the analysis of neutrino oscillation experiments.

- Elastic scattering
- Charge exchange
- Pion Production
- Absorption

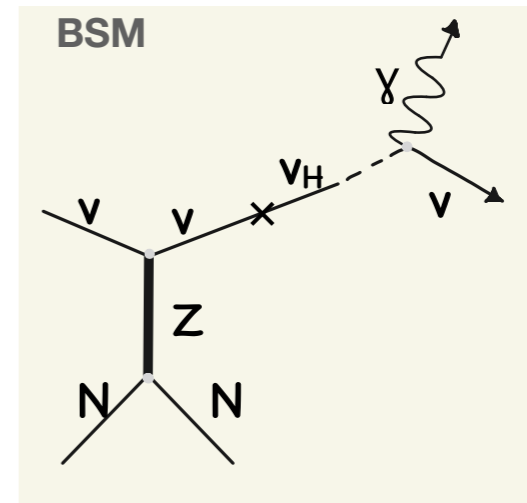


Summary

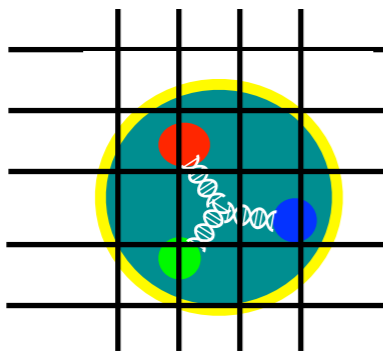
Nuclear Physics:



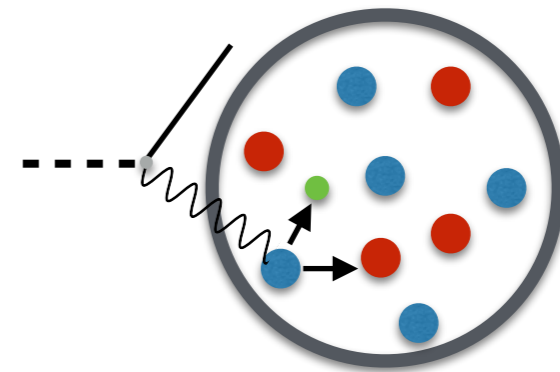
Simulate neutrino-nucleus cross sections to untangle neutrino oscillations from the measured interactions



Lattice QCD :



Event Generator :



Thank you for your attention!